Distribution Agreement

In presenting this thesis or dissertation as a partial fulfillment of the requirements for an advanced degree from Emory University, I hereby grant to Emory University and its agents the non-exclusive license to archive, make accessible, and display my thesis or dissertation in whole or in part in all forms of media, now or hereafter known, including display on the world wide web. I understand that I may select some access restrictions as part of the online submission of this thesis or dissertation. I retain all ownership rights to the copyright of the thesis or dissertation. I also retain the right to use in future works (such as articles or books) all or part of this thesis or dissertation.

Signature:

_____ _____

Susan O. Kim Date

Substrate-dependent effects of myeloperoxidase-derived oxidants on the metabolome and transcriptome of human airway epithelial cells

By

Susan O. Kim
Doctor of Philosophy

Graduate Division of Biological and Biomedical Science
Biochemistry, Cell, and Developmental Biology

_____
Joshua D. Chandler, Ph.D.
Co-advisor

_____
Rabindra M. Tirouvanziam, Ph.D.
Co-advisor

_____
Michael H. Koval, Ph.D.
Committee Member

_____
Judith L. Fridovich-Keil, Ph.D.
Committee Member

_____
Christine M. Dunham, Ph.D.
Committee Member

_____
Nicholas T. Seyfried, Ph.D.
Committee Member

Accepted:

_____
Kimberly Jacob Arriola, Ph.D., MPH
Dean of the James T. Laney School of Graduate Studies

_____
Date

Substrate-dependent effects of myeloperoxidase-derived oxidants on the metabolome and transcriptome of human airway epithelial cells

By

Susan O. Kim

B.S., University of North Carolina Chapel Hill, 2016

Advisors: Joshua Chandler, Ph.D. and Rabindra Tirouvanziam, Ph.D.

An abstract of

A dissertation submitted to the Faculty of the

James T. Laney School of Graduate Studies of Emory University

in partial fulfillment of the requirements for the degree of

Doctor of Philosophy

in Graduate Division of Biological and Biomedical Science

Biochemistry, Cell, and Developmental Biology

2023

Abstract

Substrate-dependent effects of myeloperoxidase-derived oxidants on the metabolome and transcriptome of human airway epithelial cells

By Susan O. Kim

Chronic inflammatory lung diseases, including genetic diseases such as cystic fibrosis (CF) and acquired diseases such as chronic obstructive pulmonary diseases (COPD), collectively impact millions of people worldwide. While the etiology is diverse, a convergence between these inflammatory lung diseases is the burden of airway leukocytes, often dominated by neutrophils, that consequently impede quality of life despite advances in treatment options. Neutrophils play a vital role in innate immunity by killing pathogens using a variety of mechanisms including mobilization of myeloperoxidase (MPO), a heme peroxidase enzyme, that catalyzes the production of potent oxidants that includes hypochlorous acid (HOCl), hypobromous acid (HOBr), and hypothiocyanous acid (HOSCN). However, chronic exposure to MPO-derived oxidants has the potential to cause severe oxidative stress and result in accumulation of off-target damage to host tissue. Hallmarks of MPO-derived oxidant exposure have been observed in patients with CF and COPD and these signatures correlate with structural lung damage in young children with CF. Thus, it is imperative to understand the global impact of MPO-derived oxidants on the host airway epithelial cells (AECs) in order to elucidate mechanisms of adaptation to oxidant exposure and to discover potential biomarkers of disease progression that will guide better means of monitoring and/or treating inflammatory airway diseases.

The research presented in this dissertation aims to address two main areas of chronic inflammatory lung diseases centered around neutrophilic inflammation: 1) the effects of MPO-derived oxidants on the metabolome of AECs and the translational implications in early CF and

2) the effects of MPO-derived oxidants on the global transcriptional programming of AECs. This dissertation advances the knowledge of metabolic and transcriptional (mal)adaptation of AECs exposed to MPO-derived oxidants by demonstrating global substrate-dependent divergent responses and our *in vitro* findings had implications for early cystic fibrosis by revealing dehydromethionine, a candidate metabolite biomarker of lung disease.

Substrate-dependent effects of myeloperoxidase-derived oxidants on the metabolome and transcriptome of human airway epithelial cells

By

Susan O. Kim

B.S., University of North Carolina Chapel Hill, 2016

Advisors: Joshua D. Chandler, Ph.D. and Rabindra M. Tirouvanziam, Ph.D.

A dissertation submitted to the Faculty of the

James T. Laney School of Graduate Studies of Emory University

in partial fulfillment of the requirements for the degree of

Doctor of Philosophy

in Graduate Division of Biological and Biomedical Science

Biochemistry, Cell, and Developmental Biology

2023

Acknowledgements

This work would not have been possible without the endless support and inspiration from my co-advisors Drs. Joshua Chandler and Rabin Tirouvanziam. I am eternally grateful to Joshua who fostered my passion for metabolomics and mass spec and embodies what it means to be an inclusive, patient, and brilliant mentor. I have a profound appreciation for Rabin whose motivating speeches and candidness are unmatched. Thank you both for challenging me to be an independent and confident scientist, while always expressing compassion and empathy.

I'm most grateful to have met remarkable investigators and scientists that have supported my work and encouraged me to grow. Thank you to my committee members Drs. Christine Dunham, Judy Fridovich-Keil, Mike Koval and Nick Seyfried for all the guidance, feedback, and advocacy. Many thanks to all our collaborators from the multinational SYNERGY CF consortium and Emory's IMPEDE-CF consortium with whom I've had the pleasure to work with during this dissertation project and other related projects.

I want to thank all the Chandler and Tirouvanzuam lab members (current and former) that have been a significant source of support both academically and personally. I can't express enough how much delight it has brought me to have such wonderful colleagues. I'd like to thank Dr. Kirsten Cottrill whom I have so much appreciation and admiration for and thank you to Justin Hosten for being a source of amusement during the trying times.

A special thanks to my former research mentors that are strong women in science. Thank you to my role models Dr. Natasha Snider, Dr. Kaoru Inoue, and Dr. Natalie Shaw. You have all inspired me and empowered me to be a great scientist. I am so grateful for the research opportunities and training that I received.

Words cannot convey the deep gratitude I have for my friends for their unconditional emotional support and continuous patience. Thank you for being there through the hard times, cheering me on and celebrating each accomplishment throughout my entire PhD journey: Toni Barreto, Jeanne Powell, Millie Ferguson, and Christine Bowen (and Finn). Thank you to my 1419 friends who kept me grounded during the COVID-19 pandemic: Dr. Jamie Hamilton, Erica Modeste, and Dr. Raques McGill.

I sincerely thank my family who has been so generous with their love and encouragement. Thank you to my parents, Yoon and Yong Kim, for their countless sacrifices. I am incredibly grateful for my sister, Jenny Kim, brother-in-law, Ryan Hice, and nephew, Ethan Hice – thank you for always being there. This endeavor would not have been possible without your unwavering care and support.

Finally, I thank with so much love to my dog, Ranger Kim. You have been a daily source of companionship, not only during graduate school but for the past eight years you've been alive. You are the best boy in the world.

Table of Contents

List of tables and figures

List of Abbreviations

AEC	Airway epithelial cells
Ala	Alanine
ALDH1A3	Aldehyde dehydrogenase 1 family member A3
ARE	Antioxidant response element
BAL	Bronchoalveolar lavage
BCAAs	Branched chain amino acids
Br-	Bromide
Bx	Bronchiectasis
CF	Cystic fibrosis
CFTR	Cystic fibrosis transmembrane conductance regulator
Cl-	Chloride
CoA	Acetyl coenzyme
COPD	Chronic obstructive pulmonary disease
Cys	Cysteine
CySS	Cystine
DEG	Differentially expressed gene
dhMet	Dehydromethionine
ECM	Extracellular matrix
EGF	Epidermal growth factors
EPO	Eosinophil peroxidase
ESI	Electrospray ionization
Fe3+	Ferric
FGF	Fibroblast growth factor
GAPDH	Glyceraldehyde 3-phosphate dehydrogenase
GCLM	Glutamate-cysteine ligase modifier subunit
Glu	Glutamate
GO	Gene ontology
GOX	Glucose oxidase
GSA	Glutathione sulfonamide
GSEA	Gene set enrichment analysis
GSH	Glutathione
GSSG	Glutathione disulfide
H2O2	Hydrogen peroxide
HMOX1	Heme oxygenase 1
HOBr	Hypobromous acid
HOCl	Hypochlorous acid
HOSCN	Hypothiocyanous acid
HOX	Hypohalous acids
HRMS	high resolution mass spectrometry
IL	Interleukin
Keap1	Kelch like ECH associated protein 1
KLF2	KLF transcription factor 2
LC-MS	liquid chromatography mass spectrometry

LDH	Lactate dehydrogenase
LPC	lysophosphatidylcholines
LPO	Lactoperoxidase
MAF	Musculoaponeurotic fibrosarcoma
Maff	MAF Basic Leucine Zipper Transcription Factor F
Mafg	MAF Basic Leucine Zipper Transcription Factor G
MAPK	Mitogen-activated protein kinases
Met	Methionine
MetO	Methionine sulfoxide
MPO	Myeloperoxidase
MS2	Tandem mass spectrometry
NADPH	Nicotinamide adenine dinucleotide phosphate
NET	Neutrophil extracellular trap
NF-κB	Nuclear factor kappa B
NOX2	NADPH oxidase 2
NQO1	NAD(P)H quinone dehydrogenase 1
Nrf2	Nuclear factor erythroid 2-related factor 2
$O2^{\bullet-}$	Superoxide
PC	phosphatidylcholines
PCA	Principal component analysis
PE	phosphatidylethanolamines
PLS-DA	Partial least squares-discriminant analysis
PPP	Pentose phosphate pathway
Prx3	Peroxiredoxin 3
PTPs	Protein tyrosine phosphatases
PXDN	Peroxidasin
QC	Quality control
ROS	Reactive oxygen species
SCN-	Thiocyanate
SLC7A11	Solute Carrier Family 7 Member 11
TCA	Tricarboxylic acid
TNF-α	Tumor necrosis factor alpha
TNFRSF10D	TNF receptor superfamily member 10d
TPO	Thyroid peroxidase
TSC22D3	TSC22 domain family member 3
TXNRD1	Thioredoxin reductase 1
VIP	Variable importance projection

Chapter 1

Introduction

1.1 Neutrophils in chronic lung diseases

1.2 Role of neutrophils in airway inflammation

- 1.2.1 Pathogen killing mechanisms
- 1.2.2 Oxidative burst

1.3 Myeloperoxidase

1.4 Hypohalous acids

- 1.4.1 Reactivity and selectivity
- 1.4.2 Cellular effects on airway epithelium
- 1.4.3 HOX redox and cell signaling in airway epithelium
- 1.4.4 Therapeutic potential of thiocyanate

1.5 Dissertation direction

1.1 Neutrophils in chronic lung diseases

Inflammatory lung diseases, including chronic obstructive pulmonary disease (COPD), cystic fibrosis (CF) and asthma, collectively represent a major global public health challenge and economic burden[1–5]. A common pathological theme among these lung diseases is the persistent presence of airway leukocytes, particularly neutrophils, and cellular byproducts that associate with lung disease severity and progression[6–12]. Neutrophils form an essential component of the innate immune response, particularly through their ability to mount an oxidative burst, a metabolic process that generates potent reactive oxygen species prinicipally to eliminate pathogens. The enzyme myeloperoxidase (MPO) is key to this mechanism, catalyzing the production of hypohalous acids (HOX), including hypochlorous acid (HOCl), hypobromous acid (HOBr), and hypothiocyanous acid (HOSCN). While these HOX are crucial for antimicrobial activity, their excessive or aberrant production may lead to oxidative stress and tissue damage, thereby potentially contributing to chronic inflammatory lung diseases. Each HOX also has variable implications in disease – HOCl/HOBr oxidation byproducts have been associated with increased bronchiectasis in CF, but patients with higher levels of airway SCN^- have better lung function, suggesting a protective role for HOSCN[11,13–15]. Studies have elucidated potential biological targets of HOX and cellular responses of host tissue cells to HOX exposure, however, we currently lack a comprehensive understanding of the global impact of HOX in airway epithelial cells (AEC), potential targets of oxidative burden and injury in chronic lung diseases.

1.2 Role of neutrophils in airway inflammation

Neutrophils are a major component of innate and adaptive immunity – they are the most abundant white blood cell in circulation, comprising up to 70% of all leukocytes circulating in

human bloods[16]. They are remarkably multifaceted with critical roles as the initial mediators of innate host defense and as modulators of the adaptive immune response through the recruitment and activation of lymphocytes[17,18]. Neutrophils are generated continuously in the bone marrow (upwards of $1x10^{11}$ cells daily) where they are derived from myeloid progenitor cells and released into the bloodstream once they reach maturation in approximately a week[19]. Once in circulation, neutrophils can survive for less than 24 hours[20,21], although other studies have reported a lifespan of several days[22]. In response to pro-inflammatory cues (i.e., chemoattractants such as IL-8), neutrophils mobilize to sites of inflammation, traversing the extracellular matrix (ECM) and ultimately tissue cells to arrive at their destination[23,24]. Once they do so, neutrophils deploy an array of effector functions to rapidly eliminate harmful microorganisms and viruses, discussed in depth in the next section. These short-lived cells are expected to then die via apoptosis to restrict their destructive capacity in the surrounding tissue and promote an anti-inflammatory response in macrophages, which clear the dead cells and aid in resolving the inflammation[25].

1.2.1 Pathogen killing mechanisms

Neutrophils display an impressive range of phenotypic heterogeneity in the pursuit of pathogen destruction through three primary fates: phagocytosis, degranulation, and neutrophil extracellular trap (NET) formation (i.e., NETosis) (**Figure 1.1**). To aid in these processes, neutrophils harbor four types of granules (primary/azurophilic, secondary/specific, tertiary/gelatinase, and secretory) that each contain a specific repertoire of inflammatory mediators, including proteases and oxidant-generating enzymes[26–31]. The first fate, phagocytosis, is a process by which neutrophils engulf and internalize pathogens into a digestive vacuole called

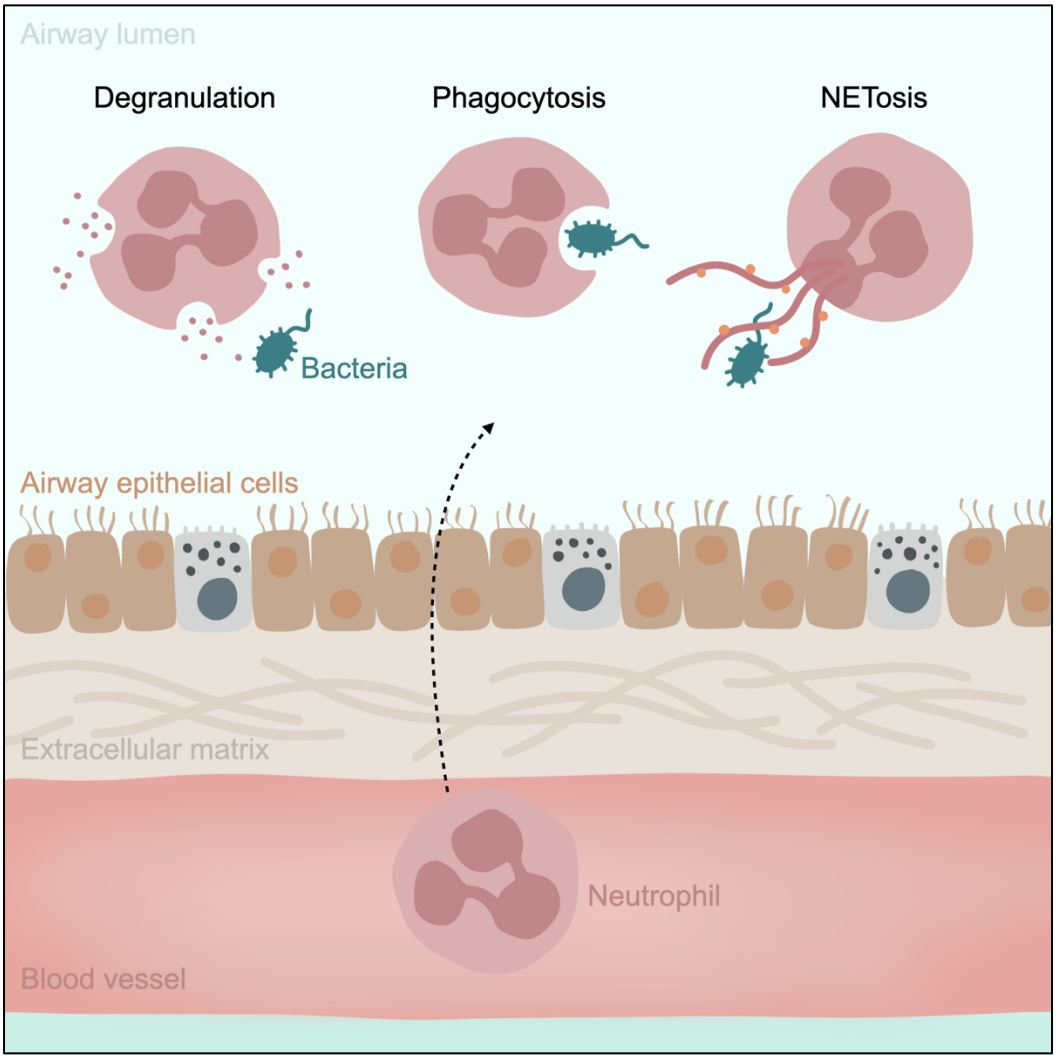

Figure 1.1 Functional fates of neutrophils during host defense. During inflammation, neutrophils circulating in the bloodstream mobilize to the airway, interacting with both the extracellular matrix and airway epithelial cells. Once at the site of infection, neutrophils exert at least three effector functions to eliminate pathogens: degranulation, phagocytosis, and neutrophil extracellular net formation, also referred to as NETosis.

the phagosome[32,33]. In the phagosome, neutrophil membrane proteins and granule contents fuse to rapidly form reactive oxygen species (ROS) that confer antimicrobial activity[34]. In addition to eliminating pathogens, phagocytosis is important for tissue homeostasis through clearance of dead cells and tissue debris[35]. The second fate, degranulation, also leverages the rapid production of ROS through exocytosis of granules containing oxidant-generating enzymes into the extracellular space[36–38]. The third fate that neutrophils undergo during host defense is NETosis – a specialized process involving the extrusion of a meshwork of modified chromatin strands containing citrullinated histones and bactericidal proteins that can trap and kill pathogens that are attracted to the material by ionic interactions[39–42].

1.2.2 Oxidative burst

To generate the lethal ROS that directly acts on pathogens within all three fates, neutrophils undergo a metabolic process known as "oxidative burst" (also referred to as "respiratory burst") (**Figure 1.2**). In the first step of oxidative burst, membrane-bound enzyme NADPH oxidase 2 (NOX2) rapidly consumes oxygen by transferring one electron from NADPH to oxygen to produce superoxide ($O_2^{\bullet-}$)[43–46]. Next, $O_2^{\bullet-}$ dismutates to oxygen and hydrogen peroxide (H_2O_2). H_2O_2 can then be reduced by MPO to produce HOCl, HOBr, and HOSCN via 2-electron oxidation of a (pseudo)halide such as chloride (Cl^-), bromide (Br^-) or thiocyanate (SCN^-), respectively[47–49]. The peroxidase-derived oxidants are a unique group of ROS collectively categorized as HOX that not only have a role in host defense, but also cell signaling to host cells[50–58]. Each HOX can effectively eliminate various pathogens (e.g., bacteria, fungi, and viruses) once released extracellularly into the luminal airway microenvironment or intracellularly in the phagolysosome[59,59–66]. While the initial ROS products (e.g., $O_2^{\bullet-}$ and H_2O_2)

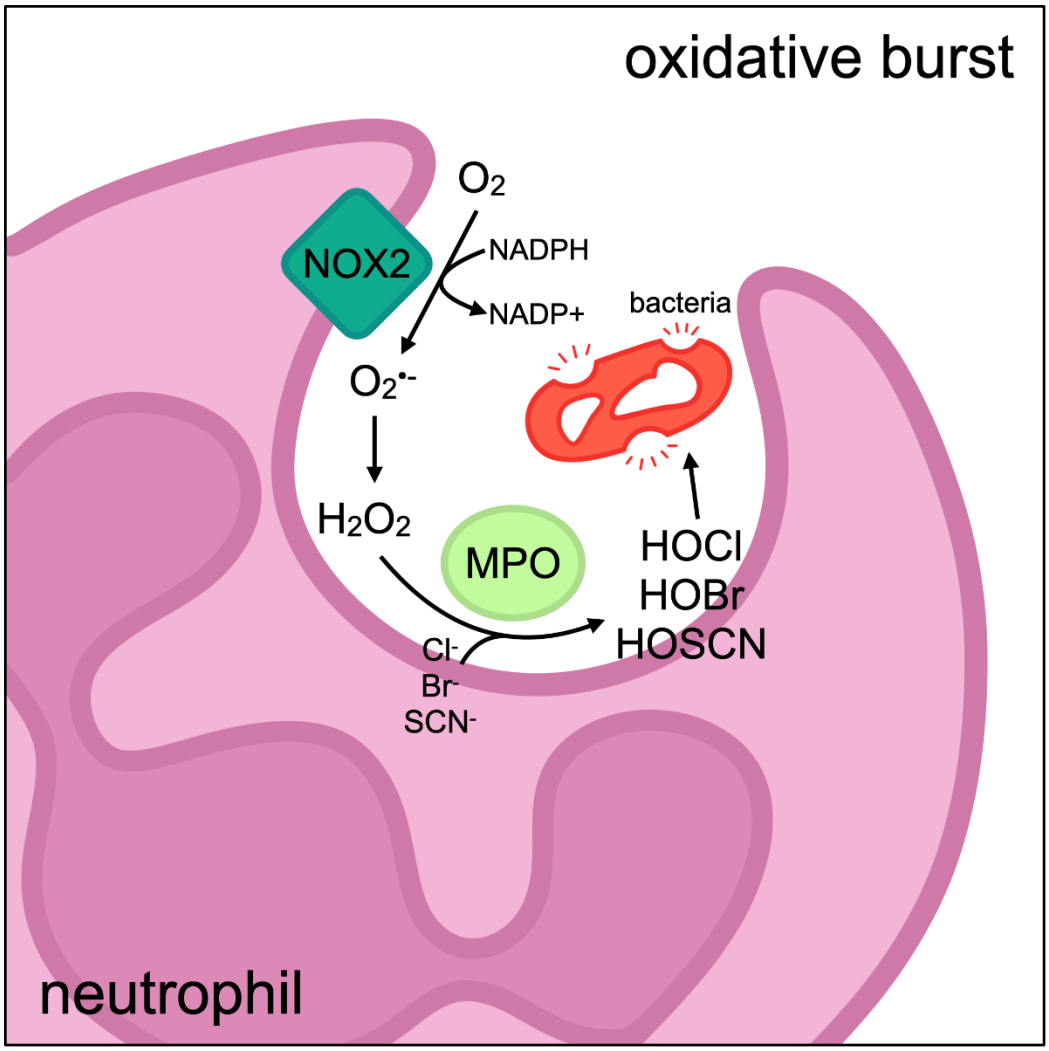

Figure 1.2 NOX2 and MPO in neutrophil oxidative burst. During phagocytosis, oxygen consumption rises through activity of NADPH oxidase 2 (NOX2) that results in the production of superoxide ($O_2^{\bullet-}$). Dismutation of $O_2^{\bullet-}$ generates hydrogen peroxide (H_2O_2). Then, myeloperoxidase (MPO) catalyzes the reaction of H_2O_2 with halides (Cl^-, Br^-) or pseudohalide (SCN^-) to produce the powerful microbicidal oxidants HOCl, HOBr, and HOSCN.

could have some contribution to the direct bacterial killing mechanism, HOX are ultimately responsible for the bulk of the antimicrobial activity in the oxidative burst[46,67–70].

A shared feature of numerous inflammatory diseases including COPD, CF, and asthma is excessive neutrophil degranulation in the airway, exemplified by significantly elevated levels of primary granule components such as MPO in CF airway clinical samples[9,11,71–73]. Additionally, excessive degranulation has been observed with *in vitro* models of neutrophil transmigration through AECs to diluted CF sputum, mimicking airway transmigration *in vivo*[10,74–76]. Bacterial killing capacity by neutrophils is reduced in many chronic lung disease models, which coincides with recurring polymicrobial infections observed in patients with chronic lung disease[77–82].

1.3 Myeloperoxidase

MPO is a heme peroxidase enzyme that is mainly produced by neutrophils during development in the bone marrow and abundantly packaged in the primary granules, constituting up to 5% of the dry mass of neutrophils[83,84]. Monocytes also express MPO in lysosomes to a significantly lesser extent, however, *in vitro* studies have shown MPO is lost when monocytes are differentiated into tissue macrophages[85–87]. Although it is somewhat controversial whether macrophages express MPO[88,89], it is expected that MPO detected in clinical airway samples are contributed to neutrophils.

Previously named verdoperoxidase due to its heme-derived green hue[90], MPO is a member of the chordata peroxidase subfamily that includes eosinophil peroxidase (EPO), lactoperoxidase (LPO), and thyroid peroxidase (TPO) – all mammalian heme peroxidases that share a number of conserved features in the heme-binding pocket, including two ester linkages between the heme and the protein backbone (Ala280, Glu408)[91,92]. The structure of MPO has

previously been described in detail[93–97]. EPO, LPO, and peroxidasin (PXDN) can also produce HOX, yet MPO is the only peroxidase that can produce HOCl, the HOX with the greatest reduction potential (i.e., tendency to accept electrons), under physiological conditions[98,99]. The exclusive chlorinating potential of MPO is owed to its structure – MPO contains an additional sulfonium linkage from heme to the peptide backbone (Met409) that increases its reduction potential, enabling it to oxidize chloride ion[98,100,101]. In the catalytic reaction pathway of MPO, formally termed "halogenation cycle", H_2O_2 first reacts with ferric (Fe^{3+}) MPO to generate the 2-electron oxidized Compound I (an oxy-ferryl species, Fe^{4+}=O, with a porphyrin π-cation radical) and a H_2O molecule. Then, Compound I is converted back to ferric MPO through the 2-electron reduction of a halide (Cl^-, Br^-) or pseudohalide (SCN^-) anion, thus producing HOCl, HOBr, and HOSCN[92].

1.4 Hypohalous acids

ROS have traditionally been regarded as toxic byproducts of metabolism that disrupt cellular redox homeostasis, leading to pathophysiological conditions. However, as Paracelsus famously said, "All things are poison, and nothing is without poison; the dosage alone makes it so a thing is not a poison"[102]. At physiological levels, ROS can function as important intra- and intercellular messengers in signaling pathways that maintain immune homeostasis and control infection[103]. HOX, are no exception – not only can they directly kill microbes through the destruction of the bacterial cell wall and oxidation of important biomolecules, but they can also induce signaling cascades and adaptive responses in various cells[50–52,55–58,104–106]. However, at pathophysiological levels, ROS, particularly HOX, can cause serve oxidative stress and harm to the host tissue as exemplified in chronic inflammatory diseases[107].

The production of HOX by MPO is largely dependent on the substrate availability, concentration, and reactivity. Cl^- is assumed the primary physiological substrate of MPO in the airway due to high concentrations (~50-100 mM) in plasma and airway surface liquid with evidence suggesting HOCl is the predominant byproduct of MPO activity[108–111]. The lung airway fluid contains ~30-650 μm of SCN^-, which in the higher range is enough to displace the majority of HOCl production by MPO in favor of SCN^-[62,112,113]. HOCl also accounts for at least 28% of oxygen consumed during oxidative burst, although 40% and 72% have been reported[109,114,115]. MPO can oxidize Cl^- with a high second-order rate constant ($4.5x10^2$ $M^{-1}s^{-1}$), however, MPO preferentially oxidizes Br^- ($2.7x10^4$ $M^{-1}s^{-1}$) and favors the pseudohalide SCN^- ($3.3x10^5$ $M^{-1}s^{-1}$) as a substrate the most[49]. With specificity constants of 1:60:730 for Cl^-, Br^-, and SCN^-, respectively, MPO will favorably form HOSCN > HOBr > HOCl[47,49].

1.4.1 Reactivity and selectivity

Despite a unifying role in host defense, there are stark differences in reactivity of HOCl, HOBr, and HOSCN with a diversity of compounds (e.g, amines, amides, thiols, thioethers, disulfides, nucleobases, nucleosides, nucleotides, lipids, sterols, etc) in biomolecules (e.g., proteins, metabolites, lipid membranes, DNA) at varying rates of reactions[116–122] (**Figure 1.3**). HOCl has the greatest reduction potential ($E'^\circ_{pH\ 7}$ = +1280 mV) out of the group of HOX, followed by HOBr ($E'^\circ_{pH\ 7}$ = +1130 mV) and HOSCN ($E'^\circ_{pH\ 7}$ = +560 mV)[98]. HOCl and HOBr are quite indiscriminate in their reactivity with biomolecules, although HOBr is more reactive with aromatic rings and double bonds[118]. In contrast, HOSCN is highly selective for thiols and selenols[92,121,122]. This alludes to HOSCN having a more specific and controlled role since the

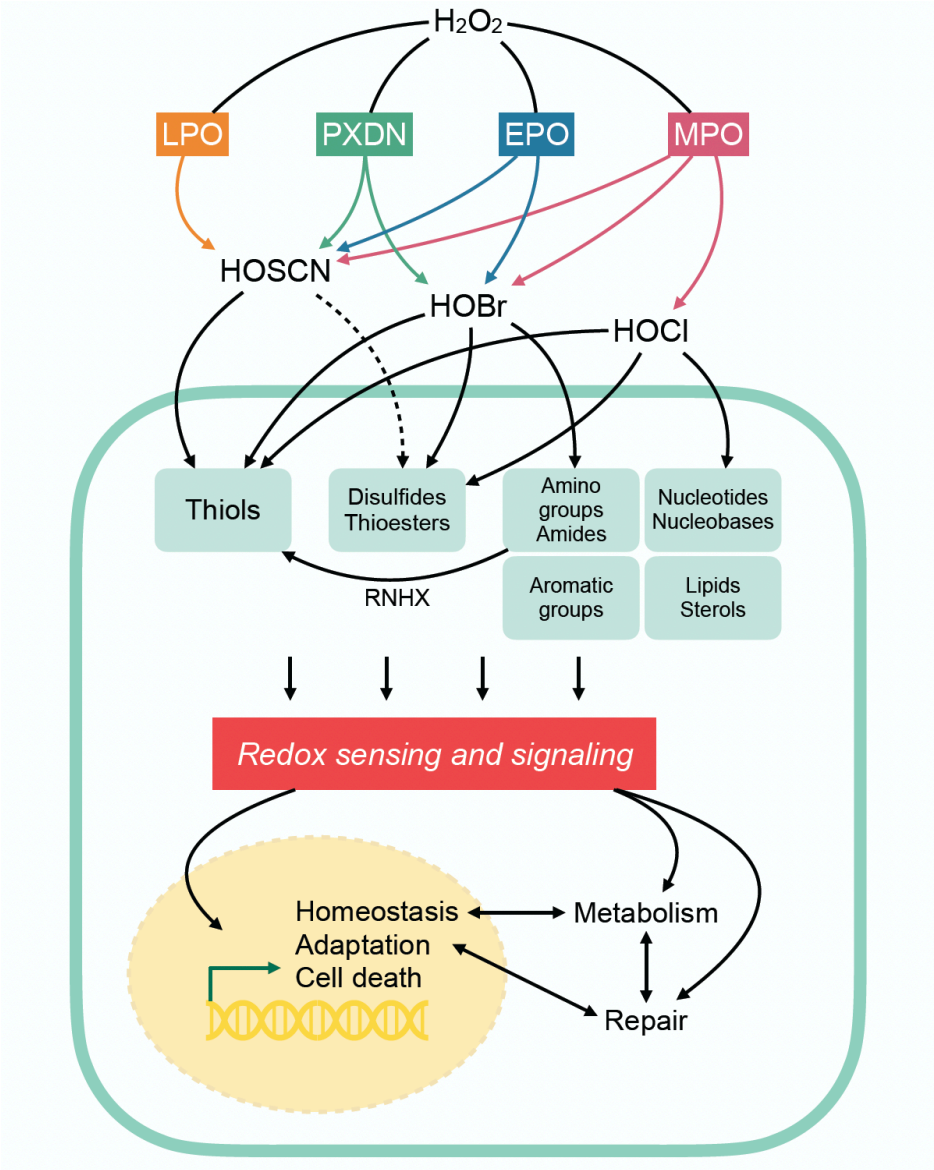

Figure 1.3 The production and reactivities of hypohalous acids (HOX) promote diverse cellular responses. HOX are produced by the mammalian peroxidases lactoperoxidase (LPO), peroxidasin (PXDN), eosinophil peroxidase (EPO), and myeloperoxidase (MPO), which can all generate HOSCN and HOBr. However, only MPO can uniquely produce HOCl. The different reactivities and selectivity of HOX with biological molecules can induce cellular redox sensing and signaling, ultimately influencing cellular fate. Adapted from Chandler JD, Mammalian Heme Peroxidases (1st Ed.), 2021[123].

thiol group in cysteine proteins can undergo reversible oxidative posttranslational modifications that modulate its activity and function[124]. HOCl reacts fastest

with nucleophiles containing sulfur (e.g., thiols and thioether) or nitrogen (e.g., amines) atoms, thus making cysteine and methionine residues in proteins and glutathione (GSH) prime targets of HOCl[92]. Although HOCl is promiscuously reactive, certain chlorinated byproducts (i.e., chloramines and chloramides) react more selectively and could contribute injury to host tissue in chronic lung pathologies via specific pathways[92]. The comprehensive reactivity and reaction rates of HOX have been well reviewed elsewhere[92,117,118]. Altogether, the differences in reactivity and selectivity of HOX influence their targets, thus impacting various redox sensing and signaling pathways that can dictate cellular fate and influence the progression of inflammatory lung pathologies.

1.4.2 Cellular effects on airway epithelium

Knowledge about the cellular impact of HOX on AECs is particularly limited. Studies assessing the cytotoxic effects of HOX on host cells were primarily performed on macrophages and endothelial cells due to their significant relevance in cardiovascular disease[92,125,126]. HOX exposure observed *in vitro* that causes cell death can often be owed to concentrations of HOX that reflect pathological conditions and potentially experimental exposures like bolus dosing that can overwhelm the cells beyond their capacity to adapt. The lethality of HOX exposure in cells is also influenced by the components within its microenvironment that can scavenge it, such as SCN^- and GSH, and negate cell death. HOX-induced injury to AECs occurs on the apical side of the cells where neutrophils are excessively recruited and aberrantly activated in chronic airway diseases such as CF and COPD. However, in chronic airway diseases, significant damage from

MPO and HOX is proposed to occur in the ECM where the basolateral side of AECs are in direct contact. The ECM is a complex and dynamic network of macromolecules that make up the interstitial matrix and basement membrane, providing structural and mechanical properties to the tissues, but it is also important for immune regulation[127]. MPO can be released or leaked into the ECM during neutrophil transmigration to the inflamed airway and it can bind to numerous ECM proteins, consequently localizing it in the ECM where it can produce HOCl and HOBr[24,128]. Not only can this lead to degradation of ECM components but it could potentially cause damage to AECs from the basolateral side.

Additionally, HOX are involved in a number of metabolic processes and could profoundly impact primary metabolism pathways in AECs[57,106,129–131]. Evidence suggests a metabolic rewiring of energy metabolism in cells by HOSCN occurs to support adaptation to oxidative stress[106,123,132]. HOSCN can redirect the glycolytic flux of glucose to pyruvate and lactate through the inactivation of glyceraldehyde 3-phosphate dehydrogenase (GAPDH), which has a redox-sensitive cysteine residue in the enzyme active site[106,132]. This is presumably to enhance pentose phosphate pathway (PPP) activity, which would increase the production of nicotinamide adenine dinucleotide phosphate (NADPH), an electron donor that provides the reducing power to restore redox balance[133]. HOSCN can also target the glycolytic enzymes fructose-bisphosphate aldolase and triose-phosphate isomerase, which are also susceptible to modulation of activity via thiol modification[106]. It has been proposed that the diminished levels of pyruvate due to the attenuation of glycolysis by HOSCN contributes to the inhibition of mitochondrial respiration and consequent decrease in ATP that has been observed in macrophages[134]. Currently, the impact of HOX on primary energy metabolism in AECs and how that may translate into cellular (mal)adaptation remains underexplored.

1.4.3 HOX redox and cell signaling in airway epithelium

ROS at physiological levels can modulate immune, antioxidant and various cellular processes through redox signaling. One of the essential regulators of redox homeostasis and antioxidant defense is the transcription factor Nrf2 (nuclear factor erythroid 2-related factor 2). Nrf2 is constitutively expressed in the cytoplasm where it is sequestered and inactivated by Keap1 (kelch like ECH associated protein 1), a protein that functions as a thiol-based redox sensor and facilitates ubiquitination for proteasomal degradation of Nrf2 under homeostatic conditions[135,136]. When the active site cysteine thiols of Keap1 become modified, Nrf2 is released and translocated to the nucleus to activate the transcription of antioxidant response element (ARE) genes[137]. In AECs, HOCl can induce the expression of Nrf2 transcriptional coactivators *MAFF* (MAF Basic Leucine Zipper Transcription Factor F) and *MAFG* (MAF Basic Leucine Zipper Transcription Factor G) and continued exposure can activate Nrf2 to induce the expression of ARE genes *TXNRD1* (thioredoxin reductase 1), *HMOX1* (heme oxygenase 1), *ALDH1A3* (aldehyde dehydrogenase 1 family member A3), *NQO1* (NAD(P)H quinone dehydrogenase 1), and *GCLM* (glutamate-cysteine ligase modifier subunit) – enzymes of antioxidant defense and detoxification[56]. Nrf2 conferred cytoprotection in AECs from HOCl-induced cytotoxicity at HOCl doses ranging from 0.6-1.5 mM. This suggests an early adaptive mechanism via Nrf2 signaling that could help to prevent tissue injury during acute inflammation. Currently, whether HOBr or HOSCN can activate Nrf2 signaling specifically in AECs has not yet been shown.

HOX can also activate other essential signaling pathways that elicit cytoprotective or destructive responses to cellular stress. HOX activation of the MAPK (mitogen-activated protein

kinases) signaling pathway and NF-κB (nuclear factor kappa B) signaling pathway have been observed in various cell types, but these pathways in AECs are much less characterized[51,56–58]. MAPK signal transduction regulates a plethora of cellular processes including cell stress response, differentiation, proliferation, survival, metabolism, inflammation, and death[138]. Three mammalian MAPK families have been extensively characterized (i.e., ERK1/2, JNK, and p38) and can be initiated by diverse stimuli including TNF-α (tumor necrosis factor alpha), EGFs (epidermal growth factors), and FGFs (fibroblast growth factors)[138]. In macrophages, HOCl and HOSCN can cause phosphorylation of JNK and p38, but they decrease phosphorylation of ERK1/2[51]. In AECs, HOCl can promote phosphorylation of JNK, p38, and ERK1/2, presumably through EGFR[56]. Interestingly, when SCN^- is added to HOCl, there are no changes in JNK, p38, ERK1/2 (de)phosphorylation which suggest SCN^- prevents HOCl-induced modulation of MAPKs that may be causing cell death[51]. It is unclear if HOBr and HOSCN promote the phosphorylation of MAPKs in AECs, but MAPKs have redox-sensitive cysteine residues within or near its substrate recognition sites that could potentially be a direct target of HOX[139].

The transcription factor NF-κB governs many critical innate and adaptive immune functions such as the expression of pro-inflammatory genes to often promote cell survival[140–142]. AECs, alongside resident macrophages, are the primary cells in the airway that initially sense pathogens and respond by releasing cytokines through the NF-κB pathway to recruit and activate neutrophils[140,141]. Studies have demonstrated that HOCl and HOSCN can increase the expression of pro-inflammatory genes (e.g., IL-1β, TNF-α, IL-6, IL-8) in macrophages through NF-κB pathway activation and that HOCl can inhibit NF-κB activation in melanoma tumor cells, but whether HOX activate this pathway in AECs is currently unresolved[50–52]. Given that AECs can express and release NF-κB -dependent inflammatory molecules in response to pathogens and

NF-κB is a redox-sensitive factor[143,144], it is plausible that HOX induce NF-κB signaling in AECs to mount an immune response, which could promote neutrophil recruitment and activation in chronic airway pathologies.

1.4.4 Therapeutic potential of thiocyanate

There is mounting evidence that HOCl is a causative agent of pathogenesis in multiple lung diseases[92]. As a result, SCN^- has been studied for its antioxidant properties against HOCl-induced damage[51,145–147] and has been studied as a potential therapeutic intervention[62,63,148,149]. The goal of SCN^- therapy for chronic airway diseases is to decrease the levels of HOCl by supplementing the airway with a pharmacologic dose of SCN^-, essentially replacing HOCl with HOSCN, a less harmful oxidant that retains pathogen killing capabilities (**Figure 1.4**). It has become increasingly evident that secretory epithelium is tolerant of HOSCN exposure[150,151]. In adults with CF, the concentration of saliva SCN^- is significantly decreased compared to non-CF control subjects[14]. Additionally, CF patients with higher levels of SCN^- had better lung function than those with lower levels[15]. SCN^- therapy could be especially beneficial to patients with CF where the levels of SCN^- are inherently reduced due to the nature of the disease. CF is caused by mutations to *CFTR* (cystic fibrosis transmembrane conductance regulator), which encodes for an ion channel for which SCN^- is one substrate[150]. Because anion transport is defective in CF, SCN^- levels in the airway may be decreased and reduce HOCl scavenging capacity, consequently leaving the airway more vulnerable than normal to pathological HOCl exposure[152]. CFTR mutations are currently categorized into five classes according to how function is lost, but it is not obvious whether certain mutations have greater or lesser impact on SCN^- channeling

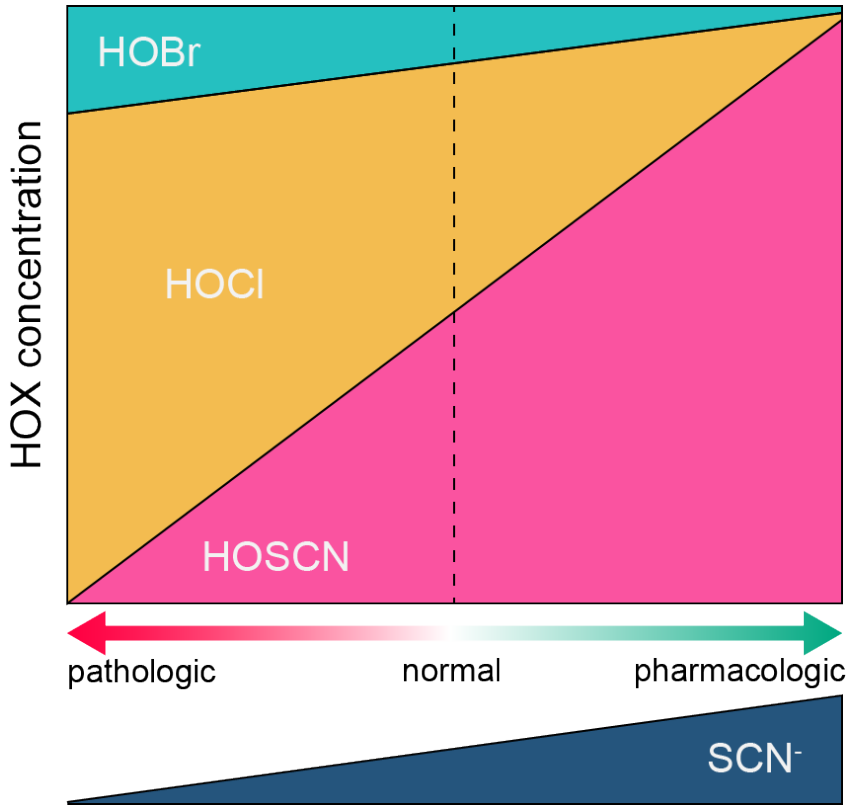

Figure 1.4 Qualitative graph demonstrating the impact of increasing thiocyanate (SCN^-) on the relative ratios of HOX concentration within plasma. Decreased SCN^- levels, as observed in cystic fibrosis, are associated with pathophysiological outcomes. However, a pharmacologic dose of SCN^- can alter the proportion of HOX to favor HOSCN formation, thus attenuating HOCl-induced toxicity. Adapted from review by Chandler JD and Day BJ, Free Radical Research, 2014[148].

specifically[153]. The promising outcomes of SCN^- supplementation thus far warrant further investigation of its use to prevent HOCl-mediated damage[61,62,146,148,150].

1.6 Dissertation direction

The redundancy of HOX exposure and lung function decline in chronic lung diseases necessitate a greater understanding of the impact of HOX on AECs to ultimately mitigate damage. AECs function as the first barrier in airway host defense. This places AECs at the forefront of infection and within the crossfire of inflammation. Hence, this dissertation seeks to define the global impact and cellular fate of HOX exposure on AECs. Leveraging a multi-omics approach (i.e., metabolomics and transcriptomics) and complimentary reductionist techniques in an *in vitro* oxidant exposure model, we delineated the substrate-dependent impact of HOX on AEC viability, redox status, and global metabolite profile, allowing us to identify potential metabolite biomarkers of early CF lung disease (**Chapter 2**), as well as the transcriptional programming of AECs exposed to HOX that may contribute to their (mal)adaptation in chronic lung disease (**Chapter 3**).

1.7 References

1. Adeloye, D. et al. Global, regional, and national prevalence of, and risk factors for, chronic obstructive pulmonary disease (COPD) in 2019: a systematic review and modelling analysis. The Lancet Respiratory Medicine 10, 447–458 (2022).
2. Safiri, S. et al. Burden of chronic obstructive pulmonary disease and its attributable risk factors in 204 countries and territories, 1990-2019: results from the Global Burden of Disease Study 2019. BMJ 378, e069679 (2022).
3. Guo, J., Garratt, A. & Hill, A. Worldwide rates of diagnosis and effective treatment for cystic fibrosis. Journal of Cystic Fibrosis 21, 456–462 (2022).
4. Braman, S. S. The Global Burden of Asthma. CHEST 130, 4S-12S (2006).
5. Nunes, C., Pereira, A. M. & Morais-Almeida, M. Asthma costs and social impact. Asthma Research and Practice 3, 1 (2017).
6. Jasper, A. E., McIver, W. J., Sapey, E. & Walton, G. M. Understanding the role of neutrophils in chronic inflammatory airway disease. F1000Res 8, F1000 Faculty Rev-557 (2019).
7. Lonergan, M. et al. Blood neutrophil counts are associated with exacerbation frequency and mortality in COPD. Respiratory Research 21, 166 (2020).
8. Giacalone, V. D., Dobosh, B. S., Gaggar, A., Tirouvanziam, R. & Margaroli, C. Immunomodulation in Cystic Fibrosis: Why and How? IJMS 21, 3331 (2020).
9. Sly, P. D. et al. Risk Factors for Bronchiectasis in Children with Cystic Fibrosis. N Engl J Med 368, 1963–1970 (2013).

10. Margaroli, C. et al. Elastase Exocytosis by Airway Neutrophils Is Associated with Early Lung Damage in Children with Cystic Fibrosis. Am J Respir Crit Care Med 199, 873–881 (2019).
11. Chandler, J. D. et al. Myeloperoxidase oxidation of methionine associates with early cystic fibrosis lung disease. Eur Respir J 52, 1801118 (2018).
12. Garratt, L. W. et al. Matrix metalloproteinase activation by free neutrophil elastase contributes to bronchiectasis progression in early cystic fibrosis. European Respiratory Journal 46, 384–394 (2015).
13. Dickerhof, N. et al. Oxidized glutathione and uric acid as biomarkers of early cystic fibrosis lung disease. Journal of Cystic Fibrosis 16, 214–221 (2017).
14. Minarowski, Ł. et al. Thiocyanate concentration in saliva of cystic fibrosis patients. Folia Histochem Cytobiol 46, 245–246 (2008).
15. Lorentzen, D. et al. Concentration of the antibacterial precursor thiocyanate in cystic fibrosis airway secretions. Free Radic Biol Med 50, 1144–1150 (2011).
16. Hollowell, J. G. et al. Hematological and iron-related analytes--reference data for persons aged 1 year and over: United States, 1988-94. Vital Health Stat 11 1–156 (2005).
17. Rosales, C. Neutrophils at the crossroads of innate and adaptive immunity. Journal of Leukocyte Biology 108, 377–396 (2020).
18. Mantovani, A., Cassatella, M. A., Costantini, C. & Jaillon, S. Neutrophils in the activation and regulation of innate and adaptive immunity. Nat Rev Immunol 11, 519–531 (2011).
19. Dancey, J. T., Deubelbeiss, K. A., Harker, L. A. & Finch, C. A. Neutrophil kinetics in man. https://www.jci.org/articles/view/108517/pdf (1976) doi:10.1172/JCI108517.

20. Bonilla, M. C. et al. How Long Does a Neutrophil Live?—The Effect of 24 h Whole Blood Storage on Neutrophil Functions in Pigs. Biomedicines 8, 278 (2020).
21. Tak, T., Tesselaar, K., Pillay, J., Borghans, J. A. M. & Koenderman, L. What's your age again? Determination of human neutrophil half-lives revisited. Journal of Leukocyte Biology 94, 595–601 (2013).
22. Pillay, J. et al. In vivo labeling with 2H2O reveals a human neutrophil lifespan of 5.4 days. Blood 116, 625–627 (2010).
23. Lee, S., Bowrin, K., Hamad, A. R. & Chakravarti, S. Extracellular matrix lumican deposited on the surface of neutrophils promotes migration by binding to beta2 integrin. J Biol Chem 284, 23662–23669 (2009).
24. Zhu, Y. et al. Interplay between Extracellular Matrix and Neutrophils in Diseases. J Immunol Res 2021, 8243378 (2021).
25. Ortega-Gómez, A., Perretti, M. & Soehnlein, O. Resolution of inflammation: an integrated view. EMBO Molecular Medicine 5, 661–674 (2013).
26. Borregaard, N. & Cowland, J. B. Granules of the human neutrophilic polymorphonuclear leukocyte. Blood 89, 3503–3521 (1997).
27. Bainton, D. F. & Farquhar, M. G. ORIGIN OF GRANULES IN POLYMORPHONUCLEAR LEUKOCYTES : Two Types Derived from Opposite Faces of the Golgi Complex in Developing Granulocytes. Journal of Cell Biology 28, 277–301 (1966).
28. Bainton, D. F., Ullyot, J. L. & Farquhar, M. G. THE DEVELOPMENT OF NEUTROPHILIC POLYMORPHONUCLEAR LEUKOCYTES IN HUMAN BONE

MARROW : ORIGIN AND CONTENT OF AZUROPHIL AND SPECIFIC GRANULES. Journal of Experimental Medicine 134, 907–934 (1971).

29. BIOCHEMICAL AND MORPHOLOGICAL CHARACTERIZATION OF AZUROPHIL AND SPECIFIC GRANULES OF HUMAN NEUTROPHILIC POLYMORPHONUCLEAR LEUKOCYTES | Journal of Cell Biology | Rockefeller University Press. https://rupress.org/jcb/article/63/1/251/18461/BIOCHEMICAL-AND-MORPHOLOGICAL-CHARACTERIZATION-OF.
30. West, B. C., Rosenthal, A. S., Gelb, N. A. & Kimball, H. R. Separation and Characterization of Human Neutrophil Granules. Am J Pathol 77, 41–66 (1974).
31. Gallin, J. I. Neutrophil specific granules: a fuse that ignites the inflammatory response. Clin Res 32, 320–328 (1984).
32. Metchnikoff, E. Immunity in Infective Diseases. (University Press, 1905).
33. Hampton, M. B., Kettle, A. J. & Winterbourn, C. C. Inside the Neutrophil Phagosome: Oxidants, Myeloperoxidase, and Bacterial Killing. Blood 92, 3007–3017 (1998).
34. Huynh, K. K., Kay, J. G., Stow, J. L. & Grinstein, S. Fusion, Fission, and Secretion During Phagocytosis. Physiology 22, 366–372 (2007).
35. Jaumouillé, V. & Waterman, C. M. Physical Constraints and Forces Involved in Phagocytosis. Front Immunol 11, 1097 (2020).
36. Lacy, P. & Eitzen, G. Control of granule exocytosis in neutrophils. Front Biosci 13, 5559–5570 (2008).
37. Baggiolini, M. & Dewald, B. Exocytosis by Neutrophils. in Regulation of Leukocyte Function (ed. Snyderman, R.) 221–246 (Springer US, 1984). doi:10.1007/978-1-4757-4862-8_8.

38. Baggiolini, M. The enzymes of the granules of polymorphonuclear leukocytes and their functions. Enzyme 13, 132–160 (1972).
39. Takei, H., Araki, A., Watanabe, H., Ichinose, A. & Sendo, F. Rapid killing of human neutrophils by the potent activator phorbol 12-myristate 13-acetate (PMA) accompanied by changes different from typical apoptosis or necrosis. J Leukoc Biol 59, 229–240 (1996).
40. Brinkmann, V. et al. Neutrophil extracellular traps kill bacteria. Science 303, 1532–1535 (2004).
41. Steinberg, B. E. & Grinstein, S. Unconventional roles of the NADPH oxidase: signaling, ion homeostasis, and cell death. Sci STKE 2007, pe11 (2007).
42. Fuchs, T. A. et al. Novel cell death program leads to neutrophil extracellular traps. J Cell Biol 176, 231–241 (2007).
43. Sbarra, A. J. & Karnovsky, M. L. The biochemical basis of phagocytosis. I. Metabolic changes during the ingestion of particles by polymorphonuclear leukocytes. J Biol Chem 234, 1355–1362 (1959).
44. Iyer, G. Y. N., Islam, M. F. & Quastel, J. H. Biochemical Aspects of Phagocytosis. Nature 192, 535–41 (1961).
45. Segal, A. W. & Abo, A. The biochemical basis of the NADPH oxidase of phagocytes. Trends Biochem Sci 18, 43–47 (1993).
46. Babior, B. M., Kipnes, R. S. & Curnutte, J. T. Biological defense mechanisms. The production by leukocytes of superoxide, a potential bactericidal agent. J Clin Invest 52, 741–744 (1973).
47. Furtmüller, P. G., Burner, U. & Obinger, C. Reaction of Myeloperoxidase Compound I with Chloride, Bromide, Iodide, and Thiocyanate. Biochemistry 37, 17923–17930 (1998).

48. Chapman, A. L. P., Skaff, O., Senthilmohan, R., Kettle, A. J. & Davies, M. J. Hypobromous acid and bromamine production by neutrophils and modulation by superoxide. Biochem J 417, 773–781 (2009).
49. van Dalen, C. J., Whitehouse, M. W., Winterbourn, C. C. & Kettle, A. J. Thiocyanate and chloride as competing substrates for myeloperoxidase. Biochem J 327, 487–492 (1997).
50. Pan, G. J., Rayner, B. S., Zhang, Y., van Reyk, D. M. & Hawkins, C. L. A pivotal role for NF-κB in the macrophage inflammatory response to the myeloperoxidase oxidant hypothiocyanous acid. Arch Biochem Biophys 642, 23–30 (2018).
51. Guo, C., Davies, M. J. & Hawkins, C. L. Role of thiocyanate in the modulation of myeloperoxidase-derived oxidant induced damage to macrophages. Redox Biology 36, 101666 (2020).
52. Wang, J.-G. et al. The principal eosinophil peroxidase product, HOSCN, is a uniquely potent phagocyte oxidant inducer of endothelial cell tissue factor activity: a potential mechanism for thrombosis in eosinophilic inflammatory states. Blood 107, 558–565 (2006).
53. Wang, Y., Chuang, C. Y., Hawkins, C. L. & Davies, M. J. Activation and Inhibition of Human Matrix Metalloproteinase-9 (MMP9) by HOCl, Myeloperoxidase and Chloramines. Antioxidants 11, 1616 (2022).
54. Pi, J. et al. Activation of Nrf2-mediated oxidative stress response in macrophages by hypochlorous acid. Toxicology and Applied Pharmacology 226, 236–243 (2008).
55. Woods, C. G. et al. Dose-dependent transitions in Nrf2-mediated adaptive response and related stress responses to hypochlorous acid in mouse macrophages. Toxicology and Applied Pharmacology 238, 27–36 (2009).

56. Zhu, L. et al. Identification of Nrf2-dependent airway epithelial adaptive response to proinflammatory oxidant-hypochlorous acid challenge by transcription profiling. Am J Physiol Lung Cell Mol Physiol 294, L469-477 (2008).
57. Lane, A. E., Tan, J. T. M., Hawkins, C. L., Heather, A. K. & Davies, M. J. The myeloperoxidase-derived oxidant HOSCN inhibits protein tyrosine phosphatases and modulates cell signalling via the mitogen-activated protein kinase (MAPK) pathway in macrophages. Biochem J 430, 161–169 (2010).
58. Liu, T. W., Gammon, S. T., Yang, P., Fuentes, D. & Piwnica-Worms, D. Myeloid cell-derived HOCl is a paracrine effector that trans-inhibits IKK/NF-κB in melanoma cells and limits early tumor progression. Sci Signal 14, eaax5971 (2021).
59. A, U. & Li, L. The effects of neutrophil-generated hypochlorous acid and other hypohalous acids on host and pathogens. Cellular and molecular life sciences : CMLS 78, (2021).
60. Nauseef, W. M. Myeloperoxidase in human neutrophil host defence. Cell Microbiol 16, 1146–1155 (2014).
61. Chandler, J. D. et al. Antiinflammatory and Antimicrobial Effects of Thiocyanate in a Cystic Fibrosis Mouse Model. Am J Respir Cell Mol Biol 53, 193–205 (2015).
62. Chandler, J. D. & Day, B. J. Thiocyanate: a potentially useful therapeutic agent with host defense and antioxidant properties. Biochem Pharmacol 84, 1381–1387 (2012).
63. Day, B. J. The science of licking your wounds: Function of oxidants in the innate immune system. Biochemical Pharmacology 163, 451–457 (2019).
64. Palau, M. et al. In Vitro and In Vivo Antimicrobial Activity of Hypochlorous Acid against Drug-Resistant and Biofilm-Producing Strains. Microbiology Spectrum 10, e02365-22 (2022).

65. Tsai, S.-Y., Liu, Y.-M., Lin, Z.-W. & Lin, C.-P. Antimicrobial activity effects of electrolytically generated hypochlorous acid-treated pathogenic microorganisms by isothermal kinetic simulation. J Therm Anal Calorim 148, 1613–1627 (2023).
66. Hatanaka, N., Yasugi, M., Sato, T., Mukamoto, M. & Yamasaki, S. Hypochlorous acid solution is a potent antiviral agent against SARS-CoV-2. J Appl Microbiol 132, 1496–1502 (2022).
67. Hyslop, P. A. et al. Hydrogen peroxide as a potent bacteriostatic antibiotic: implications for host defense. Free Radic Biol Med 19, 31–37 (1995).
68. Klebanoff, S. J. Role of the superoxide anion in the myeloperoxidase-mediated antimicrobial system. J Biol Chem 249, 3724–3728 (1974).
69. Babior, B. M., Curnutte, J. T. & Kipnes, R. S. Biological defense mechanisms. Evidence for the participation of superoxide in bacterial killing by xanthine oxidase. J Lab Clin Med 85, 235–244 (1975).
70. Rosen, H. & Klebanoff, S. J. Bactericidal activity of a superoxide anion-generating system. A model for the polymorphonuclear leukocyte. J Exp Med 149, 27–39 (1979).
71. Kettle, A. J. et al. Myeloperoxidase and Protein Oxidation in the Airways of Young Children with Cystic Fibrosis. Am J Respir Crit Care Med 170, 1317–1323 (2004).
72. Sagel, S. D., Chmiel, J. F. & Konstan, M. W. Sputum Biomarkers of Inflammation in Cystic Fibrosis Lung Disease. Proc Am Thorac Soc 4, 406–417 (2007).
73. Vasu, V. T. et al. Evaluation of thiol-based antioxidant therapeutics in cystic fibrosis sputum: Focus on myeloperoxidase. Free Radical Research 45, 165–176 (2011).

74. Forrest, O. A. et al. PATHOLOGICAL CONDITIONING OF HUMAN NEUTROPHILS RECRUITED TO THE AIRWAY MILIEU IN CYSTIC FIBROSIS. J Leukoc Biol 104, 665–675 (2018).
75. Mitchell, T. C. A GRIM fate for human neutrophils in airway disease. J Leukoc Biol 104, 657–659 (2018).
76. Giacalone, V. D., Margaroli, C., Mall, M. A. & Tirouvanziam, R. Neutrophil Adaptations upon Recruitment to the Lung: New Concepts and Implications for Homeostasis and Disease. International Journal of Molecular Sciences 21, 851 (2020).
77. Margaroli, C. et al. Macrophage PD-1 associates with neutrophilia and reduced bacterial killing in early cystic fibrosis airway disease. J Cyst Fibros 21, 967–976 (2022).
78. Dickerhof, N., Isles, V., Pattemore, P., Hampton, M. B. & Kettle, A. J. Exposure of Pseudomonas aeruginosa to bactericidal hypochlorous acid during neutrophil phagocytosis is compromised in cystic fibrosis. J Biol Chem 294, 13502–13514 (2019).
79. Jennings, S. et al. Neutrophil defect and lung pathogen selection in cystic fibrosis. Journal of Leukocyte Biology 113, 604–614 (2023).
80. Bonvillain, R. W., Painter, R. G., Ledet, E. M. & Wang, G. Comparisons of resistance of CF and Non-CF pathogens to Hydrogen Peroxide and Hypochlorous Acid Oxidants In Vitro. BMC Microbiology 11, 112 (2011).
81. Butler, A., Walton, G. M. & Sapey, E. Neutrophilic Inflammation in the Pathogenesis of Chronic Obstructive Pulmonary Disease. COPD: Journal of Chronic Obstructive Pulmonary Disease 15, 392–404 (2018).

82. Yang, X., Li, H., Ma, Q., Zhang, Q. & Wang, C. Neutrophilic Asthma Is Associated with Increased Airway Bacterial Burden and Disordered Community Composition. Biomed Res Int 2018, 9230234 (2018).
83. Schultz, J. & Kaminker, K. Myeloperoxidase of the leucocyte of normal human blood. I. Content and localization. Archives of Biochemistry and Biophysics 96, 465–467 (1962).
84. Nauseef, W. M. How human neutrophils kill and degrade microbes: an integrated view. Immunological Reviews 219, 88–102 (2007).
85. Nakagawara, A., Nathan, C. F. & Cohn, Z. A. Hydrogen peroxide metabolism in human monocytes during differentiation in vitro. J Clin Invest 68, 1243–1252 (1981).
86. Locksley, R. M., Nelson, C. S., Fankhauser, J. E. & Klebanoff, S. J. Loss of granule myeloperoxidase during in vitro culture of human monocytes correlates with decay in antiprotozoa activity. Am J Trop Med Hyg 36, 541–548 (1987).
87. Amanzada, A. et al. Myeloperoxidase and elastase are only expressed by neutrophils in normal and in inflamed liver. Histochem Cell Biol 135, 305–315 (2011).
88. Brown, K. E., Brunt, E. M. & Heinecke, J. W. Immunohistochemical detection of myeloperoxidase and its oxidation products in Kupffer cells of human liver. Am J Pathol 159, 2081–2088 (2001).
89. McMillen, T. S., Heinecke, J. W. & LeBoeuf, R. C. Expression of human myeloperoxidase by macrophages promotes atherosclerosis in mice. Circulation 111, 2798–2804 (2005).
90. K, A. Verdoperoxidase : a ferment isolated from leucocytes. Acta Physiol. Scand. 2, 1–64 (1941).

91. Zamocky, M., Jakopitsch, C., Furtmüller, P. G., Dunand, C. & Obinger, C. The peroxidase–cyclooxygenase superfamily: Reconstructed evolution of critical enzymes of the innate immune system. Proteins: Structure, Function, and Bioinformatics 72, 589–605 (2008).
92. Davies, M. J. & Hawkins, C. L. The Role of Myeloperoxidase in Biomolecule Modification, Chronic Inflammation, and Disease. Antioxid Redox Signal 32, 957–981 (2020).
93. Grishkovskaya, I. et al. Structure of human promyeloperoxidase (proMPO) and the role of the propeptide in processing and maturation. J Biol Chem 292, 8244–8261 (2017).
94. Fiedler, T. J., Davey, C. A. & Fenna, R. E. X-ray crystal structure and characterization of halide-binding sites of human myeloperoxidase at 1.8 A resolution. J Biol Chem 275, 11964–11971 (2000).
95. Battistuzzi, G. et al. Influence of the covalent heme-protein bonds on the redox thermodynamics of human myeloperoxidase. Biochemistry 50, 7987–7994 (2011).
96. Blair-Johnson, M., Fiedler, T. & Fenna, R. Human myeloperoxidase: structure of a cyanide complex and its interaction with bromide and thiocyanate substrates at 1.9 A resolution. Biochemistry 40, 13990–13997 (2001).
97. Carpena, X. et al. Essential role of proximal histidine-asparagine interaction in mammalian peroxidases. J Biol Chem 284, 25929–25937 (2009).
98. Arnhold, J. et al. Kinetics and Thermodynamics of Halide and Nitrite Oxidation by Mammalian Heme Peroxidases. European Journal of Inorganic Chemistry 2006, 3801–3811 (2006).
99. van Dalen, C. J. & Kettle, A. J. Substrates and products of eosinophil peroxidase. Biochem J 358, 233–239 (2001).

100. Furtmüller, P. G., Arnhold, J., Jantschko, W., Pichler, H. & Obinger, C. Redox properties of the couples compound I/compound II and compound II/native enzyme of human myeloperoxidase. Biochem Biophys Res Commun 301, 551–557 (2003).
101. Heme to protein linkages in mammalian peroxidases: impact on spectroscopic, redox and catalytic properties - Natural Product Reports (RSC Publishing). https://pubs.rsc.org/en/content/articlelanding/2007/NP/B604178G.
102. Hartmann, F. The Life of Philippus Theophrastus Bombast of Hohenheim, Known by the Name of Paracelsus: And the Substance of His Teachings Concerning Cosmology, Anthropology, Pneumatology, Magic and Sorcery, Medicine, Alchemy and Astrology, Philosophy and Theosophy. (Theosophical Publishing Company, 1896).
103. Dumas, A. & Knaus, U. G. Raising the 'Good' Oxidants for Immune Protection. Frontiers in Immunology 12, (2021).
104. Hawkins, C. L. The role of hypothiocyanous acid (HOSCN) in biological systems. Free Radical Research 43, 1147–1158 (2009).
105. Klebanoff, S. J. Myeloperoxidase: friend and foe. Journal of Leukocyte Biology 77, 598–625 (2005).
106. Love, D. T. et al. Cellular targets of the myeloperoxidase-derived oxidant hypothiocyanous acid (HOSCN) and its role in the inhibition of glycolysis in macrophages. Free Radic Biol Med 94, 88–98 (2016).
107. Forrester, S. J., Kikuchi, D. S., Hernandes, M. S., Xu, Q. & Griendling, K. K. Reactive Oxygen Species in Metabolic and Inflammatory Signaling. Circulation Research 122, 877–902 (2018).

108. Foote, C. S., Goyne, T. E. & Lehrer, R. I. Assessment of chlorination by human neutrophils. Nature 301, 715–716 (1983).

109. Jiang, Q., Griffin, D. A., Barofsky, D. F. & Hurst, J. K. Intraphagosomal Chlorination Dynamics and Yields Determined Using Unique Fluorescent Bacterial Mimics. Chem. Res. Toxicol. 10, 1080–1089 (1997).

110. Jayaraman, S., Song, Y., Vetrivel, L., Shankar, L. & Verkman, A. S. Noninvasive in vivo fluorescence measurement of airway-surface liquid depth, salt concentration, and pH. J Clin Invest 107, 317–324 (2001).

111. Colon, S., Page-McCaw, P. & Bhave, G. Role of Hypohalous Acids in Basement Membrane Homeostasis. Antioxid Redox Signal 27, 839–854 (2017).

112. Thomson, E. et al. Identifying peroxidases and their oxidants in the early pathology of cystic fibrosis. Free Radical Biology and Medicine 49, 1354–1360 (2010).

113. Wijkstrom-Frei, C. et al. Lactoperoxidase and human airway host defense. Am J Respir Cell Mol Biol 29, 206–212 (2003).

114. Thomas, E. L., Grisham, M. B. & Jefferson, M. M. Myeloperoxidase-dependent effect of amines on functions of isolated neutrophils. J Clin Invest 72, 441–454 (1983).

115. Weiss, S. J., Klein, R., Slivka, A. & Wei, M. Chlorination of Taurine by Human Neutrophils: EVIDENCE FOR HYPOCHLOROUS ACID GENERATION. https://www.jci.org/articles/view/110652/pdf (1982) doi:10.1172/JCI110652.

116. Pattison, D. I. & Davies, M. J. Absolute Rate Constants for the Reaction of Hypochlorous Acid with Protein Side Chains and Peptide Bonds. Chem. Res. Toxicol. 14, 1453–1464 (2001).

117. Pattison, D. I., Davies, M. J. & Hawkins, C. L. Reactions and reactivity of myeloperoxidase-derived oxidants: differential biological effects of hypochlorous and hypothiocyanous acids. Free Radic Res 46, 975–995 (2012).
118. Pattison, D. I. & Davies, M. J. Reactions of myeloperoxidase-derived oxidants with biological substrates: gaining chemical insight into human inflammatory diseases. Curr Med Chem 13, 3271–3290 (2006).
119. Storkey, C., Davies, M. J. & Pattison, D. I. Reevaluation of the rate constants for the reaction of hypochlorous acid (HOCl) with cysteine, methionine, and peptide derivatives using a new competition kinetic approach. Free Radic Biol Med 73, 60–66 (2014).
120. Pattison, D. I. & Davies, M. J. Kinetic Analysis of the Reactions of Hypobromous Acid with Protein Components: Implications for Cellular Damage and Use of 3-Bromotyrosine as a Marker of Oxidative Stress. Biochemistry 43, 4799–4809 (2004).
121. Skaff, O., Pattison, D. I. & Davies, M. J. Hypothiocyanous acid reactivity with low-molecular-mass and protein thiols: absolute rate constants and assessment of biological relevance. Biochem J 422, 111–117 (2009).
122. Skaff, O. et al. Selenium-containing amino acids are targets for myeloperoxidase-derived hypothiocyanous acid: determination of absolute rate constants and implications for biological damage. Biochem J 441, 305–316 (2012).
123. Chandler, J. D. Global Profiling of Cell Responses to (Pseudo)Hypohalous Acids. in Mammalian Heme Peroxidases (CRC Press, 2021).
124. Winterbourn, C. C. & Hampton, M. B. Thiol chemistry and specificity in redox signaling. Free Radic Biol Med 45, 549–561 (2008).

125. Nicholls, S. J. & Hazen, S. L. Myeloperoxidase and Cardiovascular Disease. Arteriosclerosis, Thrombosis, and Vascular Biology 25, 1102–1111 (2005).

126. Barrett, T. J. & Hawkins, C. L. Hypothiocyanous Acid: Benign or Deadly? Chem. Res. Toxicol. 25, 263–273 (2012).

127. Yue, B. Biology of the Extracellular Matrix: An Overview. J Glaucoma S20–S23 (2014) doi:10.1097/IJG.0000000000000108.

128. Hawkins, C. L. & Davies, M. J. Role of myeloperoxidase and oxidant formation in the extracellular environment in inflammation-induced tissue damage. Free Radic Biol Med 172, 633–651 (2021).

129. Chandler, J. D., Nichols, D. P., Nick, J. A., Hondal, R. J. & Day, B. J. Selective Metabolism of Hypothiocyanous Acid by Mammalian Thioredoxin Reductase Promotes Lung Innate Immunity and Antioxidant Defense. Journal of Biological Chemistry 288, 18421–18428 (2013).

130. McCall, A. S. et al. Bromine is an essential trace element for assembly of collagen IV scaffolds in tissue development and architecture. Cell 157, 1380–1392 (2014).

131. Cook, N. L., Moeke, C. H., Fantoni, L. I., Pattison, D. I. & Davies, M. J. The myeloperoxidase-derived oxidant hypothiocyanous acid inhibits protein tyrosine phosphatases via oxidation of key cysteine residues. Free Radic Biol Med 90, 195–205 (2016).

132. Barrett, T. J. et al. Inactivation of thiol-dependent enzymes by hypothiocyanous acid: role of sulfenyl thiocyanate and sulfenic acid intermediates. Free Radic Biol Med 52, 1075–1085 (2012).

133. Mullarky, E. & Cantley, L. C. Diverting Glycolysis to Combat Oxidative Stress. in Innovative Medicine: Basic Research and Development (eds. Nakao, K., Minato, N. & Uemoto, S.) (Springer, 2015).
134. Love, D. T. et al. The role of the myeloperoxidase-derived oxidant hypothiocyanous acid (HOSCN) in the induction of mitochondrial dysfunction in macrophages. Redox Biology 36, 101602 (2020).
135. Sihvola, V. & Levonen, A.-L. Keap1 as the redox sensor of the antioxidant response. Arch Biochem Biophys 617, 94–100 (2017).
136. Taguchi, K., Motohashi, H. & Yamamoto, M. Molecular mechanisms of the Keap1–Nrf2 pathway in stress response and cancer evolution. Genes to Cells 16, 123–140 (2011).
137. Tonelli, C., Chio, I. I. C. & Tuveson, D. A. Transcriptional Regulation by Nrf2. Antioxidants & Redox Signaling 29, 1727–1745 (2018).
138. Cargnello, M. & Roux, P. P. Activation and Function of the MAPKs and Their Substrates, the MAPK-Activated Protein Kinases. Microbiol Mol Biol Rev 75, 50–83 (2011).
139. Hampton, L., Postiglione, A., Keyes, J., Poole, L. B. & Newman, R. H. Impact of Redox Modification on MAPK Global Substrate Selection. The FASEB Journal 34, 1–1 (2020).
140. Schuliga, M. NF-kappaB Signaling in Chronic Inflammatory Airway Disease. Biomolecules 5, 1266–1283 (2015).
141. Liu, T., Zhang, L., Joo, D. & Sun, S.-C. NF-κB signaling in inflammation. Sig Transduct Target Ther 2, 1–9 (2017).
142. Barnabei, L., Laplantine, E., Mbongo, W., Rieux-Laucat, F. & Weil, R. NF-κB: At the Borders of Autoimmunity and Inflammation. Front Immunol 12, 716469 (2021).

143. Flohé, L., Brigelius-Flohé, R., Saliou, C., Traber, M. G. & Packer, L. Redox Regulation of NF-kappa B Activation. Free Radical Biology and Medicine 22, 1115–1126 (1997).

144. Morgan, M. J. & Liu, Z. Crosstalk of reactive oxygen species and NF-κB signaling. Cell Res 21, 103–115 (2011).

145. Chandler, J. D., Min, E., Huang, J., Nichols, D. P. & Day, B. J. Nebulized thiocyanate improves lung infection outcomes in mice: Thiocyanate improves lung infection outcomes. Br J Pharmacol 169, 1166–1177 (2013).

146. Hall, L. et al. Oral pre-treatment with thiocyanate (SCN−) protects against myocardial ischaemia–reperfusion injury in rats. Sci Rep 11, 12712 (2021).

147. Ashby, M. T., Carlson, A. C. & Scott, M. J. Redox Buffering of Hypochlorous Acid by Thiocyanate in Physiologic Fluids. J. Am. Chem. Soc. 126, 15976–15977 (2004).

148. Chandler, J. D. & Day, B. J. Biochemical mechanisms and therapeutic potential of pseudohalide thiocyanate in human health. Free Radic Res 49, 695–710 (2015).

149. San Gabriel, P. T., Liu, Y., Schroder, A. L., Zoellner, H. & Chami, B. The Role of Thiocyanate in Modulating Myeloperoxidase Activity during Disease. Int J Mol Sci 21, 6450 (2020).

150. Xu, Y., Szép, S. & Lu, Z. The antioxidant role of thiocyanate in the pathogenesis of cystic fibrosis and other inflammation-related diseases. Proc Natl Acad Sci U S A 106, 20515–20519 (2009).

151. Gould, N. S. et al. Hypertonic saline increases lung epithelial lining fluid glutathione and thiocyanate: two protective CFTR-dependent thiols against oxidative injury. Respir Res 11, 119 (2010).

152. Moskwa, P. et al. A Novel Host Defense System of Airways Is Defective in Cystic Fibrosis. Am J Respir Crit Care Med 175, 174–183 (2007).
153. Types of CFTR Mutations | Cystic Fibrosis Foundation. https://www.cff.org/research-clinical-trials/types-cftr-mutations.

Chapter 2

Substrate-dependent metabolomic signatures of myeloperoxidase activity in airway epithelial cells: implications for early cystic fibrosis lung disease

Kim SO, Shapiro JP, Cottrill KA, Collins GL, Shanthikumar S, Rao P, Ranganathan S, Stick SM, Orr ML, Fitzpatrick AM, Go Y, Jones DP, Tirouvanziam RM, Chandler JD

Sections of this chapter have been published as an original research article in

Free Radical Biology and Medicine

2.1 Abstract

Myeloperoxidase (MPO) is released by neutrophils in inflamed tissues. MPO oxidizes chloride, bromide, and thiocyanate to produce hypochlorous acid (HOCl), hypobromous acid (HOBr), and hypothiocyanous acid (HOSCN), respectively. These oxidants are toxic to pathogens but may also react with host cells to elicit biological activity and potential toxicity. In cystic fibrosis (CF) and related diseases, increased neutrophil inflammation leads to increased airway MPO and airway epithelial cell (AEC) exposure to its oxidants. In this study, we investigated how equal dose-rate exposures of MPO-derived oxidants differentially impact the metabolome of human AECs (BEAS-2B cells). We utilized enzymatic oxidant production with rate-limiting glucose oxidase (GOX) coupled to MPO, and chloride, bromide (Br^-), or thiocyanate (SCN^-) as substrates. AECs exposed to GOX/MPO/SCN^- (favoring HOSCN) were viable after 24 h, while exposure to GOX/MPO (favoring HOCl) or GOX/MPO/Br^- (favoring HOBr) developed cytotoxicity after 6 h. Cell glutathione and peroxiredoxin-3 oxidation were insufficient to explain these differences. However, untargeted metabolomics revealed GOX/MPO and GOX/MPO/Br^- diverged significantly from GOX/MPO/SCN^- for dozens of metabolites. We noted methionine sulfoxide and dehydromethionine were significantly increased in GOX/MPO- or GOX/MPO/Br^--treated cells and analyzed them as potential biomarkers of lung damage in bronchoalveolar lavage fluid from 5-year-olds with CF (n=27). Both metabolites were associated with increasing bronchiectasis, neutrophils, and MPO activity. This suggests MPO production of HOCl and/or HOBr may contribute to inflammatory lung damage in early CF. In summary, our *in vitro* model enabled unbiased identification of exposure-specific metabolite products which may serve as biomarkers of lung damage *in vivo*. Continued research with this exposure model

may yield additional oxidant-specific biomarkers and reveal explicit mechanisms of oxidant byproduct formation and cellular redox signaling.

2.2 Introduction

Chronic inflammatory lung diseases, such as acquired chronic obstructive pulmonary disease (COPD) and inherited cystic fibrosis (CF), collectively affect millions of people worldwide [1,2]. A common feature of these diseases is an increased burden of airway leukocytes, contributing to airway obstruction and remodeling, with neutrophils comprising the majority of infiltrating cells [3–6]. Neutrophils kill pathogens at sites of infection by secretion of proteases and generation of a range of reactive oxygen species (ROS) [7–9]. ROS generated by neutrophils during inflammation also react with host tissue, and may result in adaptive responses and/or oxidative tissue injury, which has been reported for several chronic inflammatory diseases [3,4,10–12]. However, because different oxidants are concomitantly produced in the inflamed environment and can have overlapping reactivities with many compounds, it is difficult to predict the effects of oxidant production in the complex milieu of small molecules and macromolecules present *in vivo*.

Neutrophils express large amounts of myeloperoxidase (MPO), an enzyme packaged inside their primary granules during bone marrow development [13]. MPO secreted into the lumen of phagosomes or into the extracellular environment reduces hydrogen peroxide (H_2O_2) and oxidizes chloride (Cl^-), bromide (Br^-), or thiocyanate (SCN^-) to generate hypochlorous acid (HOCl), hypobromous acid (HOBr), and hypothiocyanous acid (HOSCN), respectively (collectively referred to as [pseudo]hypohalous acids [HOX]) [14–16]. Under physiological conditions, MPO is the only mammalian enzyme capable of oxidizing Cl^- to HOCl, which has the greatest reduction potential among HOX [17,18]. However, substrate availability is critical to determine which oxidants are generated by MPO [16,19–21]. HOX are important for anti-microbial activity, but also react with biological targets important for normal functioning of host tissue

[10,22–29]. HOCl and HOBr oxidize macromolecules including thiols, amino groups, and lipids, generating irreversible oxidation products in several cases [29–31]. HOSCN is less reactive, preferentially oxidizing thiols and selenols to form reversible products that are repaired by antioxidant systems [32,33], although HOSCN was also shown to irreversibly oxidize cysteine in reactions with isolated enzymes [34]. A growing list of enzymes in eukaryotes and bacteria are efficient HOSCN reductases, including mammalian thioredoxin reductase and the proteins encoded by har and rcla genes in S. pneumoniae and E. coli [35–37]. Because it selectively targets thiols and selenols, HOSCN can initiate redox signaling mediated by sensitive cysteine- and selenocysteine-containing protein targets [34,35,38,39]. Conversely, because HOCl and HOBr also readily oxidize amino acids and lipids not targeted by HOSCN, they have the potential to elicit different cellular responses [29,40–45].

The concept that differences in HOX reactivity may impact lung health outcomes in airways is supported by numerous studies. For example, CF patients who have increased nasal lining fluid SCN^- have increased lung function [46]. Furthermore, mice treated with SCN^- have lower airway inflammation and increases clearance of P. aeruginosa infection [47,48], and mice infected with a lethal dose of influenza virus and treated with HOSCN have increased survival and decreased morbidity [49]. Conversely, products of HOCl/HOBr but not HOSCN, such as glutathione sulfonamide (GSA) and methionine sulfoxide, have been repeatedly associated with worse lung health in patients with CF [10,50–52].

As airway epithelial cells (AECs) are exposed to HOX during inflammation, a holistic understanding of the metabolomic effects of HOX on these cells may help elucidate underlying pathways that regulate health and disease. To discern the effects of HOX on AECs in a complex chemical environment, comparable to airway fluid, we employed an *in vitro* enzymatic model of

MPO-derived oxidant exposure using noncancerous immortalized human bronchoepithelial cells (BEAS-2B cell line). The culture medium contains chloride so the addition of glucose oxidase (GOX) and MPO produces HOCl. To favor generation of HOBr or HOSCN, we added Br^- or SCN^-, respectively. We evaluated the impact of GOX/MPO and various substrates or GOX alone (H_2O_2 control) on cytotoxicity, thiol-disulfide redox state, and cellular metabolomics. Here, we demonstrate that conditions favoring formation of specific HOX had distinct effects on BEAS-2B cell cytotoxicity and metabolomics, while their effects on low molecular weight thiol-disulfide systems were largely indistinguishable. Notably, the identification of methionine oxidation products specific to GOX/MPO and GOX/MPO/Br^- exposures *in vitro* were associated with *in vivo* evidence of bronchiectasis in 5-year-old children with cystic fibrosis, supporting the hypothesis that increased chloride or bromide utilization by MPO in CF patient airways is associated with lung disease.

2.3 Methods & materials

Culture of BEAS-2B cells

BEAS-2B cells (CRL-9609), SV40-immortalized from human non-cancerous bronchoepithelial cells, were obtained from American Type Culture Collection (Manassas, VA). Cells were maintained in RPMI-1640 medium (Invitrogen) supplemented with 10% (v/v) heat inactivated fetal bovine serum (FBS, MilliporeSigma), 100 IU/ml penicillin (Corning), and 100 µg/mL streptomycin (Corning) in a humidified incubator held at 37 ˚C and 5% CO_2. Cells were seeded in 12-well plates (1 ml working volume) or 6 cm dishes (3 ml working volume) at a density of 50,000 cells per cm^2 of culture vessel growth surface area. Experiments were conducted approximately 24 h after seeding.

HOX exposure model

Prior to oxidant exposure, cells were gently washed once with PBS warmed to 37 ˚C. Growth medium was replaced with oxidant exposure medium comprised of Medium-199 (Gibco) supplemented with 100 pg/ml recombinant human epidermal growth factor (MilliporeSigma) and 0.1% FBS, which was needed to maintain cell viability during prolonged low-serum exposure. Depending on experimental conditions, various combinations of GOX (MilliporeSigma G7141) from A. niger, 200 mU/ml MPO isolated from human neutrophils (MilliporeSigma 475911), and 1 mM of either Br^- or SCN^- were added. Medium-199 contains 116 mM of NaCl which was the primary source of chloride for HOCl production. GOX was added at final 2.5 mU/ml concentration, or 2 mU/ml in a subset of experiments (low molecular weight thiol and peroxiredoxin-3 redox assays) with a GOX formulation (MilliporeSigma G0543) that exhibited higher specific activity (calibrated to the same H_2O_2 production rate as other experiments using Amplex Red). MPO was in catalytic excess so that GOX activity was

rate-limiting, standardizing oxidant production rates across conditions. Medium was supplemented with 0.1 g/l additional glucose (final 1.1 g/l) to replace the majority consumed by GOX over a 24 h exposure period. In the absence of Br^- or SCN^-, medium Cl^- was anticipated to be the major substrate for MPO.

Human subjects

Bronchoalveolar lavage (BAL) fluid samples from clinically stable 5-year-olds with CF came from participants in the Australian Respiratory Early Surveillance Team for Cystic Fibrosis (AREST CF) cohort (Human Research Ethics Committee Approval Number 25054). The AREST CF cohort has been previously described [11], with participants undergoing serial assessment of lung health by chest computed tomography (CT) scans and BAL as part of clinical surveillance and care. The main outcome of the chest CT scan is bronchiectasis, which represents altered lung structure resulting in scarring and poorer future health outcomes [53–56].

Measurement of H_2O_2 production

The production of H_2O_2 by GOX was calibrated fluorometrically using Amplex Red (Invitrogen A12222). GOX was dissolved in pre-warmed (37 ˚C) Hank's balanced salt solution and placed in humidified atmosphere at 37 ˚C with 5% CO_2. At specified times, aliquots were filtered using 10 kDa Amicon Ultra filters (Millipore) to remove GOX, then diluted with 50 mM sodium phosphate, pH 7.4. Fifty µl of samples or standards of reagent H_2O_2 (MilliporeSigma) in sodium phosphate were pipetted into black-walled 96-well plates and mixed with 50 µl of assay buffer containing 50 mM sodium phosphate buffer, pH 7.4, 100 µM Amplex Red, and 0.2 U/ml horseradish peroxidase. Fluorescent resorufin product was measured at λ_{ex} 544 nm / λ_{em} 590 nm on a SpectraMax iD3 (Molecular Devices).

Cytotoxicity of HOX

Lactate dehydrogenase (LDH) activity in the media was used as an indication of cell death, owing to loss of cell membrane integrity. LDH activity was measured spectrophotometrically according to the rate of NADH oxidation at A_{340}, as previously described [35]. Total LDH activity was defined as the sum of intracellular and extracellular LDH activity. LDH release was expressed as the percentage of LDH in the extracellular medium compared to total LDH activity. Control experiments used recombinant human LDHA (MilliporeSigma SAE0049).

Glutathione and cysteine redox

Glutathione (GSH), glutathione disulfide (GSSG), cysteine (Cys), and cystine (CySS) were analyzed as previously described [57]. Briefly, cells were gently washed with ice-cold PBS. Thiol-disulfide couples were extracted with a mixture of 10% perchloric acid, 0.2 M boric acid, and 10 µM γ-glutamylglutamate internal standard, and protein isolated by centrifugation at 14,000 g for 2 min. The extract was mixed with iodoacetic acid and pH adjusted to 9.0. Then, samples were derivatized with dansyl chloride in acetone and extracted by addition of chloroform. Samples were analyzed via high-performance liquid chromatography (HPLC) coupled to fluorescence detection, with concentrations determined by comparison to γ-glutamylglutamate. Results were normalized to protein concentration as determined by bicinchoninic acid (BCA) assay (ThermoFisher). Intracellular results normalized to nmol/mg protein were converted to mM by assuming that intracellular protein concentration was consistently 0.2 g/ml [58].

Peroxiredoxin redox western blot

Cells were washed with PBS and treated with N-ethylmaleimide to react with protein thiols as previously described [59]. 20 µg of protein was separated by SDS-PAGE using a 10% 1.5

M Tris pH 8.8 gel with a 1 cm 4% 0.5 M Tris pH 6.8 stacking gel at 100 V for 10 min and 120 V for 70 min. Proteins were transferred onto a PVDF membrane at 100 V for 60 min. Membranes were blocked with 50% PBS-T and 50% Odyssey PBS blocking buffer (Li-Cor) for 1 h at room temperature, then incubated with anti-peroxiredoxin 3 (Prx3, Abcam ab16751) overnight at 4 ˚C. Membranes were washed three times with PBS-T and incubated with IRDye 680RD goat anti-mouse IgG for 1 h at room temperature and washed three times prior to imaging. Band densities of low molecular weight Prx3 monomer and high molecular weight Prx3 dimer were quantified in ImageJ [60].

Metabolomics

Metabolites were extracted from cells as previously described, with modifications [61]. Cells grown in 60 mm dishes were washed once with 1X PBS before being scraped into 250 µl of 2:2:1 acetonitrile:methanol:water + 0.1 M formic acid. A second 250 µl was added and pooled with the first to maximize recovery. Formic acid was neutralized by 45 µl of 15% ammonium bicarbonate, and the samples were incubated at -20 ˚C for 30 min. Then samples were centrifuged at 20,000 g and 4 ˚C for 10 min. Supernatants and pellets were stored at -80 ˚C. Pellets were later redissolved at 45 ˚C in 100 mM Tris-buffered saline (pH 7.5) with 1% sodium dodecyl sulfate to assay for total protein (BCA method), confirming comparable yields per sample. A small, equal volume of each sample was pooled to make a global quality control sample and experimental group-specific quality controls.

Metabolites were extracted from 50 µl of clinical BAL fluid by 1:1:1 mixture with acetonitrile and methanol, vortexed for 5 sec, incubated on ice for 30 min followed by centrifugation at 20,000 g and 4 ˚C for 10 min. One-hundred µl of supernatant were transferred

into a new tube and stored at -80˚C. A small, equal volume of each sample was pooled with all others to make a global quality control sample.

Data acquisition was conducted using a Vanquish^{TM} Horizon Binary ultrahigh performance liquid chromatography system coupled to a Q Exactive High Field Hybrid Orbitrap mass spectrometer (ThermoFisher). Two-and-a-half µl of extract (standardized to be equivalent to 125 ng of protein, in the case of cell extracts) was injected for liquid chromatography with a 5 µm, 2.1 x 150 mm iHILIC-(P) Classic column (HILICON) pumped at 0.2 ml/min and 40 ˚C with a 15-minute gradient of water containing 15 mM ammonium acetate, pH 9.4 (mobile phase A) or acetonitrile (mobile phase B). The gradient began at 10% A and progressed to 90% A, followed by a 2-minute hold and 8-minute re-equilibration of the column at 10% A. Column eluate was introduced to a heated electrospray ionization source held at 320 ˚C and +3.5 or -2.75 kV for positive and negative ionization modes, respectively, and an ion capillary temperature of 275 ˚C. The automatic gain control (AGC) was set to $1x10^6$ ions with a maximum injection time of 200 ms. Scan range was 67-1000 m/z and Orbitrap resolution was 120,000 full width at half maximum. For data-dependent acquisition of ions for MS^2 identification, we used Top20N with dynamic exclusion of 8.0 sec, AGC of $1x10^5$, and maximum injection time of 25 ms. The data acquisition sequence was randomized before injection and a global quality control was injected every 10 samples to determine measurement reproducibility. Data was analyzed using Compound Discoverer 3.3 and FreeStyle 1.7 (Thermo Fisher Scientific). mzCloud (mzcloud.org) and LipidSearch (ThermoFisher) were used for MS/MS identifications.

Statistical analysis and data visualization

For the LDH assay and redox assays, one-way ANOVA was performed in R version 2.12.0. Statistical analyses for the metabolomic data were conducted using log-transformed peak

areas for univariate analyses (ANOVA with Tukey's post-test, comparing more than two groups, or t-test, comparing only two groups) and auto-scaled peak areas for multivariate analyses (principal component analysis [PCA], and partial least squares-discriminant analysis [PLS-DA]) in MetaboAnalyst (metaboanalyst.ca) [62]. Significance was set as $p<0.05$ and false discovery rate (applied to metabolomics data) <5%. Peak area heatmaps were z-scored per metabolite, and a hierarchical clustering analysis was performed using Euclidean distance and Ward clustering algorithm. For PLS-DA, the optimal number of components was selected according to the highest Q^2 value. The 3D scores plot was generated using the Scatter function and the heatmaps were generated using the Clustermap function from the Seaborn Python package. MetaboAnalyst was employed for pathway analyses of high confidence metabolite annotations. A global test enrichment method and relative-betweenness centrality topology analysis were used in the pathway analyses and pathways were chosen from the KEGG database for Homo sapiens [63–65]. Spearman correlation analysis were performed using SciPy stats in Python.

2.4 Results

HOX cytotoxicity and redox effects on AECs

We utilized a HOX exposure model relying on rate-limiting H_2O_2 generation, via GOX and glucose, and excess MPO (when applicable) to create equal dose-rate exposures to specific oxidants. We selected a dose of 2.5 mU/ml GOX, which linearly produced 27.8 μM H_2O_2 per h (n=2) (**Figure 2.1**). Rate of H_2O_2 production by GOX was linear for at least 4 h. This approach phenocopies H_2O_2 production through oxidase enzymes such as neutrophil NOX2 followed by superoxide dismutation, while consuming negligible amounts of media glucose in 24 h (estimated <700 μM). Excess MPO was added to catalyze the production of HOCl from GOX/MPO with the presence of media Cl^-. To favor production of HOBr or HOSCN, we added 1 mM of either NaBr (GOX/MPO/Br^-) or NaSCN (GOX/MPO/SCN^-), respectively (**Figure 2.2A**). Br^- and SCN^- are both preferred substrates for MPO in comparison to Cl^-, and can also directly react with HOCl to produce either HOBr or HOSCN [16,66].

We evaluated the cytotoxicity of HOX exposure on AECs using the LDH assay. LDH release was not increased by any oxidant exposure after 2, 4, or 6 h, while by 24 h, exposure to GOX/MPO with or without Br^-, as well as to GOX alone, significantly increased LDH release compared to control (**Figure 2.2B**). However, exposure to GOX/MPO/SCN^- was not cytotoxic even at 24 h. Recombinant LDHA was modestly inactivated by all oxidant exposures (loss of activity after 1 h, 1.7-5.4%, and after 24 h, 3.7-12.6%), but differences between experimental conditions were not large enough to suggest artefactual confounding of cytotoxicity results (**Figure 2.3A**). Furthermore, qualitative evaluation of cell morphology at 24 h agreed with LDH results (e.g., GOX/MPO/SCN^--exposed cells closely resembled naïve controls, GOX-exposed

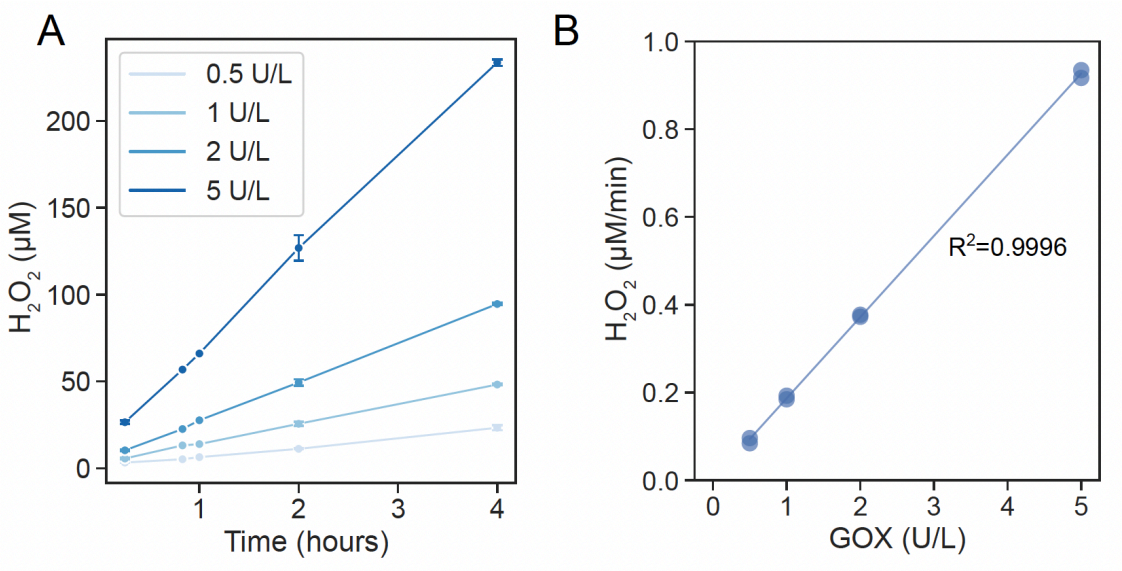

Figure 2.1 Calibration of GOX activity. (A) GOX activity was measured at a range of doses using the Amplex Red assay. (B) Linear regression of GOX activity relative to enzyme concentration. The equation is y (in units of H_2O_2, µM, per minute) = 0.185 (GOX concentration, U/L) + 0.00167, with an R^2 of 0.9996. Results are representative of two independent experiments. Error bars represent standard deviation of the mean.

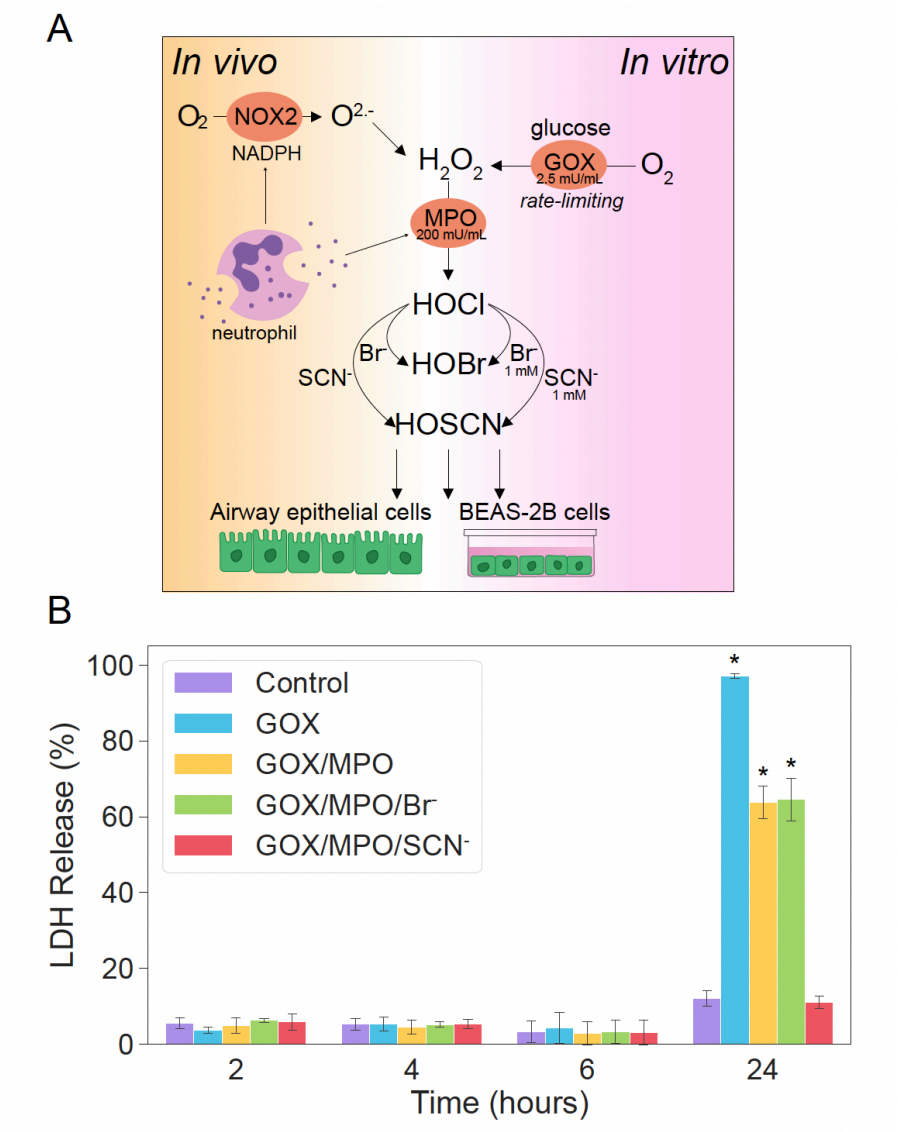

Figure 2.2 HOX exposure model. (A) Schematic of MPO-derived HOX generation *in vivo* (left) and *in vitro* using the HOX exposure model (right), with reagent concentrations indicated. (B) Viability of cells exposed to oxidants (no treatment, purple; GOX, blue; GOX/MPO, yellow; GOX/MPO/Br^-, green; GOX/MPO/SCN^-, red) were analyzed using an LDH assay. Data (n=4 per group at 2 h and n=8 per group at 4-, 6- and 24 h) expressed as mean % LDH release ± standard deviation. One-way ANOVA (24 h time point only); *$p<0.0001$ significant difference compared to untreated control.

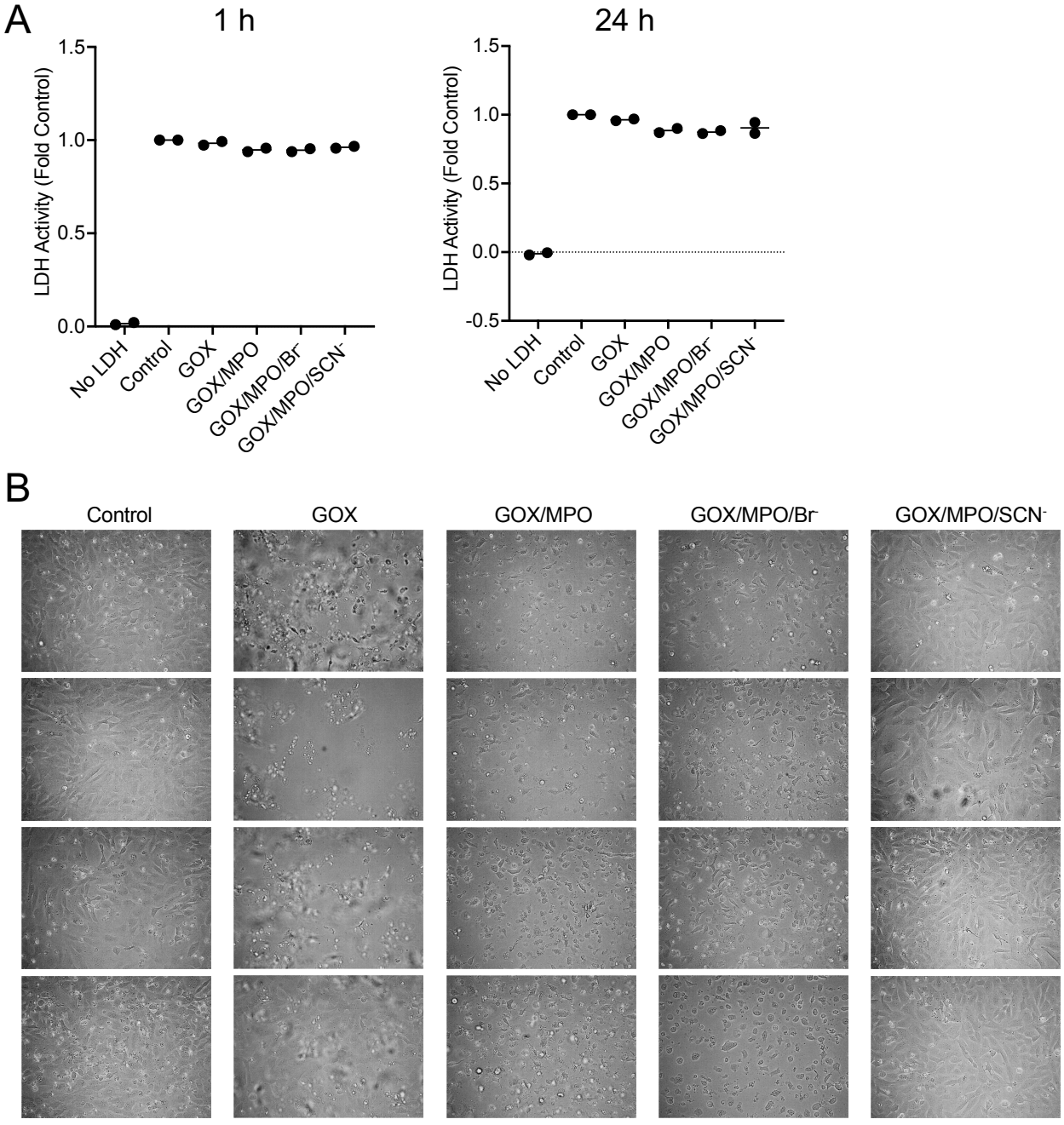

Figure 2.3 Validation of cytotoxicity results. (A) 1 U/ml (final) recombinant human LDHA was added to oxidant exposure medium and incubated with oxidants for 1 or 24 h (n=2 per group), then media was sampled, and activity measured. Results are expressed relative the rate of absorbance change of the control condition (set as 1). These results indicate LDH is not highly

sensitive to inactivation by oxidant exposures used in this study. (B) Brightfield microscopy images (Moticam 5 camera installed in an AE31E microscope set to 100X magnification) showing morphology of BEAS-2B cells exposed for 24 hours to GOX, GOX/MPO, GOX/MPO/Br^-, GOX/MPO/SCN^-, and untreated controls (n=4 per group). GOX-exposed cells are largely detached; GOX/MPO and GOX/MPO/Br^- are shrunken in size; and GOX/MPO/SCN^- closely resemble unexposed controls. Image brightness (+27-45%) and contrast (+40-71%) adjustments were manually applied to individual images for ease of morphology viewing.

cells were largely detached, and GOX/MPO or GOX/MPO/Br^- cells were mostly attached but exhibited contracted cell bodies) (**Figure 2.3B**).

We wanted to determine the impact of these exposures on cellular redox state, using three orthogonal measurements: 1) Prx3 dimerization, 2) intracellular glutathione (reduced GSH and oxidized GSSG), and 3) extracellular cysteine (reduced Cys and oxidized CySS). Analysis of glutathione (2 h and 6 h) and Prx3 (2 h) redox state in AECs revealed that only GOX, but no condition containing MPO, caused significant oxidation of these molecules (**Figure 2.4A-D**). By contrast, GOX/MPO/SCN^- caused significant Cys oxidation at 2 h, and all oxidant-producing exposures did so after 6 h (**Figure 2.4E-F**). GOX/MPO/SCN^- also caused a significant increase of media CySS at 6 h. These data indicate that the eventual divergence in the cytotoxic effects of our experimental conditions could not be explained by oxidant-specific targeting of global thiol redox state, particularly in the cytosol or mitochondria compartments.

Divergent metabolic effects of HOX exposure on AECs

We sought to use unbiased methods to determine what molecular effects preceded HOX exposures that later led to cytotoxicity (GOX/MPO, GOX/MPO/Br^-), or not (GOX/MPO/SCN^-). We used LC-MS-based metabolomics to profile a range of small molecules spanning many different pathways and functional groups in a single experiment. Cellular compounds passing QC thresholds for signal-to-noise and reproducibility of quantification included 410 in positive ionization mode and 348 in negative ionization mode. Of these, 141 compounds in positive mode and 72 compounds in negative mode were annotated as metabolites with high confidence identifications, which indicates an accurate mass and LC column retention time match to a standard, and/or tandem mass spectrometry (MS^2) spectral matches.

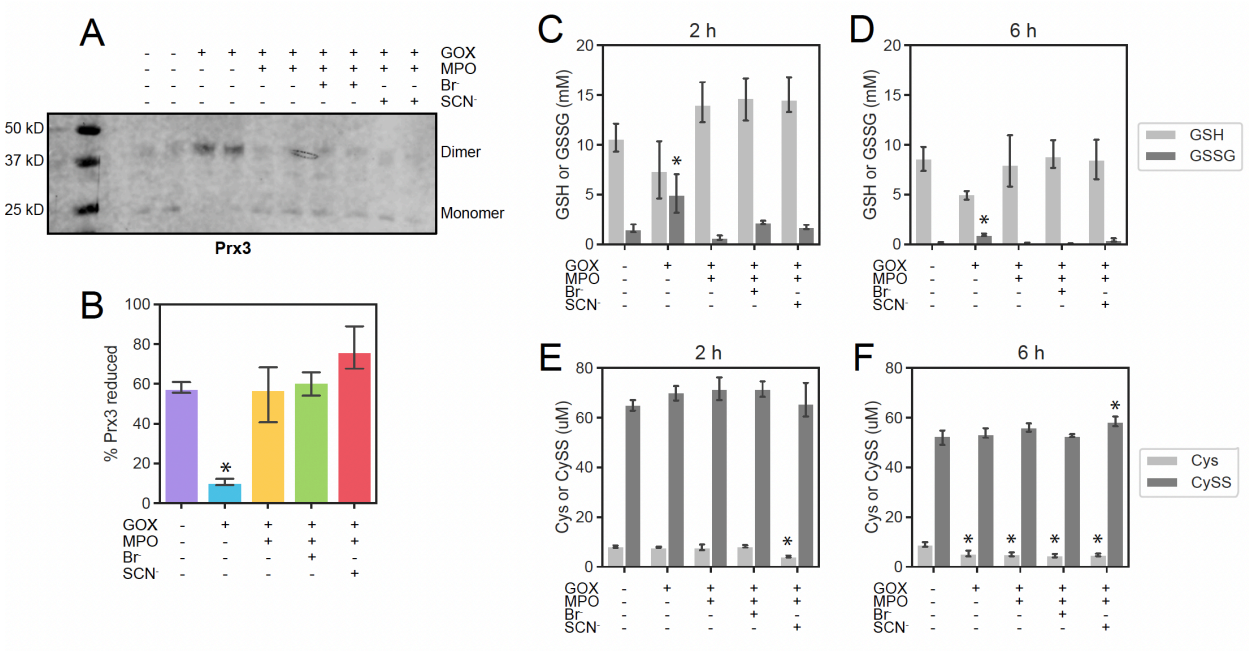

Figure 2.4 HOX effects on AEC redox state. Cells were exposed to GOX, GOX/MPO, GOX/MPO/Br^-, or GOX/MPO/SCN^-, as described for other exposures, for 2 h. (A) Cells were washed and thiols alkylated by addition of NEM, then proteins denatured in non-reducing loading buffer were resolved by SDS-PAGE followed by immunoblotting for Prx3. (B) Quantification of band intensity ratios expressed as % reduced monomer band compared to total). (C) Intracellular GSH and GSSG were analyzed via HPLC-FL for 2 h (C) and 6 h (D). Additionally, extracellular (media) Cys and CySS were quantified using the same method for 2 h (E) and 6 h (F). One-way ANOVA with Tukey's post-test. *$p<0.05$ significant difference compared to control. Data in bar plots represents mean ± standard deviation (n=4 per group).

We used multivariate analyses to assess intrinsic similarities and differences in the datasets. Partial least squares-discriminant analysis (PLS-DA) revealed distinct clustering of each group at 2 h and 6 h (**Figure 2.5A-D**), indicating broad metabolomic changes among the GOX/MPO/substrate groups. A total of 56 metabolites at 2 h and 37 metabolites at 6 h had variable importance projection (VIP) scores >1 (**Figure 2.5E-F**) in the top three PLS components. The PLS-DA model descriptors (R^2, Q^2) indicate the models were reliable (**Table 2.1**). We noted that the different exposures were well resolved from each other using this model, indicating specificity of each oxidant in overall metabolomic impact on AECs in spite of their similar effects on thiols. Notably, however, GOX/MPO and GOX/MPO/Br^- clustered closely together. Because of this, we conducted a separate PLS-DA analysis of only GOX/MPO and GOX/MPO/Br^- to determine if any metabolites could discriminate them (**Figure 2.6A-B**). Intriguingly, several phosphatidylcholines (PC), lysophosphotidylcholines (LPC) and phosphatidylethanolamines (PE) were distinct between GOX/MPO and GOX/MPO/Br^- exposures (**Figure 2.6C**). GOX/MPO/Br^- increased many of the lipids that were decreased by GOX/MPO (each compared to controls), indicating interesting divergent effects on lipids between conditions favoring HOBr or HOCl formation.

We also conducted an orthogonal univariate analysis, which also showed that different GOX/MPO/substrate exposures produce divergent metabolomic effects, from one another and GOX alone, yielding clear unsupervised clustering according to exposure (**Figure 2.7-2.8**). A total of 34 metabolites in positive mode and 27 metabolites in negative mode significantly differed at 2 h and by 6 h, 46 and 41 metabolites differed in positive mode and negative mode, respectively (ANOVA $p<0.05$, FDR<0.05). GOX/MPO and GOX/MPO/Br^- largely clustered together at both 2 h (**Figure 2.7**) and 6 h (**Figure 2.8**), congruent with the PLS-DA results.

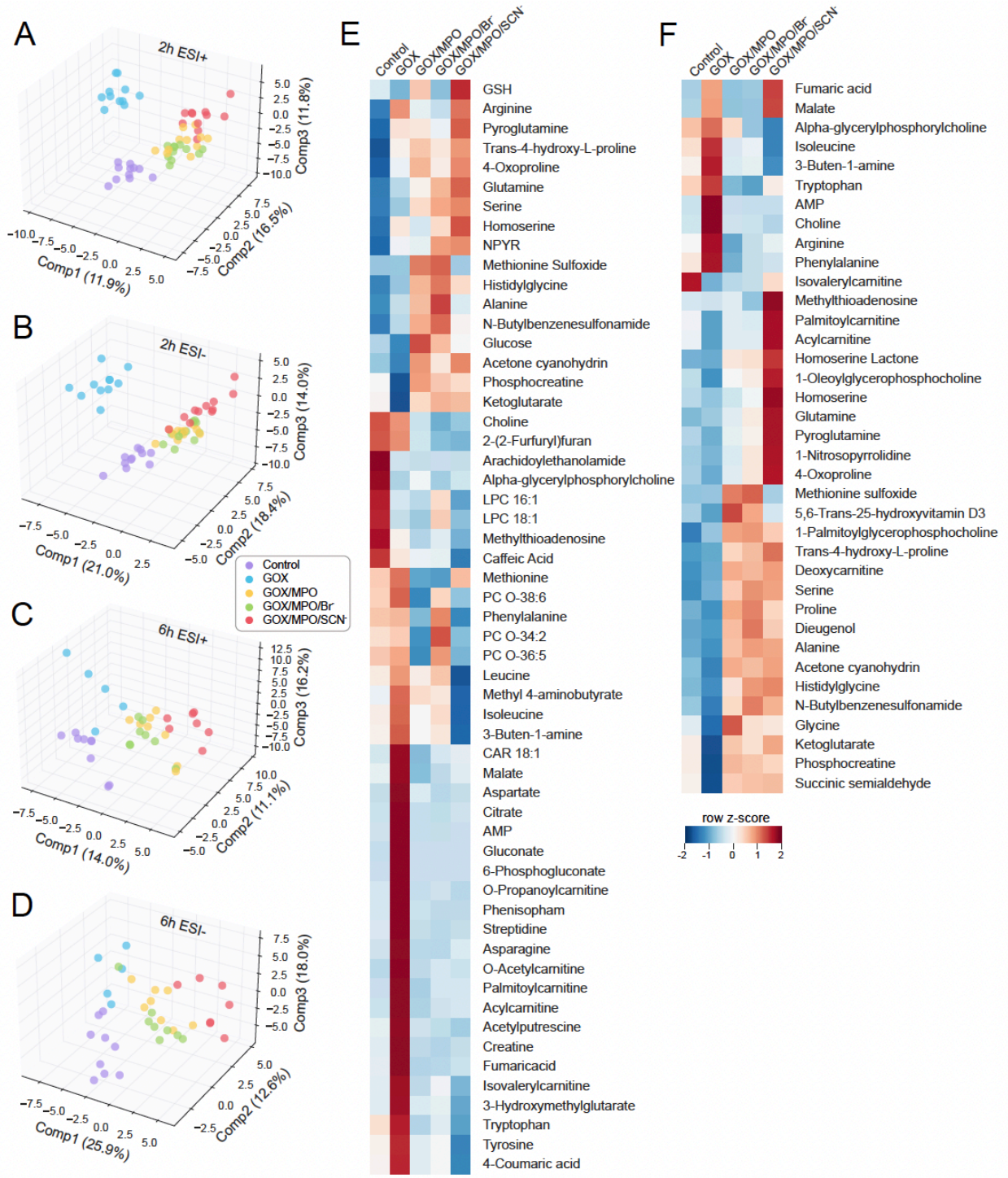

Figure 2.5 PLS-DA reveals global divergence of GOX/MPO/substrate groups from each other and from GOX alone. 3D score plots of metabolomic data from HOX and control

exposures at 2 h in positive electrospray ionization (ESI+) mode (A) and negative electrospray ionization (ESI-) mode (B) and at 6 h in ESI+ mode (C) and ESI- mode (D) reveal oxidant specific groupings. Heatmap of metabolite peak areas with VIP scores greater than 1 in the first three PLS components at 2 h (E) and 6 h (F). Peak areas of metabolites were averaged within each group and then autoscaled across each of the rows to produce z-scores, plotted on red (high) to blue (low) color scales.

ESI mode	Exposure time	Components	Q^2	R^2	Accuracy
Positive	2 hours	3	0.614	0.859	0.557
Positive	6 hours	3	0.671	0.911	0.649
Negative	2 hours	3	0.484	0.737	0.414
Negative	6 hours	3	0.722	0.878	0.514

Table 2.1 PLS-DA component contributions for discrimination (R^2) and variance (Q^2) of oxidants and controls.

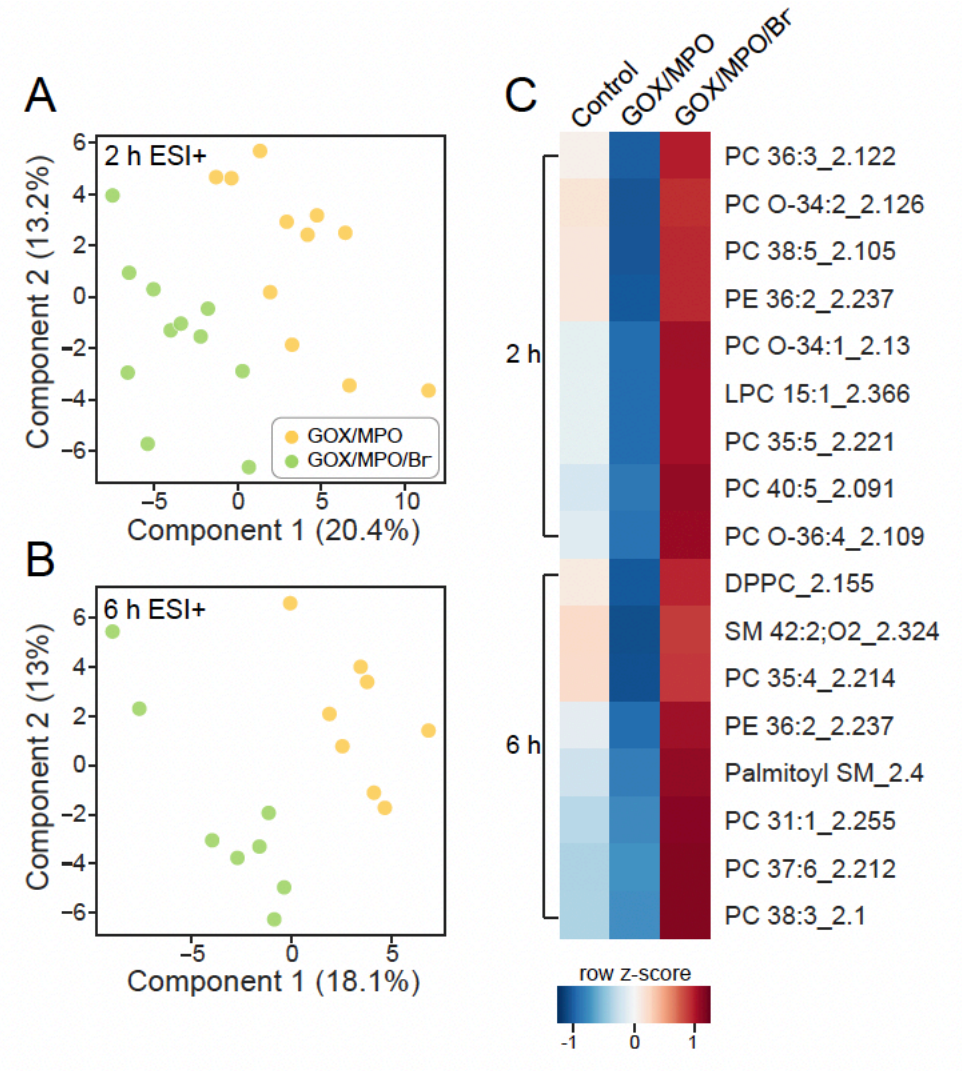

Figure 2.6 PLS-DA of conditions favoring HOBr and HOCl generation. PLS-DA of only HOBr and HOCl metabolomic data reveal an unbiased clustering of each group at both 2 h (A) and 6 h (B). Significant metabolites contributing to the variation in the first component include various lipid species. Peak areas of lipids were averaged within each group and autoscaled across rows to generate z-scores.

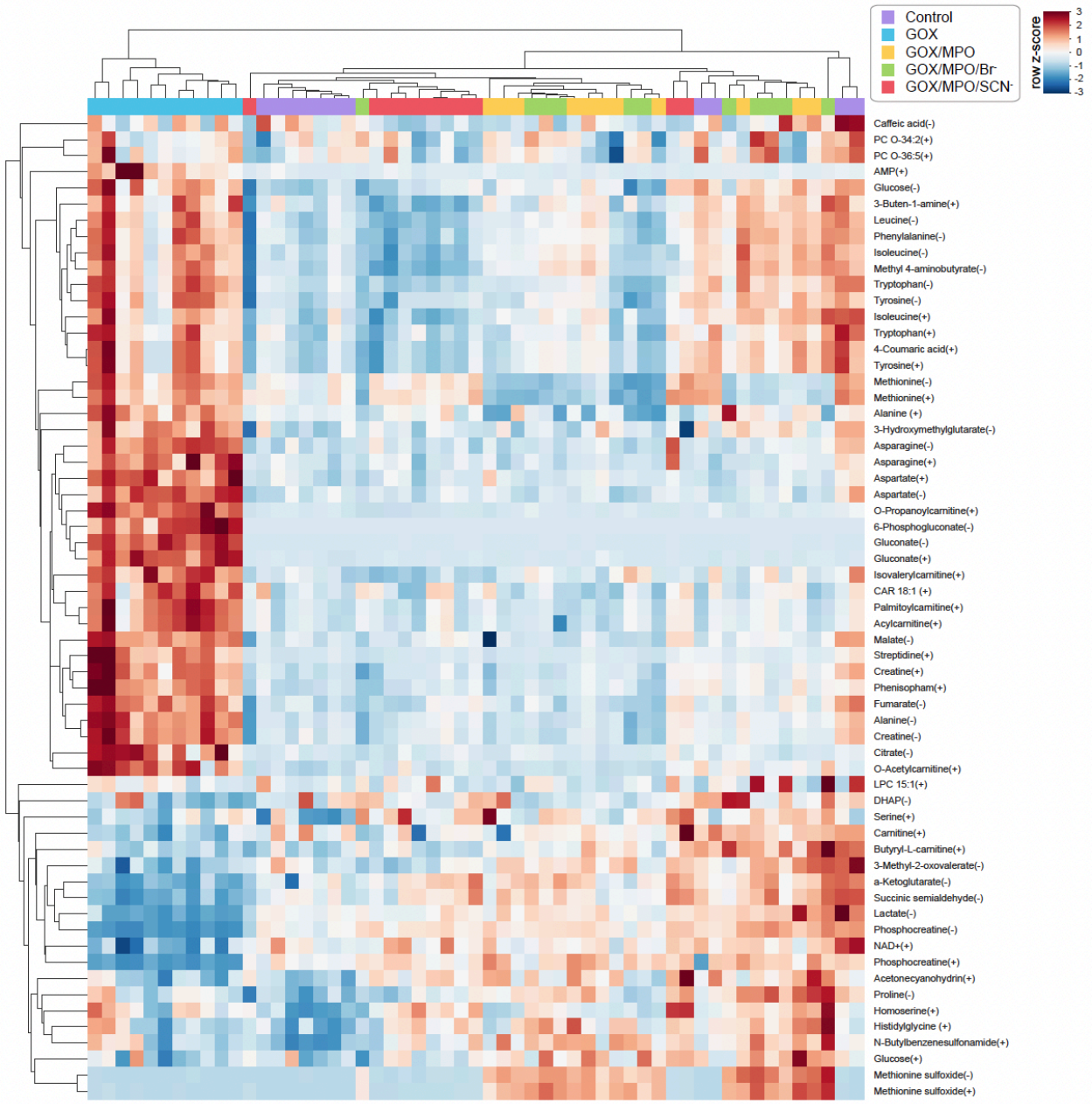

Figure 2.7 Heatmap of metabolomic differences at 2 h. Hierarchical clustering, using Euclidean distance, of significant (one-way ANOVA $p<0.05$ and FDR<0.05) metabolites at 2 h of oxidant exposure is shown. Peak areas were autoscaled to generated z-scores, row-wise, and expressed on a red (high) to blue (low) scale.

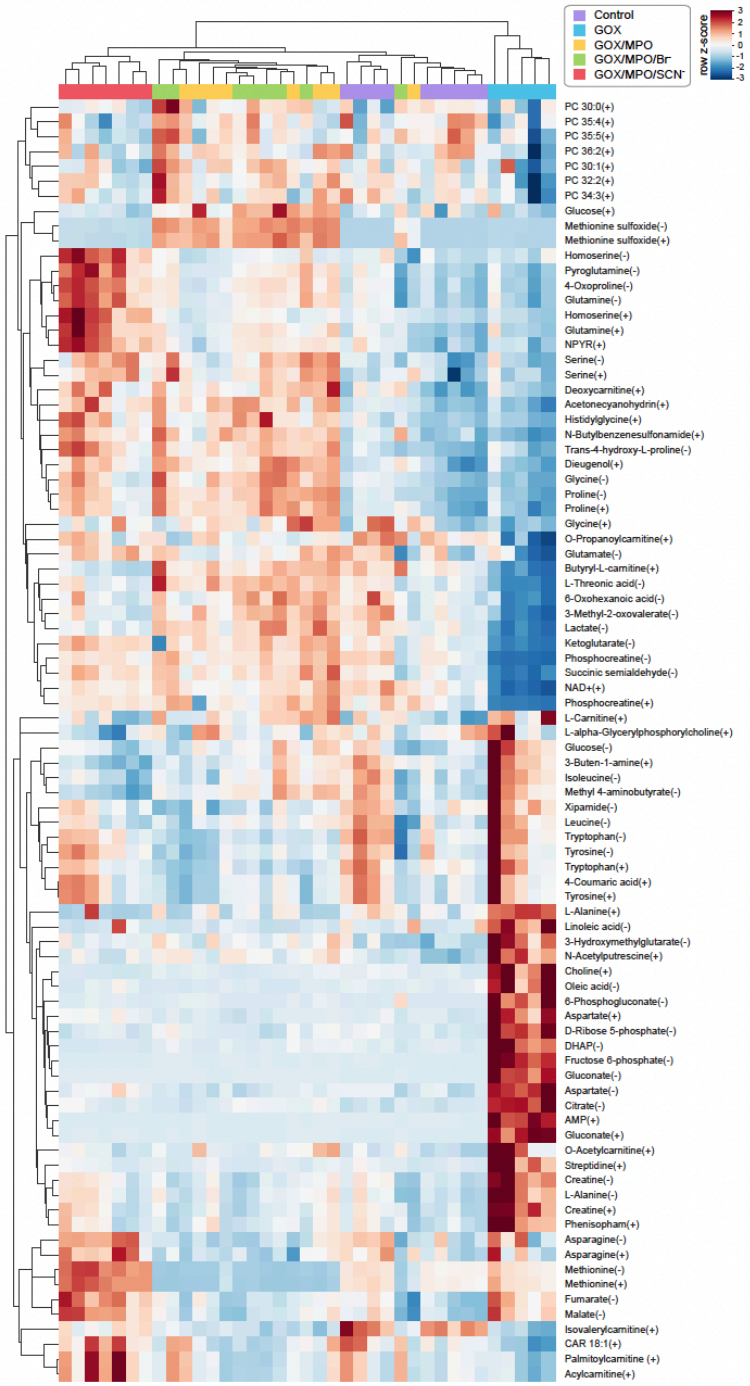

Figure 2.8 Heatmap of metabolomic differences at 6 h. Hierarchical clustering, using Euclidean distance, of significant (one-way ANOVA $p<0.05$ and FDR<0.05) metabolites at 6 h of oxidant exposure, is shown. Peak areas were autoscaled to generated z-scores, row-wise, and expressed on a red (high) to blue (low) scale.

HOX distinctly alter important metabolic pathways in AECs

Next, we performed comparisons of control cells and GOX/MPO/substrate groups using Metaboanalyst 3.0 to reveal metabolic pathways impacted by HOX exposure at 2 h and 6 h (**Figure 2.9**) based on the KEGG database. The results of pathway analyses revealed perturbation to cysteine and methionine metabolism in cells exposed to GOX/MPO and GOX/MPO/Br^- at 2 and 6 h, driven by oxidation of methionine, and in GOX/MPO/SCN^- by 6 h. These results were driven by altered abundances of methionine and methionine byproducts. We anticipate the cysteine/cystine pool may also be impacted, even if indirectly via methionine disruption, but neither metabolite was detected in the BEAS-2B cell lysates. GOX/MPO/SCN^- had the most pronounced effects on primary metabolism pathways of the GOX/MPO/substrate groups but was less potent in this effect than GOX alone. Because GOX/MPO/SCN^- was non-toxic at 24 h, we also evaluated its effects at this time. Pentose phosphate pathway (PPP) and tricarboxylic acid (TCA) cycle perturbation in HOSCN-exposed cells were evident by 24 h (**Figure 2.10B**), similar to the effects that GOX alone had on AECs by 2 h. GOX/MPO/SCN^- also increased amino acid pathways associated with glutathione synthesis such as glutamine, while primary metabolism compounds such as lactate and oxoglutarate decreased, suggesting metabolic rewiring emphasizing PPP activity for antioxidant support.

Based on experimental results and known biological importance to metabolism, we created a metabolic network map contrasting effects of different oxidant exposure on an individual metabolite basis (**Figure 2.11**). This network map of metabolites that were statistically significant in the ANOVA model highlights primary energy metabolic pathways (glycolysis, PPP, TCA cycle) and interconnected amino acid metabolic/degradation pathways related to HOX exposure. There are several nodes in this metabolic network where exposure specificity is

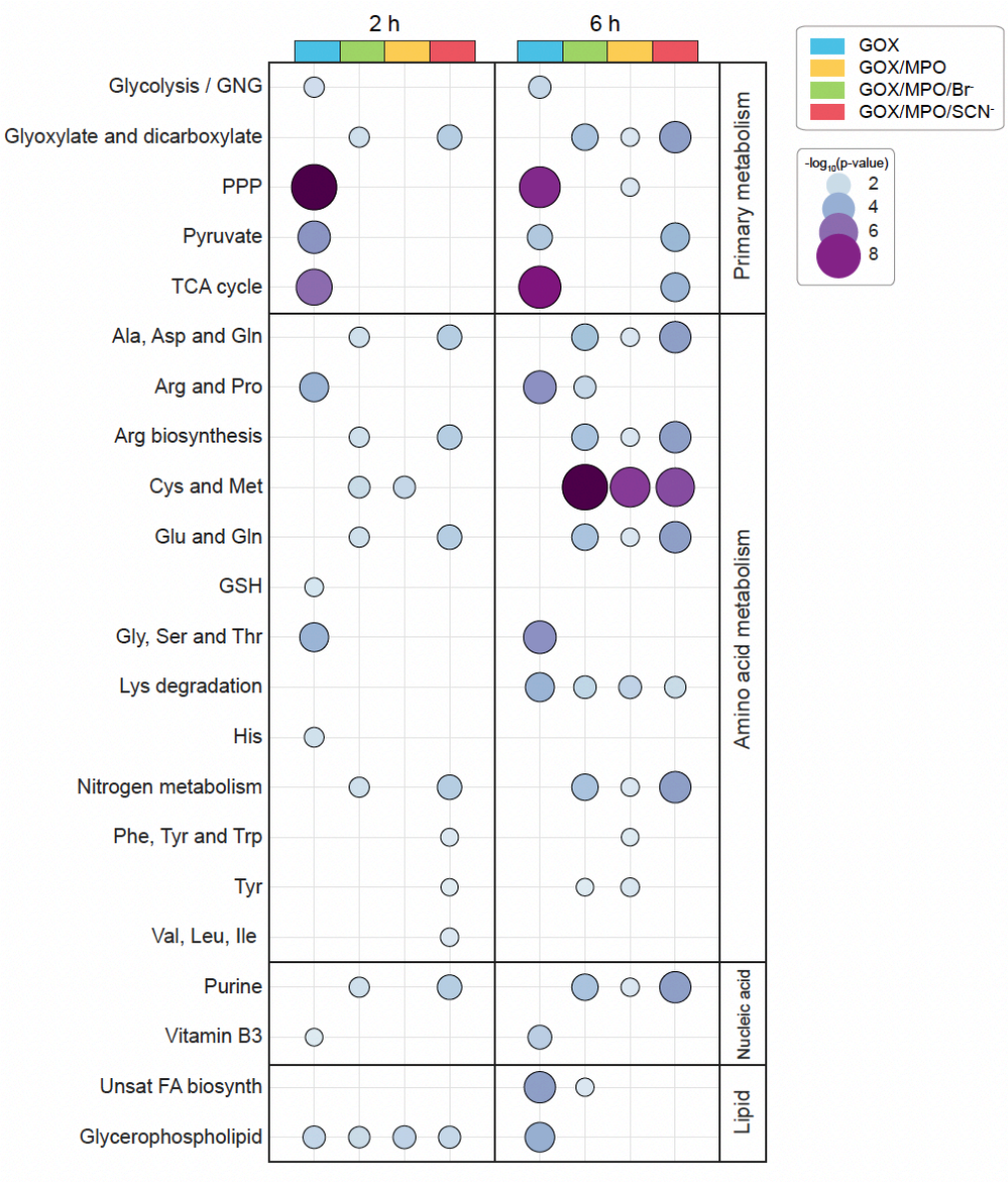

Figure 2.9 Pathway analysis of altered metabolites according to HOX exposures. Different HOX conditions were compared to untreated control at 2 h (left) and 6 h (right) performed with MetaboAnalyst. Pathway significance expressed as negative $\log_{10}$ transformed p-values which is both represented by color intensity and marker size. Results with pathway $p>0.05$ are censored for ease of viewing. Pathways were grouped by primary metabolism, amino acid metabolism, nucleic acid metabolism, and lipid metabolism (indicated on the right side of the plot).

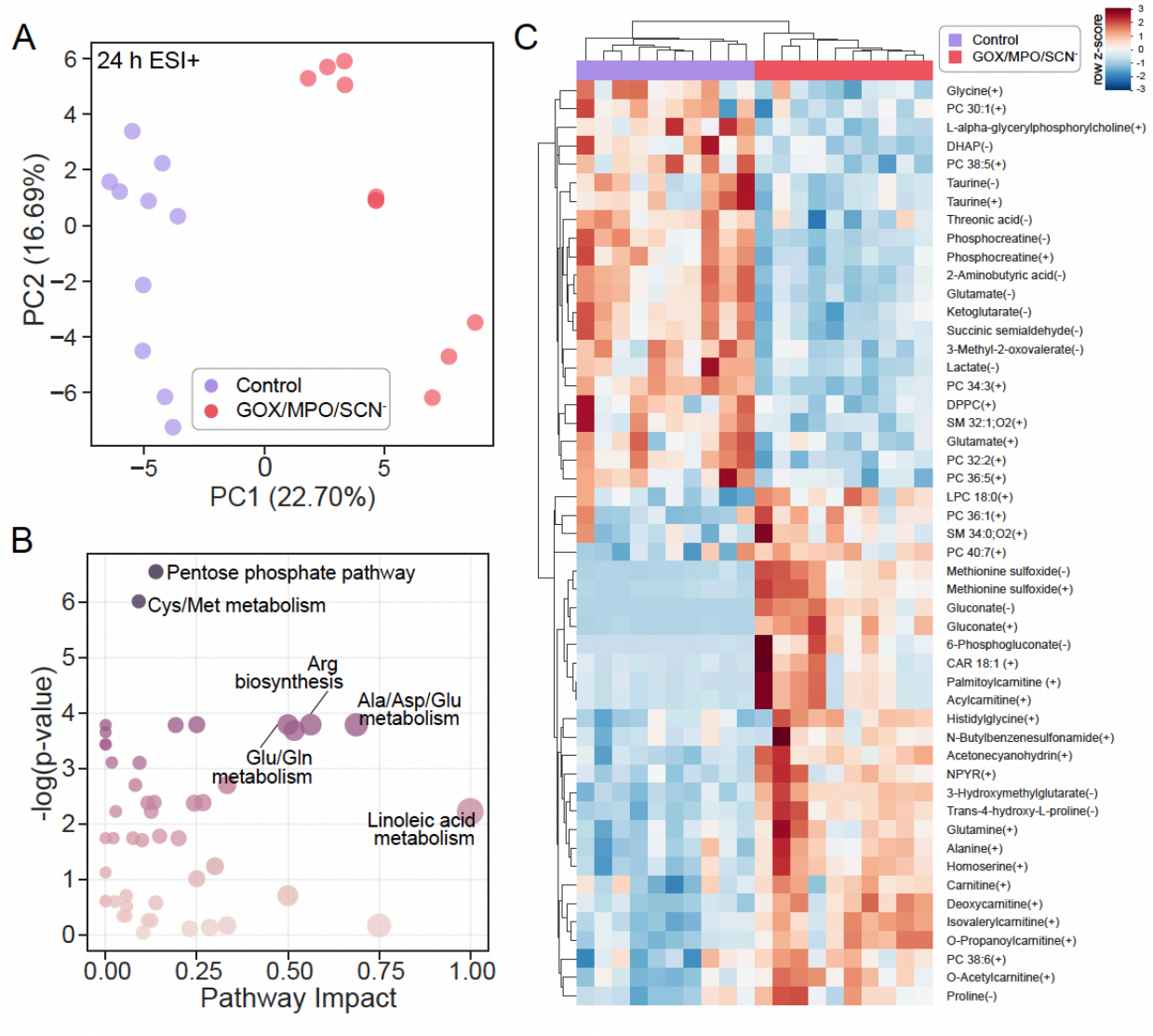

Figure 2.10 Detailed comparison of HOSCN and control conditions at 24 h. (A) PCA score plot shows separation of HOSCN-exposed data from control at 24 h. (B) Pathway analysis reveals PPP and amino acid pathways as significant metabolic pathways in cells treated with HOSCN for 24 h. (C) Clustered heatmap of significant metabolites. T-test; $p<0.05$.

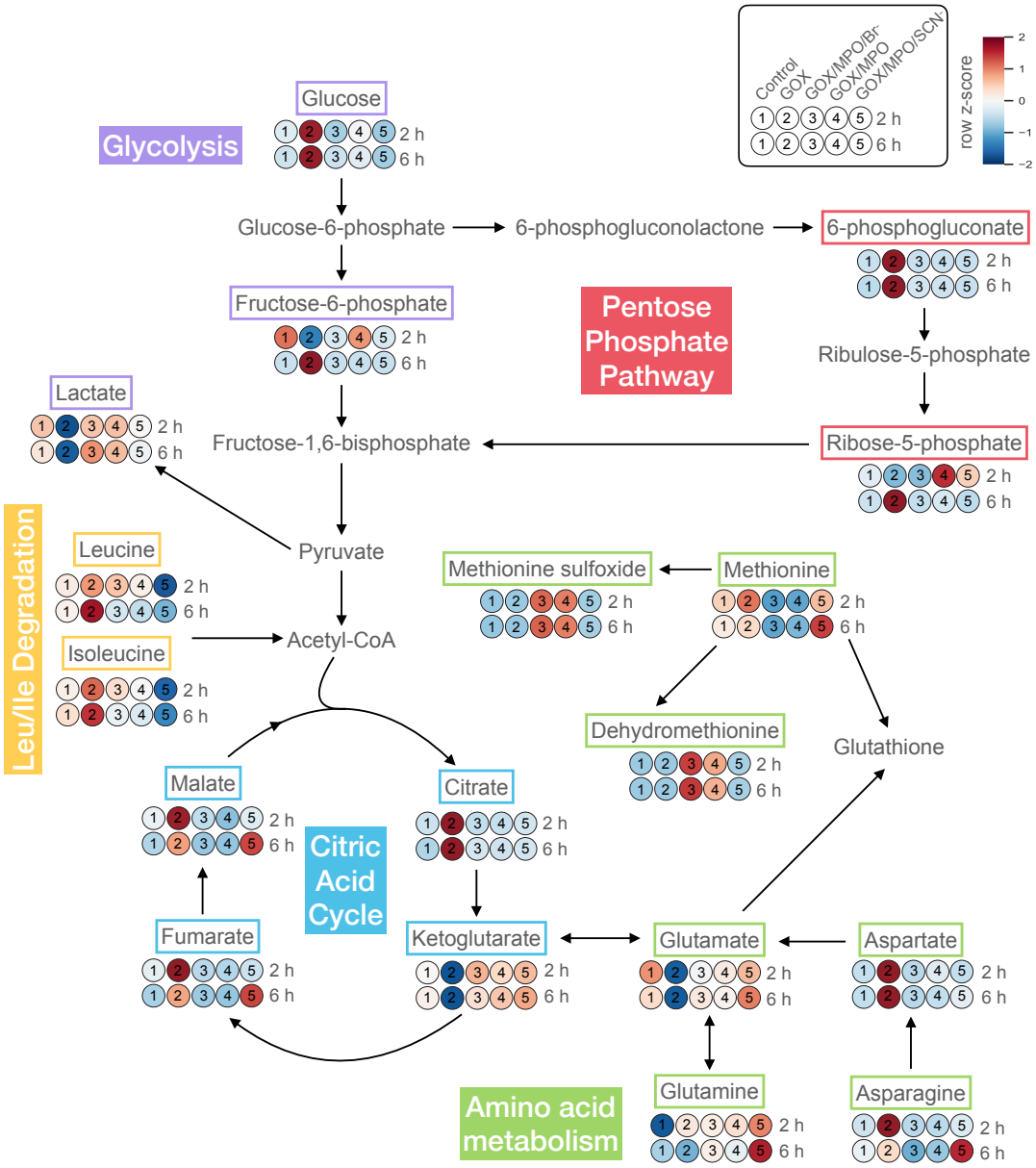

Figure 2.11 Schematic representation of metabolic pathways involving statistically significant compounds altered by HOX exposure. Arrows are suggestive of major pathway direction. In some cases, arrows include multiple reaction steps between metabolites. Metabolites depicted on the plot without heatmaps were not statistically significant or not detected and are shown in order to bridge different modules of significant metabolites. Metabolite peak areas

were averaged within each group and z-scored across rows. One-way ANOVA, $p<0.05$ and FDR<0.05 compared to control.

obvious. GOX/MPO and GOX/MPO/Br^- exhibited unique effects on methionine, which was depleted, and led to increased methionine oxidation products (discussed in more detail below). GOX/MPO/SCN^- depleted branched chain amino acids (BCAAs), which may indicate catabolism to acetyl coenzyme (CoA) and succinyl CoA for TCA support, while also increasing glutamine, fumarate (6 h only), and malate (6 h only). Additionally, GOX alone exhibited profound effects on primary metabolism (glycolysis, PPP, TCA), including depletion of lactate and accumulation of PPP products as well as accrual of TCA metabolites except for ketoglutarate, which was depleted – together suggesting rapid metabolic rewiring for antioxidant support [67]. Notably, interconnected metabolites often displayed very similar or opposite patterns, showing the utility of this approach to identify potential biological relationships and reactions.

Halogenating HOX species specifically increase methionine oxidation products also evident in early CF

One benefit of our unbiased approach is the ability to query unknown compounds of high analytical quality in addition to previously validated compounds. Analysis of statistically significant unknown compounds from the dataset led to the detection of an unidentified compound which was increased in AECs exposed to GOX/MPO and GOX/MPO/Br^-. The compound had an exact mass of 147.03541 amu and was the most significantly altered compound at 2 h (p=1.57e-46) and at 6 h (p=2.38e-27) in GOX/MPO- and GOX/MPO/Br^--exposed cells. Upon further investigation into the chemical formula of the unknown compound ($C_5H_9NO_2S$), we identified dehydromethionine (dhMet), featuring a cyclic azasulfonium group, as the probable candidate (**Figure 2.12**). We validated the identity of dhMet by making a dhMet standard from reacting reagent methionine and HOCl, a reaction which has been previously

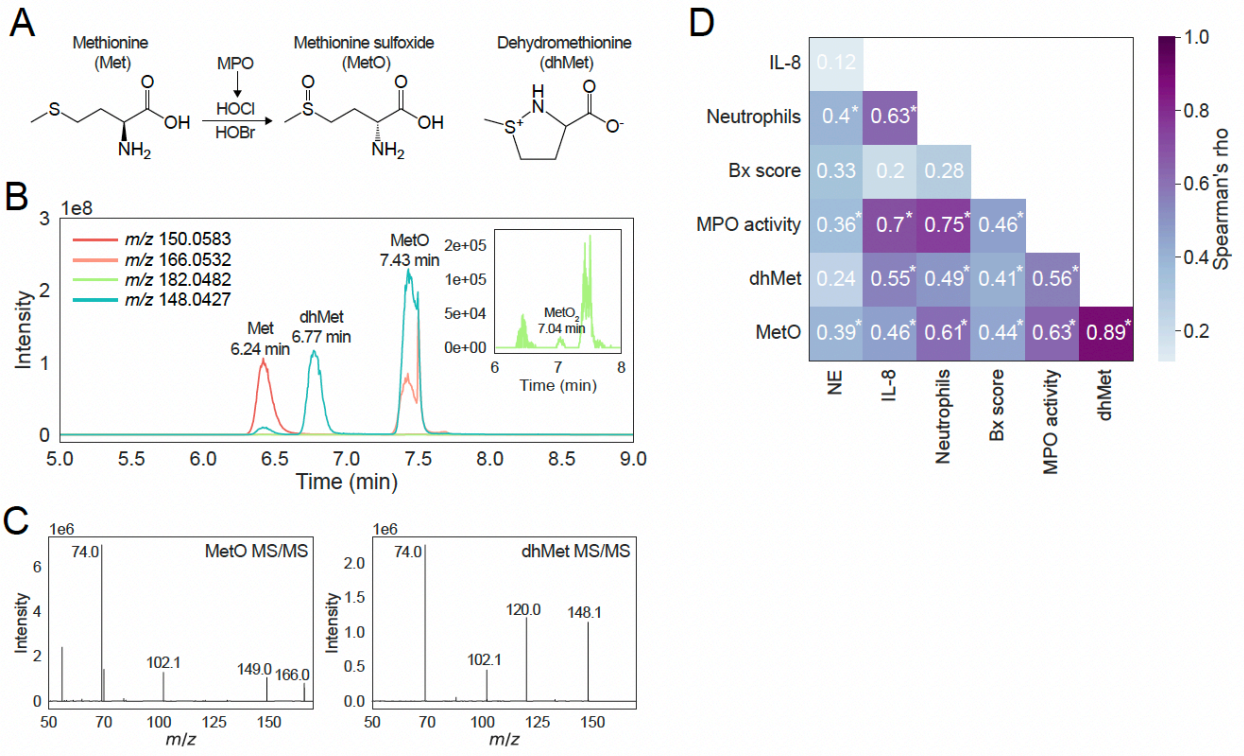

Figure 2.12 Methionine oxidation products associated with HOCl and HOBr exposures (GOX/MPO and GOX/MPO/Br$^-$) are important in early CF lung damage. (A) Schematic of Met oxidation to MetO and dhMet by HOCl/HOBr generated by MPO. (B) Mass-to-charge (m/z) ratio corresponding to dhMet in a methionine standard mixed with HOCl was validated in our LC-MS method and had a unique retention time compared to other methionine oxidation species. (C) dhMet identity was further validated with MS/MS of the retention-time resolved peak, which has a unique fragmentation pattern compared to MetO. (D) BAL fluid from children with CF aged 5-years-old (n=27) was analyzed for MPO activity, MetO, dhMet, and tested for correlation with IL-8, % of neutrophils among BAL leukocytes, and bronchiectasis (Bx) score. The stronger purple color indicates stronger Spearman rho (indicated over each pairwise cell). Spearman correlation; *p<0.05 significance.

described [68], and analyzed the retention time, MS^1, and MS^2 spectra of this standard. The reaction produced four distinct peaks, with one of the appropriate MS^1 m/z and retention time (**Figure 2.12B**). Other peaks corresponded to anticipated Met, MetO, and methionine sulfone. The MS^2 spectra of the dhMet peak had a unique fragment at m/z 120, corresponding to the loss of ethylene, and does not include a common MetO peak at m/z 149, corresponding to the loss of ammonia (**Figure 2.12C**), which matched prior MS^2 data published for dhMet [68]. dhMet was also shown in this publication to be produced by phorbol myristate acetate-stimulated neutrophils *in vitro*, along with MetO.

To investigate the clinical significance of dhMet and MetO in inflammatory airway disease, we performed retrospective LC-HRMS analysis of BAL fluid from children with CF at 5 years of age (n=27) (**Table 2.2**). We found that MetO and dhMet were detectible in early CF BAL and significantly correlated to MPO activity, neutrophil chemokine IL-8, percentage of neutrophils among BAL leukocytes, and bronchiectasis (Bx) scores from chest computed tomography scans (**Figure 2.12D**). These findings are in agreement with two previously published reports that analyzed MetO [10,52] but this result has not been reported for dhMet before. MPO activity and the methionine oxidation products had a greater association to Bx score than neutrophil elastase, a proteolytic neutrophil enzyme previously established as an important risk factor for severity of CF lung disease [11,69–72]. Thus, the oxidant-generating activity of MPO, which produces both dhMet and MetO in complex biological mixtures, is associated with an increase of neutrophil-driven inflammation and structural lung damage in children with CF.

Children n	27
Age at BAL years	5.09±0.17
Sex n	
Female	15
Male	12
F508del homozygous	19
F508del heterozygous	8
Pancreatic insufficiency	27
Positive for pathogen %	73

Table 2.2 Cystic fibrosis patient demographics. Age is given as mean ± SD.

2.5 Discussion

In this study, we compared the metabolomic effects of MPO-derived oxidants on immortalized human AECs via experimental conditions favoring HOCl (GOX/MPO), HOBr (GOX/MPO/Br^-), or HOSCN (GOX/MPO/SCN^-) production. We observed differences in cytotoxicity (via LDH release) after 24 h when comparing GOX/MPO/SCN^- to GOX/MPO or GOX/MPO/Br^-, as well as GOX. However, we saw no difference in cytosolic glutathione or mitochondrial Prx3 oxidation in response to any MPO-based exposure. In the extracellular compartment, however, Cys oxidation by GOX/MPO/SCN^- was evident earlier than other oxidant exposures. In contrast, we observed broad metabolomic differences between oxidant exposures, revealing that GOX/MPO/SCN^- affected markedly different pathways of metabolism compared to GOX/MPO or GOX/MPO/Br^-, which were similar, or GOX alone, which affected many overlapping metabolites to GOX/MPO/SCN^- but did so more rapidly and more potently. The relative similarity of GOX/MPO and GOX/MPO/Br^- generally agrees with a transcriptomic study of E. coli responses to MPO-derived oxidants [73], and is perhaps not surprising considering the similar reactivities of HOCl and HOBr [74–76].

We observed that GOX/MPO was less cytotoxic than GOX alone (as was GOX/MPO/Br^-), unlike in two previous studies collectively including 16HBE, Calu-3, Neuro2A, Min6, and human aortic endothelial cells [35,77], but in agreement with a different study using J774A.1 cells [78]. Importantly, the aforementioned studies used balanced salts rather than media, and also used shorter (≤4 h) exposures. It is possible that the presence of metabolites mitigates the impact of HOCl- and HOBr-derived cytotoxicity more so than that of H_2O_2 due to wider-ranging cross-reaction of the halogenating oxidants with media components [7980]. However, our approach has the advantage of mimicking physiological exposures, including comparable levels of media

metabolites to airway fluid (e.g., average adult CF sputum methionine has been estimated at 0.6 mM, compared to 0.1 mM methionine in Medium-199) [81]. The results suggest unmitigated H_2O_2 can be an even more potent toxicant than hypohalous acids in the context of a physiological milieu.

A stark difference of GOX/MPO and GOX/MPO/Br^- exposures compared to others was their significant effects on methionine oxidation at both 2 and 6 h. This means oxidized methionine species could function as sensitive biomarkers of HOCl and HOBr, as shown in the current study. MetO and dhMet in 5-year-old CF patient BAL were associated with MPO activity, IL-8, neutrophils, and lung damage (bronchiectasis). This study is the first, to our knowledge, to link free dhMet in airway lining fluid to CF lung health. Prior publications have also linked free MetO to MPO and CF lung health [10,52,82], and protein MetO is also increased in idiopathic pulmonary fibrosis and associated with neutrophils [83]. dhMet at the N-terminal methionine residue of S100A8 was also previously found to be increased in CF BALF compared to controls and associated with bacterial burden [84]. The reaction rate of H_2O_2 with methionine is slow, and no reaction has been conclusively demonstrated with methionine for HOSCN, so more favorable targets are expected to consume these oxidants first [85–87].

Together, these studies indicate neutrophilic inflammation in CF and other airways diseases involves significant HOCl production that may contribute to disease progression. HOBr is a minor product of MPO *in vivo* [16,20], but may also contribute to luminal methionine oxidation due to its presence in CF airways (evidenced by protein bromination) [88]. While there are many good candidate biomarkers of CF lung disease [88–91], advantages of the oxidized methionine species are their robust attribution to MPO activity favoring HOCl and HOBr, as validated in our model system, and their relatively high abundance compared to glutathione sulfonamide (which

we did not detect in the current study). Both MetO and dhMet are promising candidate biomarkers for structural lung disease in CF and other illnesses, and also for studies of lung anti-inflammatory treatment efficacy. However, MetO can be generated by other strong oxidants and flavin monooxygenases (reacting with protein methionine) [92,93], potentially lowering its specificity as a candidate biomarker.

Interestingly, GOX/MPO and GOX/MPO/Br^- also impacted abundances of phospholipids. Several long-chain phospholipids discriminated GOX/MPO and GOX/MPO/Br^-, with GOX/MPO/Br^- leading to accumulation and GOX/MPO to depletion. This difference is intriguing since both HOCl and HOBr both readily oxidize specialized PC lipids called plasmalogens, reacting at the characteristic vinyl ether bond, and PE or phosphatidylserine lipids by modifying their head groups [94–97]. Plasmalogen oxidation also gives rise to halogenated fatty acids that have biological activity [44,95]. Although the lipids that discriminated GOX/MPO from GOX/MPO/Br^- were plausible HOCl and HOBr targets (either by head group or double bonds), these results may also arise from indirect remodeling effects, possibly specific to the reactions of each oxidant considering the differential abundances between the exposures. Owing to the fact that GOX/MPO and GOX/MPO/Br^- were equally cytotoxic, their divergent lipidomic effects in this model, while interesting, were likely not the common basis of eventual cell death.

In contrast to GOX/MPO and GOX/MPO/Br^-, GOX/MPO/SCN^- favors HOSCN production. HOSCN is a weaker oxidant that primarily oxidizes thiols to reducible disulfides. In our experiments, GOX/MPO/SCN^- was the only experimental condition not toxic to AECs after 24 h. This may be due to gradual disruption of primary metabolism (PPP, TCA) and amino acids (methionine, glutamate, and glutamine), which could supply molecules important for maintenance of redox poise. Many of these effects are consistent with catalytic thiol oxidation of

key metabolic proteins. Our study did not analyze protein-bound thiols, which make up an important functional element of the redox proteome [98,99]. Prior works have found that GAPDH, aldolase, triosephosphate isomerase, and creatinine kinase are targets of HOSCN and that HOSCN can inhibit glycolysis to promote PPP activity in J774A.1 cells, similar to redox rewiring by H_2O_2 [34,67,100]. PPP was the most significantly altered pathway by 24 h in AECs exposed to GOX/MPO/SCN^-, consistent with the notion of glycolysis inhibition and metabolic rewiring. Catalytic reduction of HOSCN by mammalian thioredoxin reductase may also elicit adaptive responses if this prevents the enzyme from interacting with other substrates, or depletes NADPH to activate glucose 6-phosphate dehydrogenase [35,101]. Thus, airway cells may tolerate HOSCN by enacting a metabolic switch to increase oxidative PPP activity and increase HOSCN clearance by thioredoxin reductase, GSH, and other NADPH-dependent antioxidant systems.

GOX/MPO/SCN^- also rapidly decreased the BCAAs leucine and isoleucine, catabolites methyl 4-aminobutyrate and 3-buten-1-amine, after 2 h. This suggests increased BCAA catabolism as a mechanism of HOSCN adaptation/tolerance, which in turn may contribute to upregulation of the TCA pathway by BCAA breakdown to acetyl-CoA and succinyl-CoA. These TCA cycle intermediates could provide metabolic flexibility to protect cells against oxidative stress and loss of energy homeostasis while glycolysis is inhibited, and oxidative PPP activity increased. BCAA degradation promoted by HOSCN could also regulate cell homeostasis and metabolism through altered mTORC1 activity [102]. Alternatively, this decrease may have been a result of altered activity or expression of a BCAA transporter, such as SLC7A5 [103]. Further studies are needed to better determine the impact of HOSCN on BCAAs and the impact of this relationship on cell function.

In summary, this study demonstrates the utility of an *in vitro* HOX oxidant exposure model combined with a holistic, untargeted metabolomics method to identify plausible *in vivo* targets of HOX that can be validated in clinical samples. We showed the divergent metabolomic effects of experimental conditions favoring HOCl, HOBr, or HOSCN formation by MPO on human lung bronchoepithelial cells, adding to knowledge about the byproducts of each exposure in complex systems. Although the effects observed cannot be directly attributed to the MPO-derived oxidants but are products of both oxidants and their byproducts formed in media and cells, they confer a better understanding of how MPO-derived oxidants arising in physiological milieu ultimately affect mammalian lung tissue. Our results enabled the detection of a new candidate biomarker, free dhMet, and reinforced an existing one, free MetO, increasing our understanding of inflammation and lung damage in early CF. More studies are needed to elucidate the mechanisms underlying other metabolic effects we observed, such as phospholipid oxidation, glycolysis inhibition, and BCAA depletion, and determine their importance in both cellular function and lung health.

2.6 References

1. About Cystic Fibrosis | Cystic Fibrosis Foundation. https://www.cff.org/intro-cf/about-cystic-fibrosis.
2. Adeloye, D. et al. Global, regional, and national prevalence of, and risk factors for, chronic obstructive pulmonary disease (COPD) in 2019: a systematic review and modelling analysis. The Lancet Respiratory Medicine 10, 447–458 (2022).
3. Khan, T. Z. et al. Early Pulmonary Inflammation in Infants with Cystic Fibrosis. American Journal of Respiratory and Critical Care Medicine (2013) doi:10.1164/ajrccm/151.4.1075.
4. Margaroli, C. et al. Elastase Exocytosis by Airway Neutrophils Is Associated with Early Lung Damage in Children with Cystic Fibrosis. Am J Respir Crit Care Med 199, 873–881 (2019).
5. Ls, M. et al. Progression of early structural lung disease in young children with cystic fibrosis assessed using CT. Thorax 67, 509–516 (2011).
6. Stănescu, D. et al. Airways obstruction, chronic expectoration, and rapid decline of FEV1 in smokers are associated with increased levels of sputum neutrophils. Thorax 51, 267–271 (1996).
7. Reeves, E. P. et al. Killing activity of neutrophils is mediated through activation of proteases by K+ flux. Nature 416, 291–297 (2002).
8. Klebanoff, S. J. Myeloperoxidase-Halide-Hydrogen Peroxide Antibacterial System. J Bacteriol 95, 2131–2138 (1968).
9. Klebanoff, S. J. Myeloperoxidase: friend and foe. Journal of Leukocyte Biology 77, 598–625 (2005).

10. Chandler, J. D. et al. Myeloperoxidase oxidation of methionine associates with early cystic fibrosis lung disease. Eur Respir J 52, 1801118 (2018).
11. Sly, P. D. et al. Risk Factors for Bronchiectasis in Children with Cystic Fibrosis. N Engl J Med 368, 1963–1970 (2013).
12. Renwick, J. et al. Early Interleukin-22 and Neutrophil Proteins Are Correlated to Future Lung Damage in Children With Cystic Fibrosis. Front. Pediatr. 9, 640184 (2021).
13. Schultz, J. & Kaminker, K. Myeloperoxidase of the leucocyte of normal human blood. I. Content and localization. Archives of Biochemistry and Biophysics 96, 465–467 (1962).
14. Furtmüller, P. G., Burner, U. & Obinger, C. Reaction of Myeloperoxidase Compound I with Chloride, Bromide, Iodide, and Thiocyanate. Biochemistry 37, 17923–17930 (1998).
15. Chapman, A. L. P., Skaff, O., Senthilmohan, R., Kettle, A. J. & Davies, M. J. Hypobromous acid and bromamine production by neutrophils and modulation by superoxide. Biochem J 417, 773–781 (2009).
16. van Dalen, C. J., Whitehouse, M. W., Winterbourn, C. C. & Kettle, A. J. Thiocyanate and chloride as competing substrates for myeloperoxidase. Biochem J 327, 487–492 (1997).
17. Zgliczynski, J. M. Characteristics of Myeloperoxidase from Neutrophils and Other Peroxidases from Different Cell Types. in Biochemistry and Metabolism (eds. Sbarra, A. J. & Strauss, R. R.) 255–278 (Springer US, 1980). doi:10.1007/978-1-4615-9134-4_10.
18. Davies, M. J., Hawkins, C. L., Pattison, D. I. & Rees, M. D. Mammalian Heme Peroxidases: From Molecular Mechanisms to Health Implications. Antioxidants & Redox Signaling 10, 1199–1234 (2008).

19. Xu, S. et al. Influence of plasma halide, pseudohalide and nitrite ions on myeloperoxidase-mediated protein and extracellular matrix damage. Free Radical Biology and Medicine 188, 162–174 (2022).
20. Morgan, P. E. et al. High plasma thiocyanate levels in smokers are a key determinant of thiol oxidation induced by myeloperoxidase. Free Radic Biol Med 51, 1815–1822 (2011).
21. Arnhold, J. et al. Kinetics and Thermodynamics of Halide and Nitrite Oxidation by Mammalian Heme Peroxidases. European Journal of Inorganic Chemistry 2006, 3801–3811 (2006).
22. Hirche, T. O., Gaut, J. P., Heinecke, J. W. & Belaaouaj, A. Myeloperoxidase Plays Critical Roles in Killing Klebsiella pneumoniae and Inactivating Neutrophil Elastase: Effects on Host Defense. The Journal of Immunology 174, 1557–1565 (2005).
23. Aratani, Y. et al. Severe Impairment in Early Host Defense against Candida albicans in Mice Deficient in Myeloperoxidase. Infect Immun 67, 1828–1836 (1999).
24. Feld, M. et al. Proteinase-activated receptor-2 agonist activates anti-influenza mechanisms and modulates IFNγ-induced antiviral pathways in human neutrophils. Biomed Res Int 2013, 879080 (2013).
25. A, U. & Li, L. The effects of neutrophil-generated hypochlorous acid and other hypohalous acids on host and pathogens. Cellular and molecular life sciences : CMLS 78, (2021).
26. Arnhold, J. Heme Peroxidases at Unperturbed and Inflamed Mucous Surfaces. Antioxidants (Basel) 10, 1805 (2021).
27. Hawkins, C. L. & Davies, M. J. Role of myeloperoxidase and oxidant formation in the extracellular environment in inflammation-induced tissue damage. Free Radic Biol Med 172, 633–651 (2021).

28. Pullar, J. M., Vissers, M. C. & Winterbourn, C. C. Living with a killer: the effects of hypochlorous acid on mammalian cells. IUBMB Life 50, 259–266 (2000).
29. Pattison, D. I., Davies, M. J. & Hawkins, C. L. Reactions and reactivity of myeloperoxidase-derived oxidants: differential biological effects of hypochlorous and hypothiocyanous acids. Free Radic Res 46, 975–995 (2012).
30. Hawkins, C. L. Hypochlorous acid-mediated modification of proteins and its consequences. Essays in Biochemistry 64, 75–86 (2019).
31. Davies, M. J. & Hawkins, C. L. The Role of Myeloperoxidase in Biomolecule Modification, Chronic Inflammation, and Disease. Antioxid Redox Signal 32, 957–981 (2020).
32. Karimi, M., Crossett, B., Cordwell, S. J., Pattison, D. I. & Davies, M. J. Characterization of disulfide (cystine) oxidation by HOCl in a model peptide: Evidence for oxygen addition, disulfide bond cleavage and adduct formation with thiols. Free Radical Biology and Medicine 154, 62–74 (2020).
33. Skaff, O. et al. Selenium-containing amino acids are targets for myeloperoxidase-derived hypothiocyanous acid: determination of absolute rate constants and implications for biological damage. Biochem J 441, 305–316 (2012).
34. Barrett, T. J. et al. Inactivation of thiol-dependent enzymes by hypothiocyanous acid: role of sulfenyl thiocyanate and sulfenic acid intermediates. Free Radic Biol Med 52, 1075–1085 (2012).
35. Chandler, J. D., Nichols, D. P., Nick, J. A., Hondal, R. J. & Day, B. J. Selective Metabolism of Hypothiocyanous Acid by Mammalian Thioredoxin Reductase Promotes Lung Innate

Immunity and Antioxidant Defense. Journal of Biological Chemistry 288, 18421–18428 (2013).

36. Shearer, H. L., Pace, P. E., Paton, J. C., Hampton, M. B. & Dickerhof, N. A newly identified flavoprotein disulfide reductase Har protects Streptococcus pneumoniae against hypothiocyanous acid. Journal of Biological Chemistry 298, (2022).
37. Meredith, J. D. et al. Escherichia coli RclA is a highly active hypothiocyanite reductase. Proceedings of the National Academy of Sciences 119, e2119368119 (2022).
38. Forman, H. J. et al. Protein cysteine oxidation in redox signaling: caveats on sulfenic acid detection and quantification. Arch Biochem Biophys 617, 26–37 (2017).
39. Cook, N. L., Moeke, C. H., Fantoni, L. I., Pattison, D. I. & Davies, M. J. The myeloperoxidase-derived oxidant hypothiocyanous acid inhibits protein tyrosine phosphatases via oxidation of key cysteine residues. Free Radic Biol Med 90, 195–205 (2016).
40. McHowat, J., Shakya, S. & Ford, D. A. 2-Chlorofatty Aldehyde Elicits Endothelial Cell Activation. Frontiers in Physiology 11, (2020).
41. Hartman, C. L. et al. 2-Chlorofatty acids induce Weibel-Palade body mobilization. J Lipid Res 59, 113–122 (2018).
42. Palladino, E. N. D. et al. Peroxisome proliferator-activated receptor-α accelerates α-chlorofatty acid catabolism. J Lipid Res 58, 317–324 (2017).
43. Albert, C. J., Crowley, J. R., Hsu, F.-F., Thukkani, A. K. & Ford, D. A. Reactive brominating species produced by myeloperoxidase target the vinyl ether bond of plasmalogens: disparate utilization of sodium halides in the production of alpha-halo fatty aldehydes. J Biol Chem 277, 4694–4703 (2002).

44. Palladino, E. N. D., Hartman, C. L., Albert, C. J. & Ford, D. A. The Chlorinated Lipidome Originating from Myeloperoxidase-Derived HOCl Targeting Plasmalogens: Metabolism, Clearance, and Biological Properties. Arch Biochem Biophys 641, 31–38 (2018).
45. Baliou, S. et al. Bromamine T, a stable active bromine compound, prevents the LPS-induced inflammatory response. International Journal of Molecular Medicine 47, 1–1 (2021).
46. Lorentzen, D. et al. Concentration of the antibacterial precursor thiocyanate in cystic fibrosis airway secretions. Free Radic Biol Med 50, 1144–1150 (2011).
47. Chandler, J. D. et al. Antiinflammatory and Antimicrobial Effects of Thiocyanate in a Cystic Fibrosis Mouse Model. Am J Respir Cell Mol Biol 53, 193–205 (2015).
48. Chandler, J. D., Min, E., Huang, J., Nichols, D. P. & Day, B. J. Nebulized thiocyanate improves lung infection outcomes in mice: Thiocyanate improves lung infection outcomes. Br J Pharmacol 169, 1166–1177 (2013).
49. Ashtiwi, N. M. et al. The Hypothiocyanite and Amantadine Combination Treatment Prevents Lethal Influenza A Virus Infection in Mice. Front Immunol 13, 859033 (2022).
50. Kettle, A. J. et al. Oxidation contributes to low glutathione in the airways of children with cystic fibrosis. European Respiratory Journal 44, 122–129 (2014).
51. Dickerhof, N. et al. Oxidative stress in early cystic fibrosis lung disease is exacerbated by airway glutathione deficiency. Free Radic Biol Med 113, 236–243 (2017).
52. Dickerhof, N. et al. Oxidized glutathione and uric acid as biomarkers of early cystic fibrosis lung disease. Journal of Cystic Fibrosis 16, 214–221 (2017).

53. Loeve, M. et al. Chest computed tomography scores are predictive of survival in patients with cystic fibrosis awaiting lung transplantation. Am J Respir Crit Care Med 185, 1096–1103 (2012).
54. Brody, A. S. et al. Computed Tomography Correlates with Pulmonary Exacerbations in Children with Cystic Fibrosis. Am J Respir Crit Care Med 172, 1128–1132 (2005).
55. Tepper, L. A. et al. Impact of bronchiectasis and trapped air on quality of life and exacerbations in cystic fibrosis. European Respiratory Journal 42, 371–379 (2013).
56. Bortoluzzi, C.-F. et al. Bronchiectases at early chest computed tomography in children with cystic fibrosis are associated with increased risk of subsequent pulmonary exacerbations and chronic pseudomonas infection. Journal of Cystic Fibrosis 13, 564–571 (2014).
57. Roede, J. R., Go, Y.-M. & Jones, D. P. Redox Equivalents and Mitochondrial Bioenergetics. in Mitochondrial Bioenergetics: Methods and Protocols (eds. Palmeira, C. M. & Moreno, A. J.) 197–227 (Springer, 2018). doi:10.1007/978-1-4939-7831-1_12.
58. Milo, R. What is the total number of protein molecules per cell volume? A call to rethink some published values. BioEssays 35, 1050–1055 (2013).
59. Cox, A. G., Peskin, A. V., Paton, L. N., Winterbourn, C. C. & Hampton, M. B. Redox Potential and Peroxide Reactivity of Human Peroxiredoxin 3. Biochemistry 48, 6495–6501 (2009).
60. Schneider, C. A., Rasband, W. S. & Eliceiri, K. W. NIH Image to ImageJ: 25 years of image analysis. Nat Methods 9, 671–675 (2012).
61. Lu, W. et al. Metabolite Measurement: Pitfalls to Avoid and Practices to Follow. Annual Review of Biochemistry 86, 277–304 (2017).

62. MetaboAnalyst 5.0: narrowing the gap between raw spectra and functional insights | Nucleic Acids Research | Oxford Academic. https://academic.oup.com/nar/article/49/W1/W388/6279832.
63. Kanehisa, M. & Goto, S. KEGG: kyoto encyclopedia of genes and genomes. Nucleic Acids Res 28, 27–30 (2000).
64. Kanehisa, M., Furumichi, M., Sato, Y., Kawashima, M. & Ishiguro-Watanabe, M. KEGG for taxonomy-based analysis of pathways and genomes. Nucleic Acids Res gkac963 (2022) doi:10.1093/nar/gkac963.
65. Kanehisa, M. Toward understanding the origin and evolution of cellular organisms. Protein Sci 28, 1947–1951 (2019).
66. Ashby, M. T., Carlson, A. C. & Scott, M. J. Redox Buffering of Hypochlorous Acid by Thiocyanate in Physiologic Fluids. J. Am. Chem. Soc. 126, 15976–15977 (2004).
67. The GAPDH redox switch safeguards reductive capacity and enables survival of stressed tumour cells | Nature Metabolism. https://www.nature.com/articles/s42255-023-00781-3.
68. Peskin, A. V., Turner, R., Maghzal, G. J., Winterbourn, C. C. & Kettle, A. J. Oxidation of Methionine to Dehydromethionine by Reactive Halogen Species Generated by Neutrophils. Biochemistry 48, 10175–10182 (2009).
69. Chalmers, J. D. et al. Neutrophil Elastase Activity Is Associated with Exacerbations and Lung Function Decline in Bronchiectasis. Am J Respir Crit Care Med 195, 1384–1393 (2017).
70. Ali, H. A., Fouda, E. M., Salem, M. A., Abdelwahad, M. A. & Radwan, H. H. Sputum neutrophil elastase and its relation to pediatric bronchiectasis severity: A cross-sectional study. Health Science Reports 5, e581 (2022).

71. Brusselle, G. G. & Van Braeckel, E. Sputum Neutrophil Elastase as a Biomarker for Disease Activity in Bronchiectasis. Am J Respir Crit Care Med 195, 1289–1291 (2017).

72. Fouda, E. M., Ali, H. A., Salem, M. A. A. & Radwan, H. H. Sputum Neutrophil Elastase in pediatric cystic fibrosis and non-cystic fibrosis bronchiectasis. QJM: An International Journal of Medicine 114, hcab113.027 (2021).

73. Groitl, B., Dahl, J.-U., Schroeder, J. W. & Jakob, U. Pseudomonas aeruginosa defense systems against microbicidal oxidants. Molecular Microbiology 106, 335–350 (2017).

74. Buss, I. H. et al. 3-Chlorotyrosine as a Marker of Protein Damage by Myeloperoxidase in Tracheal Aspirates From Preterm Infants: Association With Adverse Respiratory Outcome. Pediatr Res 53, 455–462 (2003).

75. Domigan, N. M., Charlton, T. S., Duncan, M. W., Winterbourn, C. C. & Kettle, A. J. Chlorination of Tyrosyl Residues in Peptides by Myeloperoxidase and Human Neutrophils *. Journal of Biological Chemistry 270, 16542–16548 (1995).

76. Kang, Jr., J. I. & Neidigh, J. W. Hypochlorous Acid Damages Histone Proteins Forming 3-Chlorotyrosine and 3,5-Dichlorotyrosine. Chem. Res. Toxicol. 21, 1028–1038 (2008).

77. Xu, Y., Szép, S. & Lu, Z. The antioxidant role of thiocyanate in the pathogenesis of cystic fibrosis and other inflammation-related diseases. Proc Natl Acad Sci U S A 106, 20515–20519 (2009).

78. Guo, C., Sileikaite, I., Davies, M. J. & Hawkins, C. L. Myeloperoxidase Modulates Hydrogen Peroxide Mediated Cellular Damage in Murine Macrophages. Antioxidants (Basel) 9, 1255 (2020).

79. Morgan, J. F., Campbell, M. E. & Morton, H. J. The nutrition of animal tissues cultivated in vitro. I. A survey of natural materials as supplements to synthetic medium 199. J Natl Cancer Inst 16, 557–567 (1955).

80. Ashby, L. V., Springer, R., Hampton, M. B., Kettle, A. J. & Winterbourn, C. C. Evaluating the bactericidal action of hypochlorous acid in culture media. Free Radical Biology and Medicine 159, 119–124 (2020).

81. Palmer, K. L., Aye, L. M. & Whiteley, M. Nutritional Cues Control Pseudomonas aeruginosa Multicellular Behavior in Cystic Fibrosis Sputum. Journal of Bacteriology 189, 8079–8087 (2007).

82. O'Connor, J. B. et al. Network Analysis to Identify Multi-Omic Correlations in the Lower Airways of Children With Cystic Fibrosis. Front. Cell. Infect. Microbiol. 12, 805170 (2022).

83. Maier, K., Leuschel, L. & Costabel, U. Increased Levels of Oxidized Methionine Residues in Bronchoalveolar Lavage Fluid Proteins from Patients with Idiopathic Pulmonary Fibrosis. Am Rev Respir Dis 143, 271–274 (1991).

84. Magon, N. J. et al. Oxidation of calprotectin by hypochlorous acid prevents chelation of essential metal ions and allows bacterial growth: Relevance to infections in cystic fibrosis. Free Radical Biology and Medicine 86, 133–144 (2015).

85. Skaff, O., Pattison, D. I. & Davies, M. J. Hypothiocyanous acid reactivity with low-molecular-mass and protein thiols: absolute rate constants and assessment of biological relevance. Biochem J 422, 111–117 (2009).

86. Winterbourn, C. C. & Hampton, M. B. Thiol chemistry and specificity in redox signaling. Free Radic Biol Med 45, 549–561 (2008).

87. Sjöberg, B., Foley, S., Cardey, B., Fromm, M. & Enescu, M. Methionine oxidation by hydrogen peroxide in peptides and proteins: A theoretical and Raman spectroscopy study. Journal of Photochemistry and Photobiology B: Biology 188, 95–99 (2018).
88. Thomson, E. et al. Identifying peroxidases and their oxidants in the early pathology of cystic fibrosis. Free Radical Biology and Medicine 49, 1354–1360 (2010).
89. Esther, C. R. et al. Metabolomic biomarkers predictive of early structural lung disease in cystic fibrosis. Eur Respir J 48, 1612–1621 (2016).
90. Esther, C. R. et al. Metabolomic Evaluation of Neutrophilic Airway Inflammation in Cystic Fibrosis. Chest 148, 507–515 (2015).
91. Chandler, J. D. & Esther, C. R. Metabolomics of airways disease in cystic fibrosis. Curr Opin Pharmacol 65, 102238 (2022).
92. Manta, B. & Gladyshev, V. N. Regulated methionine oxidation by monooxygenases. Free Radic Biol Med 109, 141–155 (2017).
93. Lee, B. C. & Gladyshev, V. N. The biological significance of methionine sulfoxide stereochemistry. Free Radic Biol Med 50, 221–227 (2011).
94. Zoeller, R. A. et al. Plasmalogens as endogenous antioxidants: somatic cell mutants reveal the importance of the vinyl ether. Biochem J 338, 769–776 (1999).
95. Skaff, O., Pattison, D. I. & Davies, M. J. The Vinyl Ether Linkages of Plasmalogens Are Favored Targets for Myeloperoxidase-Derived Oxidants: A Kinetic Study. Biochemistry 47, 8237–8245 (2008).
96. Skaff, O., Pattison, D. I. & Davies, M. J. Kinetics of Hypobromous Acid-Mediated Oxidation of Lipid Components and Antioxidants. Chem. Res. Toxicol. 20, 1980–1988 (2007).

97. Pattison, D. I., Hawkins, C. L. & Davies, M. J. Hypochlorous Acid-Mediated Oxidation of Lipid Components and Antioxidants Present in Low-Density Lipoproteins: Absolute Rate Constants, Product Analysis, and Computational Modeling. Chem. Res. Toxicol. 16, 439–449 (2003).

98. Go, Y.-M., Chandler, J. D. & Jones, D. P. The cysteine proteome. Free Radical Biology and Medicine 84, 227–245 (2015).

99. Paulsen, C. E. & Carroll, K. S. Cysteine-mediated redox signaling: chemistry, biology, and tools for discovery. Chem Rev 113, 4633–4679 (2013).

100. Love, D. T. et al. Cellular targets of the myeloperoxidase-derived oxidant hypothiocyanous acid (HOSCN) and its role in the inhibition of glycolysis in macrophages. Free Radic Biol Med 94, 88–98 (2016).

101. Christodoulou, D. et al. Reserve Flux Capacity in the Pentose Phosphate Pathway by NADPH Binding Is Conserved across Kingdoms. iScience 19, 1133–1144 (2019).

102. Son, S. M. et al. Leucine Signals to mTORC1 via Its Metabolite Acetyl-Coenzyme A. Cell Metab 29, 192-201.e7 (2019).

103. Nwosu, Z. C., Song, M. G., di Magliano, M. P., Lyssiotis, C. A. & Kim, S. E. Nutrient transporters: connecting cancer metabolism to therapeutic opportunities. Oncogene 42, 711–724 (2023).

Chapter 3

Substrate-dependent transcriptomic signatures of myeloperoxidase-derived oxidants in airway epithelial cells

3.1 Abstract

In progressive lung diseases such as chronic obstructive pulmonary disease (COPD) and cystic fibrosis (CF), recurring airway obstruction, infection, and inflammation culminate in the decline of lung function and ultimately lead to respiratory failure. During inflammation, potent oxidants are produced by myeloperoxidase (MPO) as a defense against pathogens. These oxidants, referred to as (pseudo)hypohalous acids (HOX), include hypochlorous acid (HOCl), hypobromous acid (HOBr), and hypothiocyanous acid (HOSCN). Chronic exposure to HOX, especially HOCl, has been implicated in the pathogenesis of chronic lung diseases and can cause severe oxidative stress to airway epithelial cells (AECs), which are at the frontline of inflammation. HOX have varying cytotoxic effects and we have previously shown that AECs exposed to enzymatically generated HOX are viable during an acute exposure of 2 hours, but only HOSCN-treated AECs evade cell death during a continuous 24-hour exposure. In this study, we sought to 1) define the early transcriptional responses of AECs during HOX exposure and 2) understand how AECs adapt to HOSCN exposure to prevent cell death. Using an enzymatic oxidant exposure model with glucose oxidase (GOX) coupled to MPO and substrate (Cl^-, Br^-, or SCN^-), we compared the effects of GOX/MPO, GOX/MPO/Br^-, and GOX/MPO/SCN^- (favoring HOCl, HOBr, and HOSCN formation, respectively) on the transcriptome of normal human bronchoepithelial cells (BEAS-2B) via RNA sequencing (RNA-Seq). We observed substrate-dependent effects on gene expression in AECs *in vitro*, suggesting diverse transcriptional programs and cell signaling roles of HOX that potentially contribute to the (mal)adaptation of AECs *in vivo*. Each HOX exposure group increased expression of the pro-inflammatory cytokine genes encoding for IL-1A and IL-1B, however, GOX/MPO/SCN^- had the greatest impact in addition to inducing the expression of other cytokines (*IL24*) and chemokines (*CXCL8*, *CXCL3*,

CXCL2), suggestive of sustained neutrophilic inflammation. To circumvent oxidative stress early in exposure, evidence suggests GOX/MPO/SCN^- activates the antioxidant Nrf2 signaling pathway – apparent through the significant increase in Nrf2-target genes *GCLM*, *SLC7A11*, *TXNRD1*, *NQO1*, and *HMOX1*. While each oxidant exposure group uniquely altered diverse biological pathways, GOX/MPO/SCN^- significantly induced robust changes in gene expression related to MAPK signaling and FGFR/EGFR signaling to potentially aid in AEC survival to chronic exposure. These findings provide novel insights into the role of HOX in AECs. Future research is warranted to validate these gene targets and signaling pathways.

3.2 Introduction

Neutrophils form an essential component of the innate immune response, particularly through their ability to mount an oxidative burst, a metabolic process that generates potent reactive oxygen species (ROS) to eliminate pathogens[1]. An enzyme central to the oxidative burst is myeloperoxidase (MPO), which is abundantly released from the primary granules of neutrophils[2]. MPO reduces hydrogen peroxide (H_2O_2) and oxidizes (pseudo)halide ions (e.g., chloride; Cl^-, bromide; Br^-, and thiocyanate; SCN^-) to generate hypochlorous acid (HOCl), hypobromous acid (HOBr), and hypothiocyanous acid (HOSCN), collectively referred to as hypohalous acids (HOX)[3–5]. HOX exert powerful antimicrobial activities against invading pathogens[6–8], however, the same strong oxidizing properties can also cause injury to the host tissue, with airway epithelial cells (AECs) being at the forefront of inflammation. A greater understanding of how HOX impact the gene expression and regulation of AECs can potentially expose pathways of (mal)adaptation and ultimately modes of intervention.

The unique chemical properties of each HOX can influence its reactivity with biomolecules, potentially triggering distinct transcriptomic responses in AECs that correspond to their ability to maintain homeostatic conditions during severe oxidative stress. HOCl and HOBr are potent chlorinating/brominating and oxidizing agents – they can oxidize a range of biomolecules including proteins, lipids, and DNA and their oxidative byproducts (e.g., methionine sulfoxide, dehydromethionine, and glutathione sulfonamide) have been associated with increased lung damage in patients with CF[9–14]. Although HOSCN is less reactive, it has a greater specificity for thiols and selenols[15,16]. HOSCN can elicit redox signaling by targeting cysteine and selenocysteine-containing proteins such as protein tyrosine phosphatases (PTPs). Modification of active site cysteine resides occurs when exposed to pathophysiological amounts

of HOSCN and causes a loss of PTP activity and downstream apoptosis via the mitogen-activated protein kinase (MAPK) pathway [17]. In addition to the MAPK signaling pathway, HOX can induce a diversity of signal transduction pathways. For example, both HOSCN and HOCl can induce the expression of different pro-inflammatory gene targets of the NF-κB signaling pathway, which is crucial for the regulation of innate and adaptive immune functions[18–21]. Additionally, to maintain redox homeostasis during oxidative stress, HOCl can activate the Keap1/Nrf2 pathway and increase Nrf2-target genes (i.e., *GCLM*, *SLC7A11*, *TXNRD1*, *NQO1*, *HMOX1*) that encode for proteins involved in detoxification and elimination of ROS[18,20,22–24]. Currently, much remains to be discovered about the totality of gene expression changes and signaling alterations associated with each HOX.

This study aims to fill the knowledge gap by using RNA-Seq analysis of AECs exposed to enzymatically generated HOX *in vitro* to explore how these potent oxidants impact the transcriptome of AECs. Our findings indicate that each HOX differentially impacts the expression of many genes and alters distinct biological pathways in AECs, shedding light on potential mechanisms that AECs use to (mal)adapt to oxidative stress. Novel insights into the substrate-specific effects of MPO-derived oxidants in the context of chronic inflammatory lung diseases, may open potential new avenues for therapeutic intervention.

3.3 Methods & materials

Culture of BEAS-2B cells

BEAS-2B cells (ATCC CRL-9609) were grown in T-75 flasks with RPMI-1640 plus 10% FBS and 1X Penn-Strep in a humidified cell culture incubator with 5% CO_2 at 37°C. After reaching approximately 85% confluence, the cells were washed, detached with trypsin, and seeded in 35 mm dishes overnight to achieve near-confluence for the experiments.

HOX exposure model

Glucose oxidase (Sigma G0543) was dissolved to final 2 U/L in media, generating 0.4899 μM H_2O_2 per minute, which was measured with the Amplex Red reagent (Invitrogen A12222). Excess MPO (200 U/L) isolated from human neutrophils was added to generate hypohalous acids (no other excipients for HOCl, or 1 mM of either sodium bromide or sodium thiocyanate for HOBr or HOSCN, respectively), or no additions were made (H_2O_2 control). Cells were gently washed with pre-warmed PBS prior to exposure and then exposed to the pre-warmed reagents in Medium-199 containing 100 pg/ml recombinant human EGF (MilliporeSigma) and 0.1% FBS for 2 hours.

RNA-Seq

Immediately after oxidant exposure, the media was aspirated from the cells. Total RNA was extracted from the cells using QIAazol lysis reagent (Qiagen) and purified using Qiagen miRNeasy Mini kits (Qiagen) according to the manufacturer's instructions. Purified RNA was further processed by Emory Integrated Genomics Core (GA, USA) who subjected samples to quality control analysis, and generated RNA-Seq libraries. The quality of all RNA samples was confirmed using a Bioanalyzer, with an RNA integrity number (RIN) of ≥8.4, indicating high quality. The libraries were constructed using polyA enrichment and subjected to 50 million

paired-end reads sequencing per sample using the Illumina HiSeq v4 platform at Hudson Alpha (AL, USA). Fastq files were mapped to the Homo_sapiens.GRCh37 reference genome using HISAT2 which detected 51,276 transcripts from the RefSeq database.

To increase sensitivity and precision of differentially expressed gene detection, we filtered low-expression genes that had less than 10 counts in 70% of the samples using the EdgeR package (version 3.38.4) in RStudio (version 4.2.1), available at https://www.R-project.org. Then, we applied DESeq's normalization function median of ratios to the dataset. The results were a normalized read count of 24,389 transcripts that were considered for all downstream analyses.

Differential expression gene analysis

To identify DEGs in oxidant groups compared to the untreated control group, we used DESeq2 R package (version 1.36.0) with the criteria of Benjamini-Hochberg (BH) adjusted p-value of less than 0.05 and absolute $\log_2$ fold-change greater than 1 set as cut-off values for significant DEGs.

Gene ontology (GO) enrichment analyses

To attain shared biological processes and pathways among HOX groups, we used Metascape[25] (version 3.5, http://metascape.org) for multi-group functional enrichment analysis of the DEGs from GOX/MPO, GOX/MPO/Br^- and GOX/MPO/SCN^- samples. The lists of annotated genes were submitted to Metascape for enrichment analysis based on the significant overrepresentation of GO biological processes, KEGG pathways, Reactome pathways, Pathway Interaction Database (PID) pathways, and WikiPathways (WP). Terms with an adjusted p-value threshold of <0.05 were considered significant and were represented in the plots.

Gene set enrichment analyses

We performed ranked gene analyses using Gene set enrichment analysis (GSEA) software (version 4.3.2) to identify gene sets and gene expression changes associated with exposure of AECs with each oxidant group. Analyses were performed with log_2-transformed normalized read counts. The analysis used the Reactome gene set database with the settings of performance: 1000 permutations, gene_set for permutation type, classic for enrichment statistic, and Signal2Noise metric for ranking genes.

Statistical analysis

Principal component analysis (PCA) was used to visualize the global effect of substrate-dependent oxidant exposure. Heatmaps were z-scored per transcript, and a hierarchical clustering analysis was performed using Euclidean distance and Ward clustering algorithm. Scatterplots and heatmaps were generated using the Seaborn package (version 0.12.2) in Python (version 3.9.13), available at http://www.python.org.

3.4 Results

To study the effects of substrate-dependent HOX on the transcriptome of BEAS-2B cells, a noncancerous immortalized human bronchoepithelial cell line, we employed an *in vitro* oxidant exposure model that resembles the enzymatic production of HOX (**Figure 3.1**). The model produces equal dose-rate exposures of HOX via generation of rate-limiting H_2O_2 using GOX (2 U/L) and the addition of excess MPO (200 U/L) and (pseudo)halide substrate. The reactions were carried out in Medium-199, a nutrient-rich media chosen to reflect the complexity of the airway microenvironment. Because chloride is abundantly present in the Medium-199 at a concentration of 116 mM, HOCl (GOX/MPO) is formed upon addition of GOX and MPO. We added 1 mM NaBr or 1 mM NaSCN to favor production of HOBr (GOX/MPO/Br^-) or HOSCN (GOX/MPO/SCN^-), respectively. MPO preferably generates HOBr and HOSCN over HOCl when Br^- and SCN^- are present due to the higher specificity constant of MPO for those substrates compared to Cl^-[13,26,27]. Br^- and SCN^- can also directly interact with HOCl to produce either HOBr or HOSCN, respectively. Therefore, the predominant HOX species produced is dependent on the supplemented substrate. We included AECs exposed to GOX alone as H_2O_2 negative control in addition to including an untreated AEC control. An exposure duration of 2 hours was chosen to assess early transcriptional changes that occur from HOX exposure. The RNA-seq Illumina platform detected 51,276 transcripts annotated from the RefSeq database and after removing low-quality reads a total of 24,389 transcripts were used for all subsequent analyses.

HOX greatly differ in their global transcriptional impact on AECs

First, we assessed the unbiased global variation in the transcriptome of AECs exposed to HOX. We performed a PCA and found that each HOX clustered

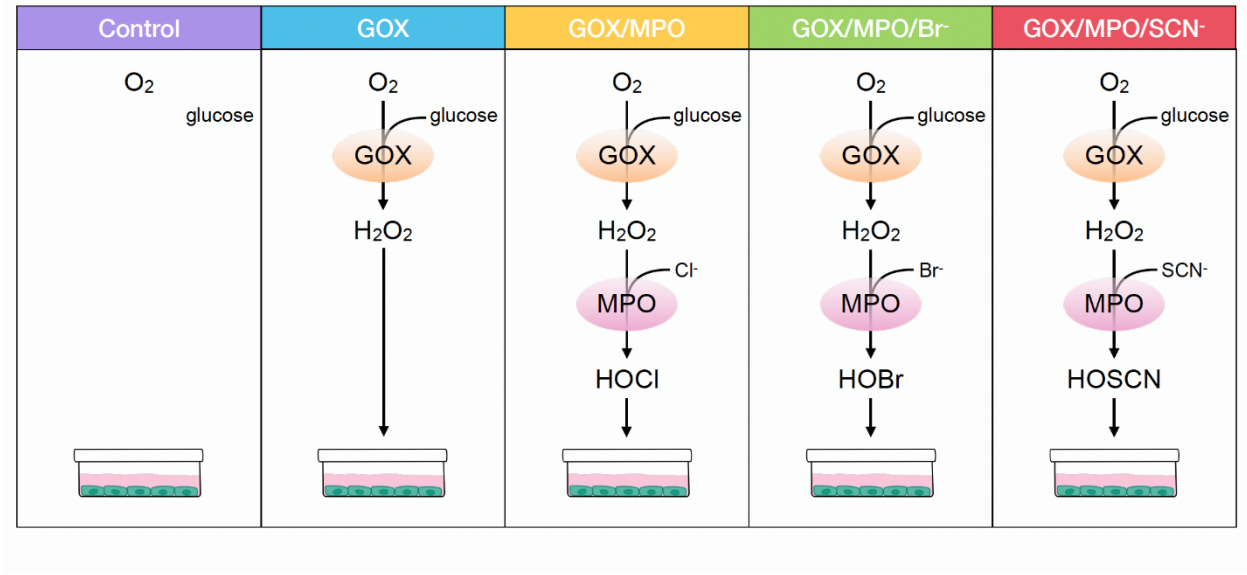

Figure 3.1 Schematic of H_2O_2 and MPO-derived HOX generation *in vitro*. The oxidant exposure model uses rate-limiting glucose oxidase (GOX) to produce H_2O_2 and the addition of excess MPO oxidizes Cl^- from the media to produce HOCl. The addition of 1 mM Br^- or 1 mM SCN^- reacts directly with MPO or HOCl to generate the favored products HOBr or HOSCN, respectively.

individually from one another and from GOX and untreated control in the first principal component (PC1) that accounted for 16.47% of the variation in the dataset (**Figure 3.2A**). The variation in PC1 was driven by GOX/MPO/SCN^- which displayed the greatest separation from all the other groups. Genes involved in immunomodulation (e.g., *CXCL8* and *CCL2*) and cell signaling (e.g., *RND3* and *TNFRSF10D*) contributed to PC1 (**Figure 3.2B**). The second principal component (PC2), which accounted for 13.79% of the variation in the dataset, shows overlap of all the HOX groups but deviation from GOX and untreated controls. The overall results from the PCA indicate that the transcriptional programming of HOCl, HOBr, and HOSCN greatly differ from one another, but the HOX still share enough similarities in their transcriptional effects on AECs that differentiate them from their precursor H_2O_2.

DEG analyses reveal HOX transcriptional signatures in AECs

DEG analyses were performed for each oxidant exposure group (GOX, GOX/MPO, GOX/MPO/Br^-, and GOX/MPO/SCN^-) compared to untreated control. A threshold of adjusted p-value of less than 5% and a $\log_2$ normalized fold-change of greater than 1 or less than -1 were applied and resulted in different total upregulated and downregulated transcripts in each oxidant group that are represented in volcano plots (**Figure 3.3A-D**). DEG analysis of GOX alone compared to untreated control revealed 22 significantly upregulated genes and 19 significantly downregulated genes (**Figure 3.3A**). GOX/MPO, which produces HOCl, resulted in 45 and 39 significantly upregulated and downregulated DEGs, respectively (**Figure 3.3C**). GOX/MPO/Br^-, which favors HOBr production, yielded 109 and 163 significantly upregulated and downregulated DEGs, respectively (**Figure 3.3B**). GOX/MPO/SCN^-, which favors HOSCN production, yielded 178 and 135 significantly upregulated and downregulated DEGs, respectively (**Figure 3.3D**).

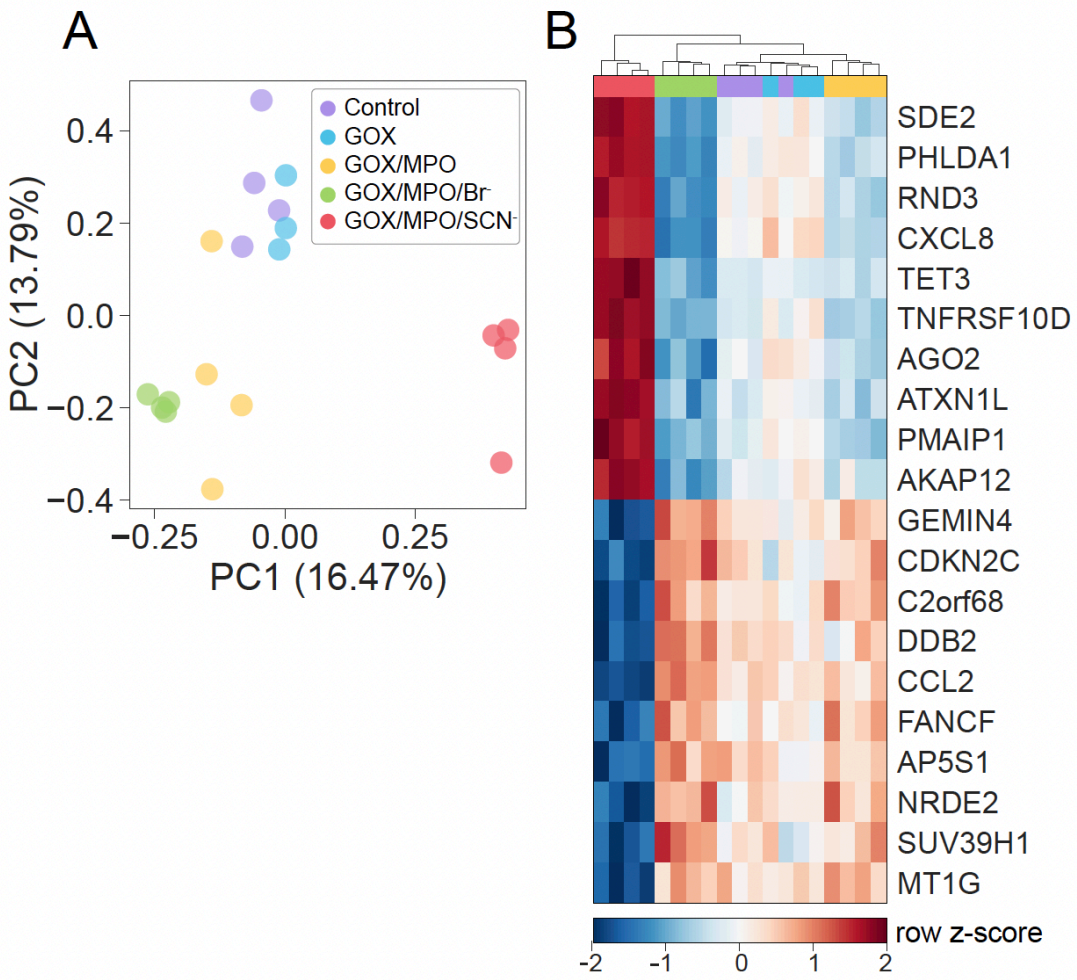

Figure 3.2 PCA score plot reveals transcriptional divergence of HOX from H_2O_2 treated and untreated AECs (A). Heatmap of the top 20 transcripts contributing to PC1 reveals genes significantly altered in GOX/MPO/SCN^- exposed AECs (B). Samples were hierarchical clustered, using Euclidean distance, and normalized read counts were z-scored across rows and expressed on a red (high) to blue (low) scale.

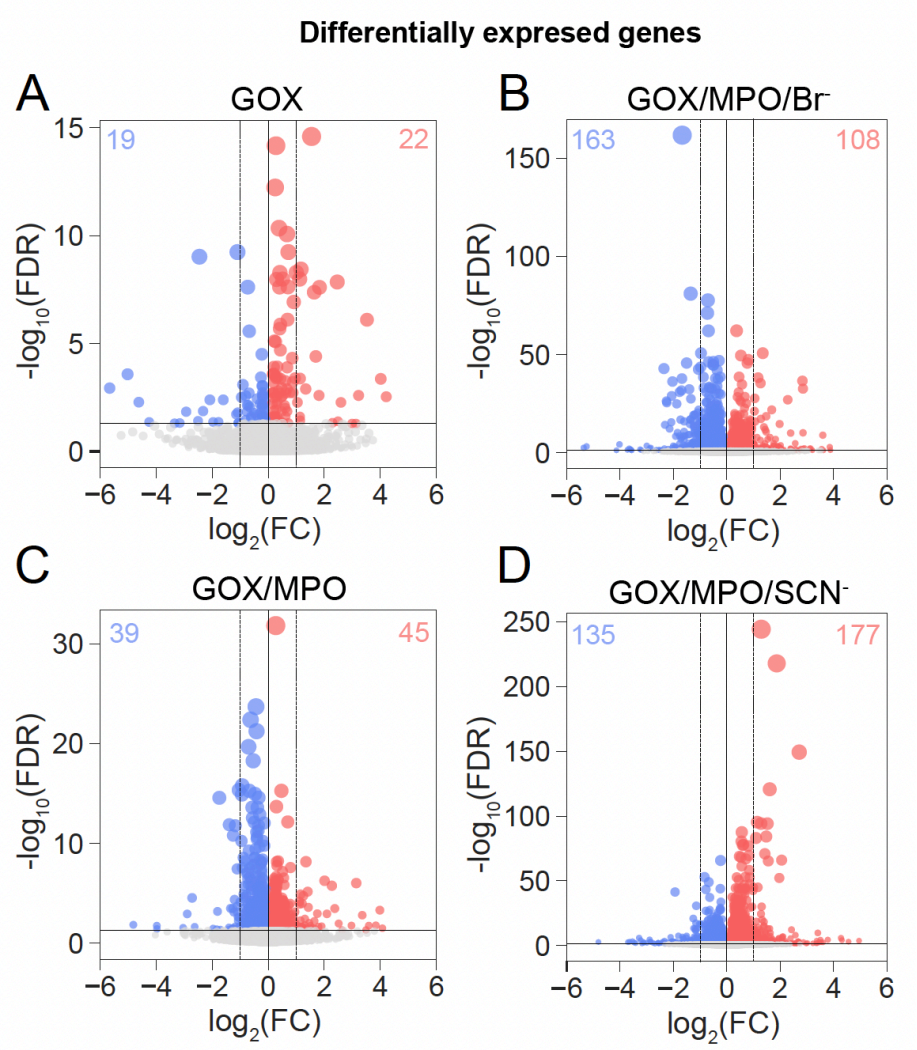

Figure 3.3 Volcano plot of the differentially expressed genes in each experimental group versus control. The significance (adjusted p-value) on the y-axis and the fold-change (oxidant/control) on the x-axis are converted to $-\log_{10}(\text{FDR})$ and $\log_2(\text{FC})$, respectively, for GOX alone (A), GOX/MPO/Br- (B), GOX/MPO (C), and GOX/MPO/SCN^- (D). The vertical and horizontal dotted lines show the cut-off of fold-change > |1|, and of FDR < 0.05, respectively. Transcripts that did not meet the significance threshold are denoted by the gray dots. Upregulated genes in the oxidant groups are represented by the red markers and downregulated genes are represented by the blue markers.

To quantify the overlap of DEGs between the oxidant exposure groups, we created four-way Venn diagrams for significantly upregulated DEGs (**Figure 3.4A**) and significantly downregulated DEGs (**Figure 3.4B**). The Venn diagrams revealed 13, 19, 76, and 136 unique upregulated DEGs for GOX, GOX/MPO, GOX/MPO/Br^-, and GOX/MPO/SCN^-, respectively, and 13, 10, 135, and 115 unique downregulated DEGs. The significant DEGs across all the groups were projected onto a heatmap, clustered using Euclidean distance, and z-scored across rows for the normalized read counts (**Figure 3.4C**). Samples clustered into their respective experimental groups without any overlap, supporting the idea that the transcriptional programming in AECs is substrate-dependent and that HOX have unique roles in AECs.

HOX impact similar biological processes, but with diverse transcriptional programs

To assess the convergent roles HOX may play in AECs, we performed a multi-group GO enrichment analysis between the significant DEG lists from GOX/MPO, GOX/MPO/Br^-, and GOX/MPO/SCN^- using Metascape. The biological processes enriched in the analysis included the regulation of cell death (GO:2001233 and GO:0010942), response to growth factor and hormones (GO:0070848 and GO:009725), and response to stress (GO:0080135) as several of the most significantly enriched terms (**Figure 3.5**). The list of significant pathways also included various cell signaling pathways and processes implicated in signal transduction such as PID/AP1 pathway (M167), diseases of signal transduction by GFRs and 2^{nd} messengers (R-HSA-5663202), nuclear receptors meta-pathway (WP2882), regulation of intracellular signal transduction (GO:1902532), and regulation of protein phosphorylation (GO:0001934).

We chose to evaluate the GO biological processes (GO:BP) regulation of cellular response to stress and response to growth factor in depth to gain an understanding of how AECs

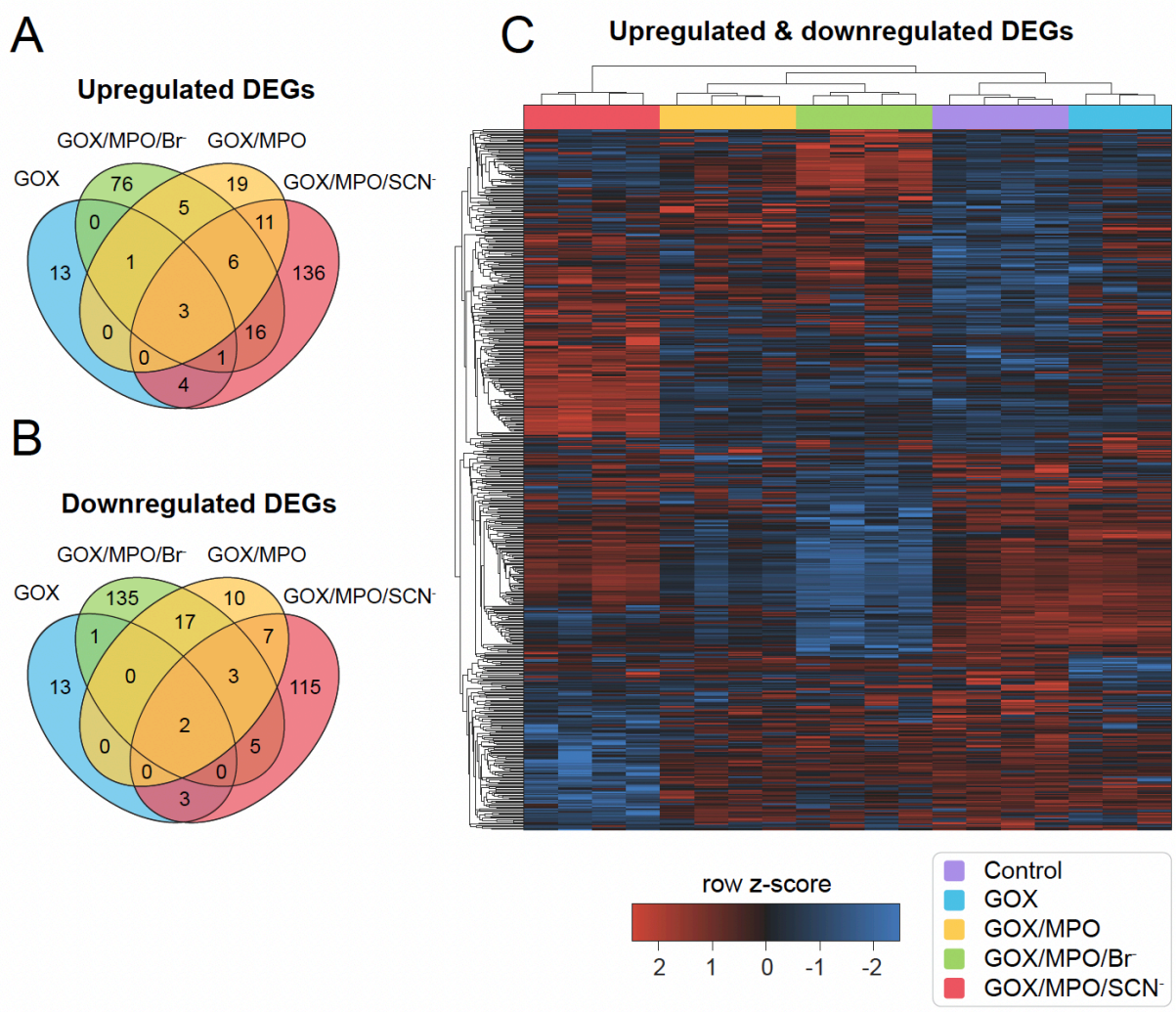

Figure 3.4 Unique transcriptomic profiles are revealed within substrate dependent MPO activity in AECs exposed to the oxidant model for 2 hours. Four-way venn diagram of upregulated differentially expressed genes (DEGs) (A) and downregulated DEGs (B) from each experimental group show a differential number of unique gene counts. Significant DEGs (FDR<0.05) were projected onto a heatmap and row z-scored with genes counts increased in red and gene counts decreased in blue (C).

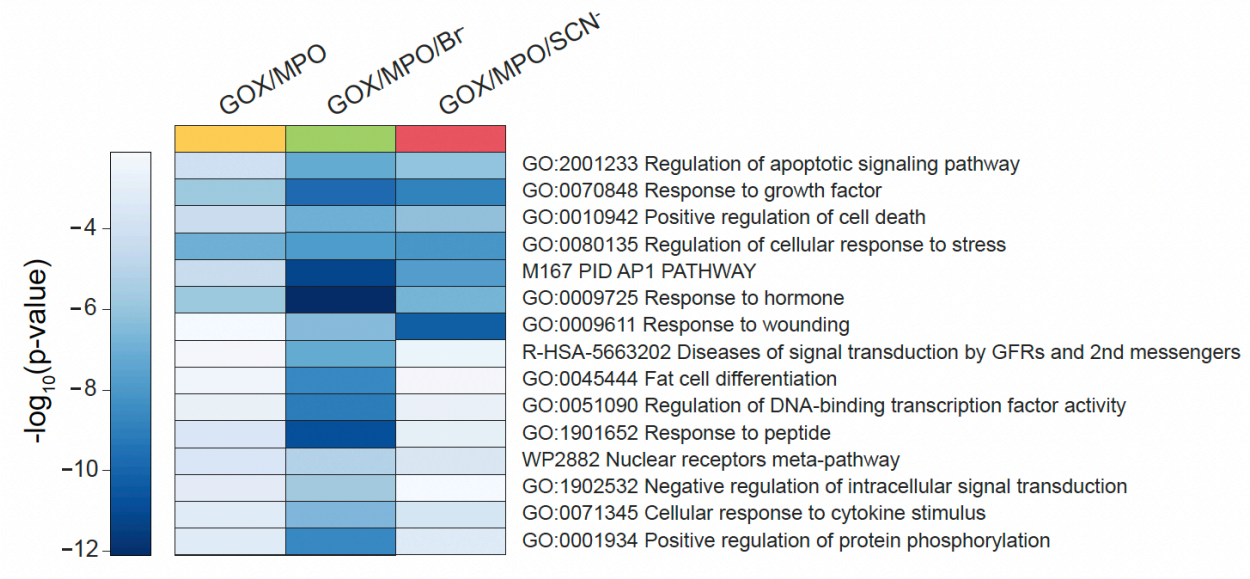

Figure 3.5 Heatmap of top 15 HOX enriched terms. Each term enriched across at least 2 experimental groups from gene ontology (GO) enrichment analysis that includes GO biological processes, KEGG pathways, Reactome pathways, Pathway Interaction Database (PID) pathways, and WikiPathways (WP). Values represent negative $\log_{10}$ transformed p-values with the increasing darker blue color corresponding to a greater significance.

may be adapting to the oxidative stress imposed by HOX. The regulation of cellular response to stress included a network of 10 GO:BP terms that primarily included response to DNA damage and regulation of DNA repair (**Figure 3.6A**). To identify HOX-specific transcriptional patterns, we projected the genes involved in the regulation of cellular response to stress onto a heatmap (**Figure 3.6B**). Three clusters of genes significantly altered in HOX compared to untreated control were evident – the first cluster included genes upregulated in GOX/MPO/Br^- exposed AECs, the second cluster included genes upregulated in GOX/MPO/SCN^- exposed AECs and a third cluster of genes uniquely downregulated in GOX/MPO and GOX/MPO/Br^- exposed AECs. Next, the response to growth factor included four GO:BP terms that included receptor protein tyrosine kinase (RTKs) signaling pathway and responses to growth factor (**Figure 3.7A**). We identified four prominent clusters of genes involved in response to growth factor that were significantly altered in HOX compared to untreated control. The first cluster included genes uniquely upregulated in GOX/MPO/Br^- exposed AECs, the second cluster included genes uniquely upregulated in AECs exposed to GOX/MPO/SCN^-, the third cluster included genes downregulated in GOX/MPO/Br^- and GOX/MPO/SCN^- exposed AECs, and the fourth cluster involved genes downregulated in GOX/MPO and GOX/MPO/Br^- exposed AECs (**Figure 3.7B**).

HOX alter diverse set of Reactome pathways in AECs

Next, we sought to determine the biological pathways that differentiate the individual oxidant exposures. We performed GSEA using Reactome GeneSets and selected the top 40 most significantly altered biological pathways to display – 20 of which were the most significantly upregulated and 20 that were most significantly downregulated in a comparison of each oxidant against all groups (**Figure 3.8-3.11**). GOX-treated cells significantly upregulated GPCR signaling and receptor binding pathways while downregulated many pathways related

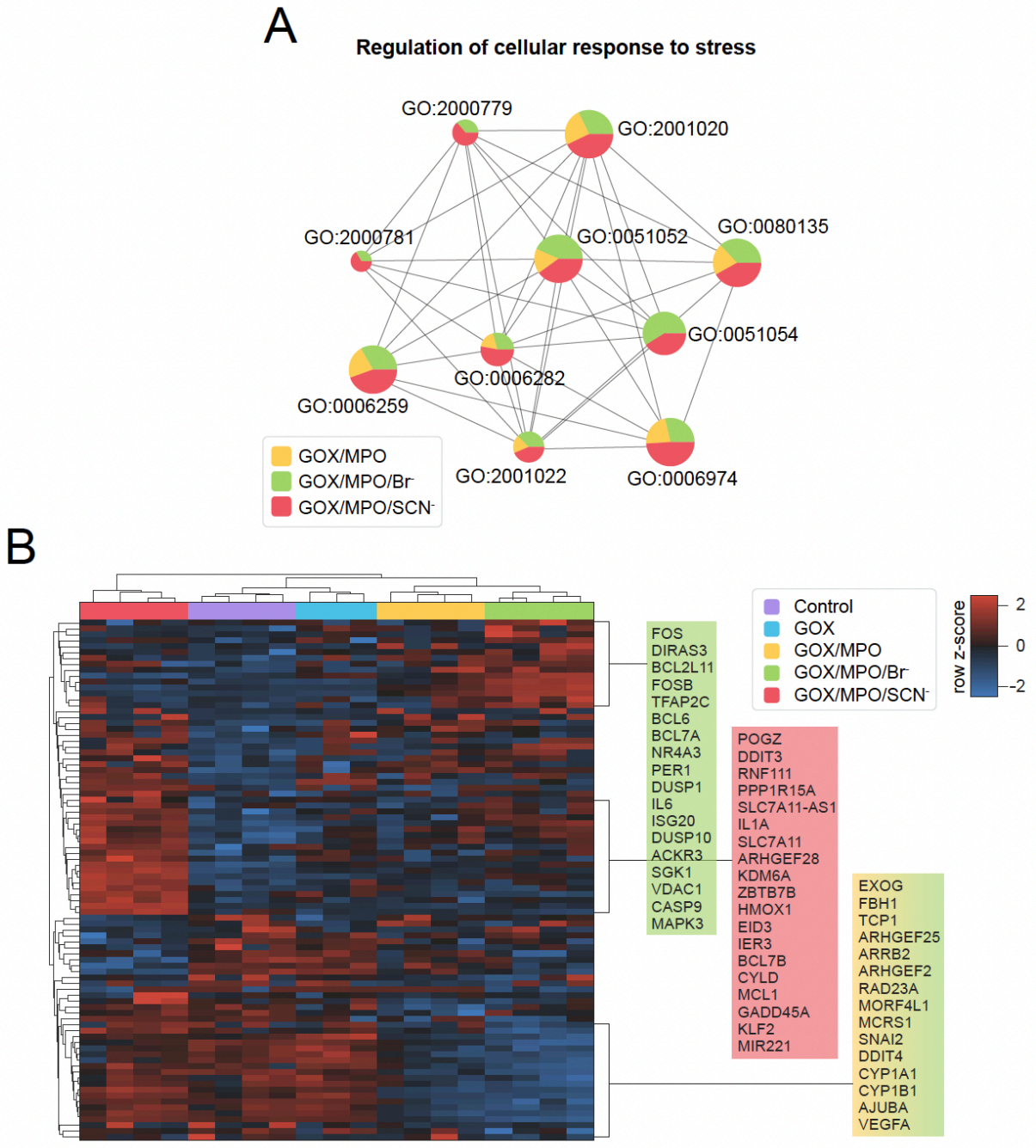

Figure 3.6 HOX may impact the regulation of cellular response to stress in AECs from diverse transcriptional programs that are substrate dependent. Network of enriched terms related to regulation of cellular response to stress represented as a pie chart where the size of the nodes is proportional to the number of genes that fall into an enriched term (A). The pie charts

are color-coded based on group: GOX/MPO (yellow), GOX/MPO/Br^- (green), and GOX/MPO/SCN^- (red), and the size of the slice represents the percentage of genes under the enriched term that came from the corresponding gene list. A heatmap of z-scored genes involved in the network of enriched terms reveal substrate-dependent effects (B). Samples and genes were hierarchically clustered, using Euclidean distance, and normalized read counts were expressed on a red (high) to blue (low) scale. Select cluster of genes are labeled to the right of the heatmap and colored based on the experimental group that is differentially expressed compared to untreated control samples (purple).

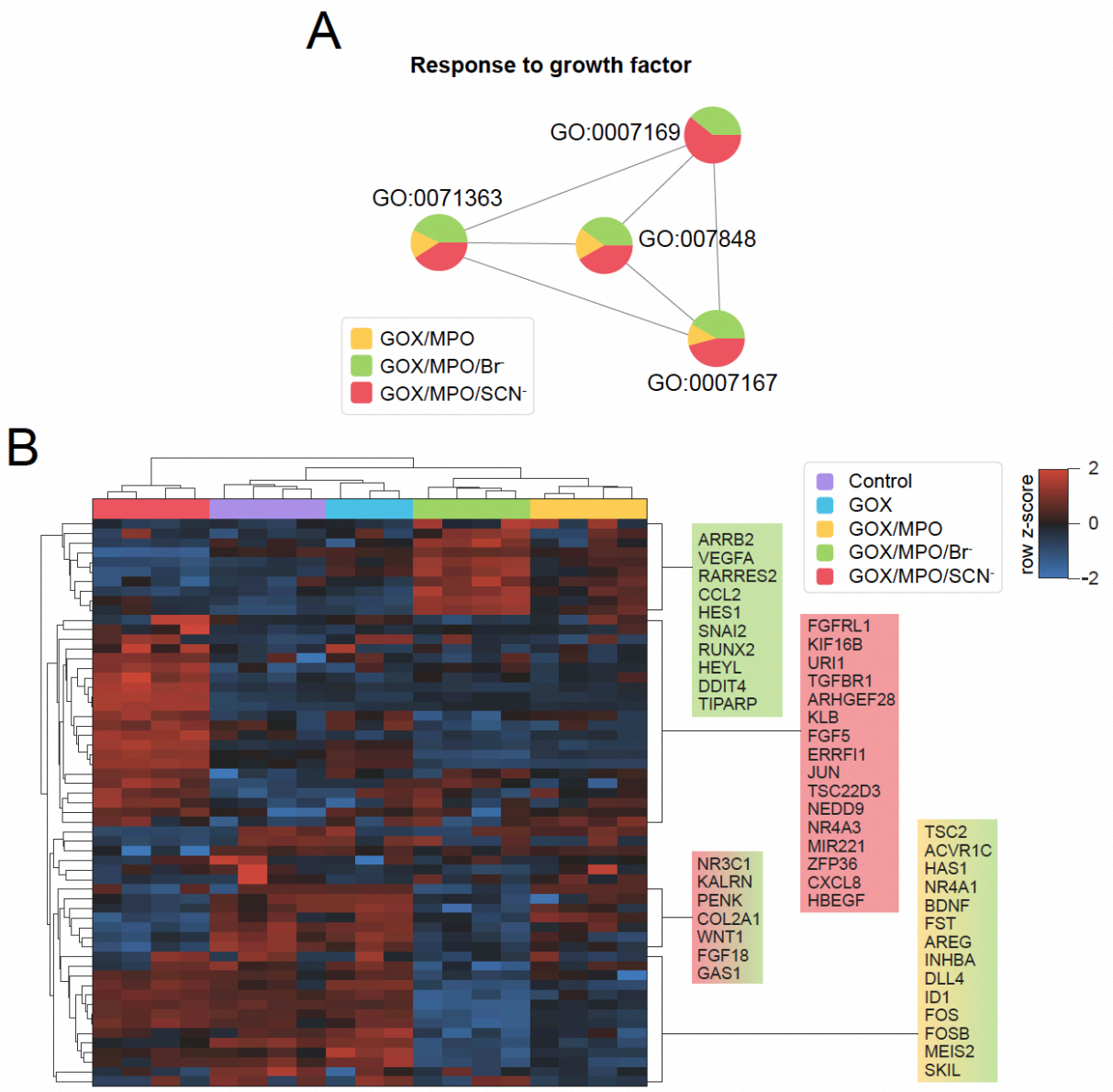

Figure 3.7 HOX may elicit responses to growth factors in AECs from diverse transcriptional programs that are substrate-dependent. Network of enriched terms related to regulation of cellular response to stress represented as a pie chart where the size of the nodes is proportional to the number of genes that fall into an enriched term (A). The pie charts are color-coded based on group: GOX/MPO (yellow), GOX/MPO/Br^- (green), and GOX/MPO/SCN^- (red), and the size of the slice represents the percentage of genes under the enriched term that came

from the corresponding gene list. A heatmap of z-scored genes involved in the network of enriched terms reveal substrate-dependent effects (B). Samples and genes were hierarchically clustered, using Euclidean distance, normalized read counts were expressed on a red (high) to blue (low) scale. Select cluster of genes are labeled to the right of the heatmap and colored based on the experimental group that is differentially expressed compared to untreated control samples (purple).

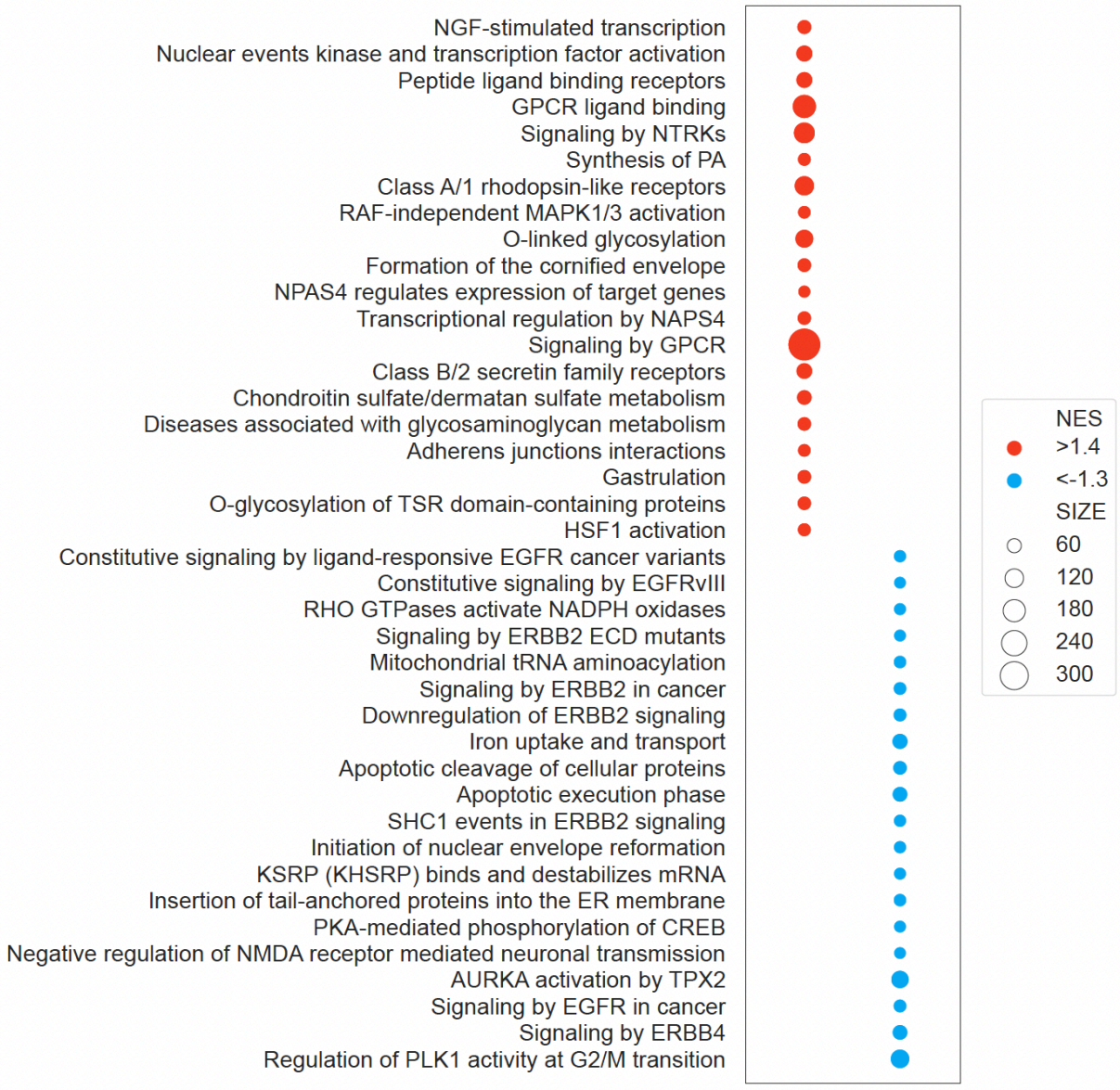

Figure 3.8 Most significant Reactome gene sets altered by GOX in AECs compared to all groups from GSEA. Top 20 upregulated pathways represented with a positive normalized enrichment score (NES) in red and top 20 downregulated pathways with a negative NES score in blue displayed by descending statistical significance. The marker size corresponds to gene count within the given gene set. GSEA $p < 0.05$ for all pathways shown.

Figure 3.9 Most significant Reactome gene sets altered by GOX/MPO in AECs compared to all groups from GSEA. Top 20 upregulated pathways represented with a positive normalized enrichment score (NES) in red and top 20 downregulated pathways with a negative NES score in blue displayed by descending statistical significance. The marker size corresponds to gene count within the given gene set. GSEA $p < 0.05$ for all pathways shown.

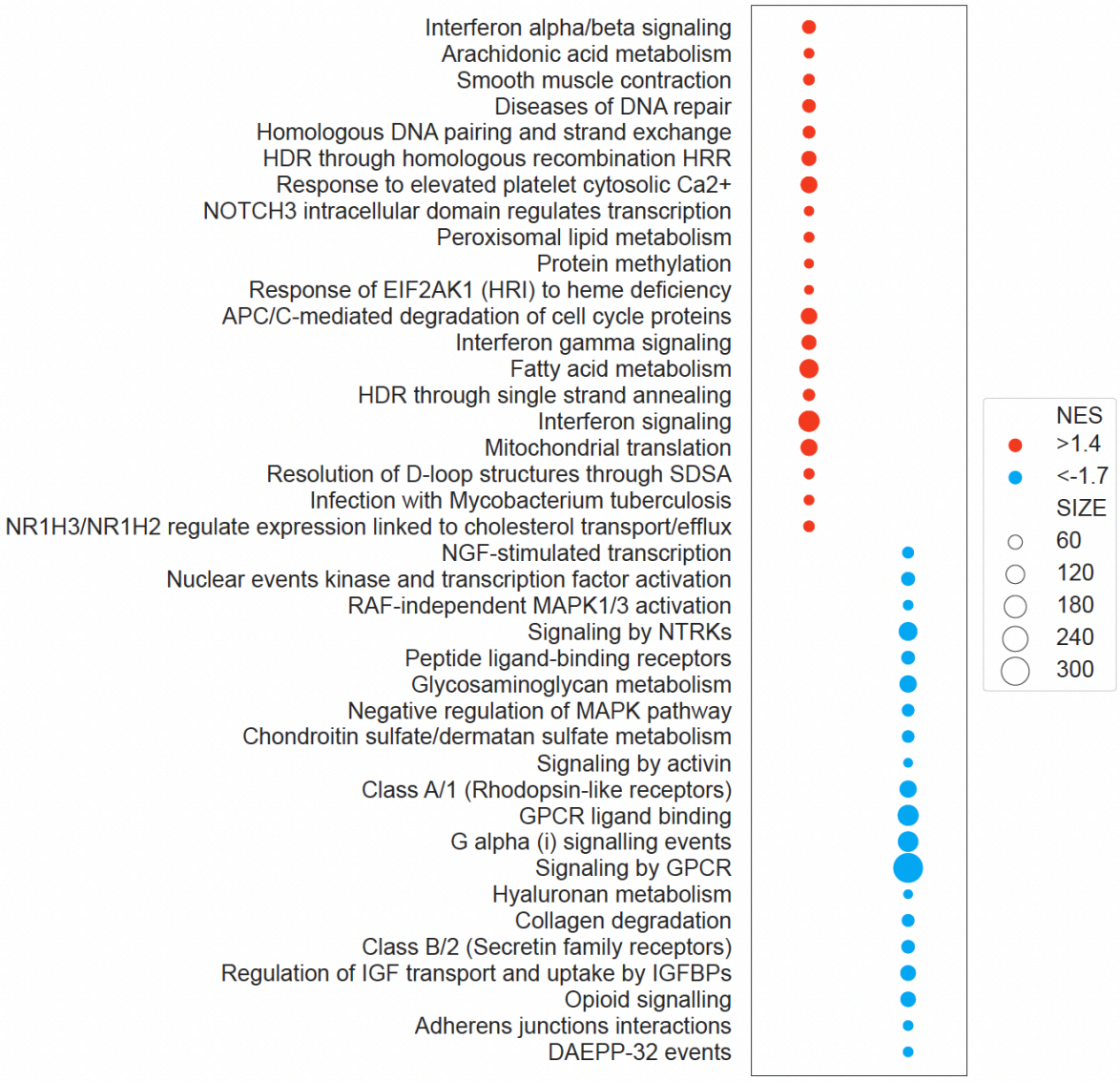

Figure 3.10 Most significant Reactome gene sets altered by GOX/MPO/Br- in AECs compared to all groups from GSEA. Top 20 upregulated pathways represented with a positive normalized enrichment score (NES) in red and top 20 downregulated pathways with a negative NES score in blue displayed by descending statistical significance. The marker size corresponds to gene count within the given gene set. GSEA $p < 0.05$ for all pathways shown.

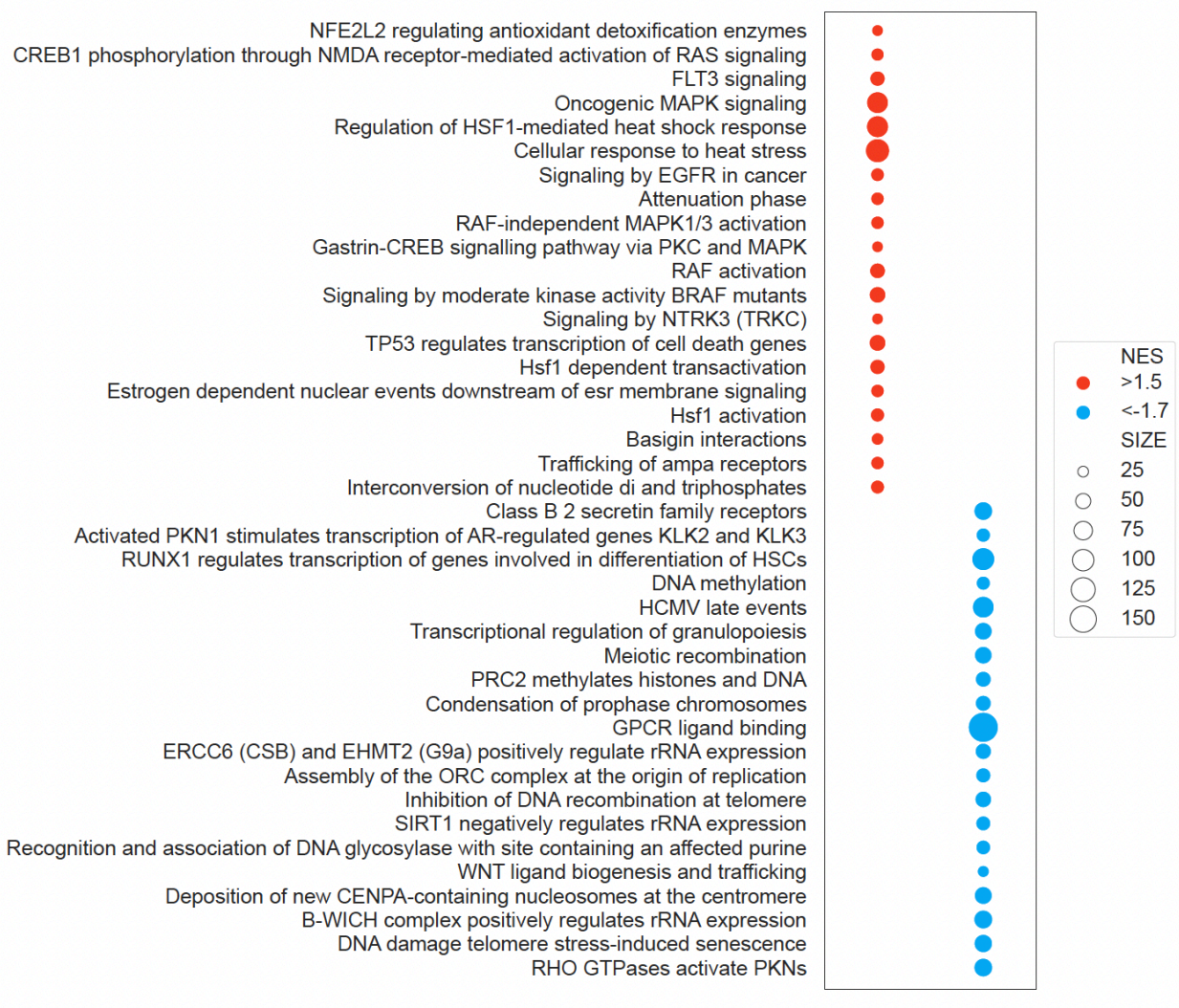

Figure 3.11 Most significant Reactome gene sets altered by GOX/MPO/SCN- in AECs compared to all groups from GSEA. Top 20 upregulated pathways represented with a positive normalized enrichment score (NES) in red and top 20 downregulated pathways with a negative NES score in blue displayed by descending statistical significance. The marker size corresponds to gene count within the given gene set. GSEA $p < 0.05$ for all pathways shown.

to ERBB2 (Erb-B2 receptor tyrosine kinase 2) signaling (**Figure 3.8**). GOX/MPO significantly upregulated pathways involved in Ca^{2+} signaling including DAG and IP3 signaling and downregulated pathways involving the cytokine IL-6 (**Figure 3.9**). GOX/MPO/Br^- significantly upregulated interferon signaling pathways and fatty acid metabolism, and downregulated GPCR related pathways (**Figure 3.10**). GOX/MPO/SCN^- significantly upregulated a pathway involving Nrf2 signaling, which was the most significant pathway impacted, and numerous pathways involving MAPK signaling (**Figure 3.11**). We also performed GSEA for each oxidant group versus untreated control and found numerous differences between the oxidants in select Reactome pathways (**Figure 3.12**) and quantified the unique pathways to each group (**Figure 3.13**).

HOX influence the expression of pro-inflammatory genes in AECs

Numerous studies have demonstrated that HOCl and HOSCN can induce the expression of genes that encode for pro-inflammatory chemokines and cytokines[18–20], so we investigated the impact HOX exposures have on these genes in AECs (**Figure 3.14**). Compared to the untreated control, GOX/MPO/SCN^- exposure caused approximately a 2-fold increase in the expression of *CXCL2* and *CXCL3*, which encode for chemokines that are potent neutrophil chemoattractants[28], and a 3-fold increase in the expression of *CXCL8*. The *CXCL8* gene encodes for IL-8, a major mediator of inflammation, which also functions as a chemotactic factor for neutrophils, in addition to other granulocytes, and stimulates phagocytosis once the cells are recruited to the site of inflammation[29,30]. On the contrary, GOX/MPO and GOX/MPO/Br^- decreased the expression of chemokine genes compared to untreated control with GOX/MPO/Br^- having a stronger suppressive effect than GOX/MPO. All HOX groups increased the expression of pro-inflammatory cytokine genes encoding for IL-1α and IL-1β with GOX/MPO/SCN^- inducing a

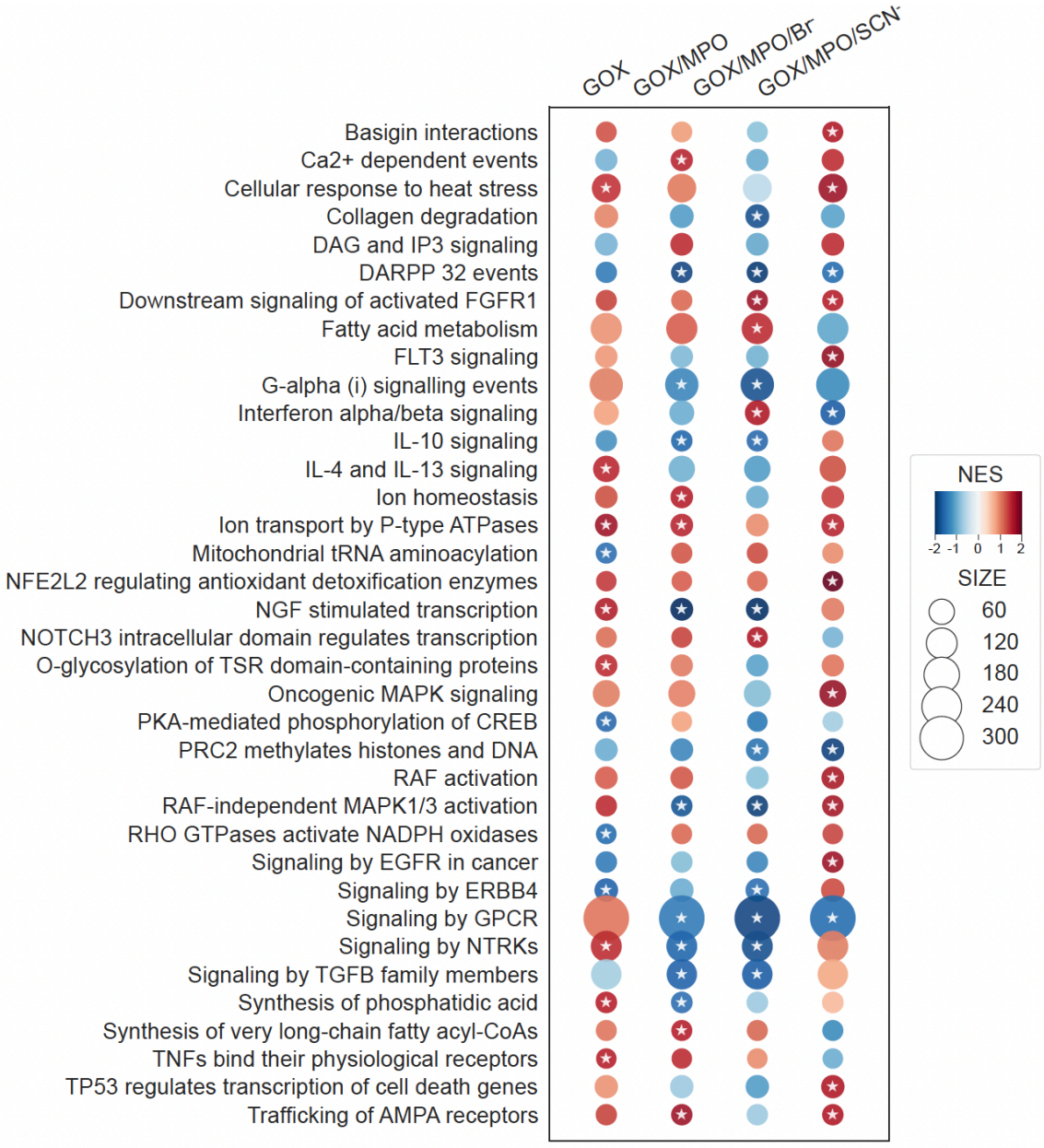

Figure 3.12 GSEA identifies differentially expressed Reactome pathways in response to oxidant exposure. Altered pathways selected by statistical significance are displayed by normalized enrichment scores (NES), with red corresponding to an upregulation compared to untreated control and blue corresponding to downregulation compared to untreated control. The marker size corresponds to gene count within the given gene set. GSEA $p < 0.05$ denoted by star marker.

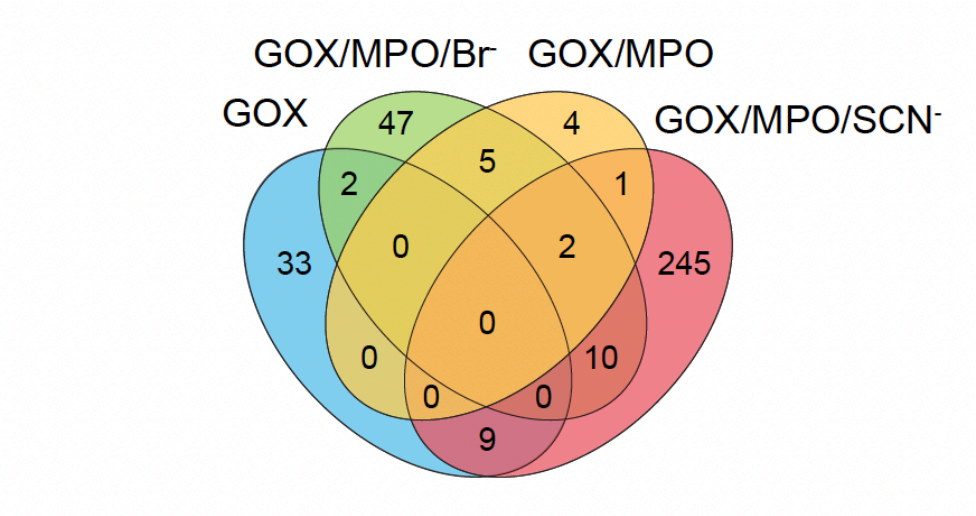

Figure 3.13 Four-way venn diagram of significant (p<0.05) Reactome gene sets. Oxidant groups: GOX (blue), GOX/MPO (yellow), GOX/MPO/Br^- (green), and GOX/MPO/SCN^- (red) shows minimal gene set overlap between oxidant groups.

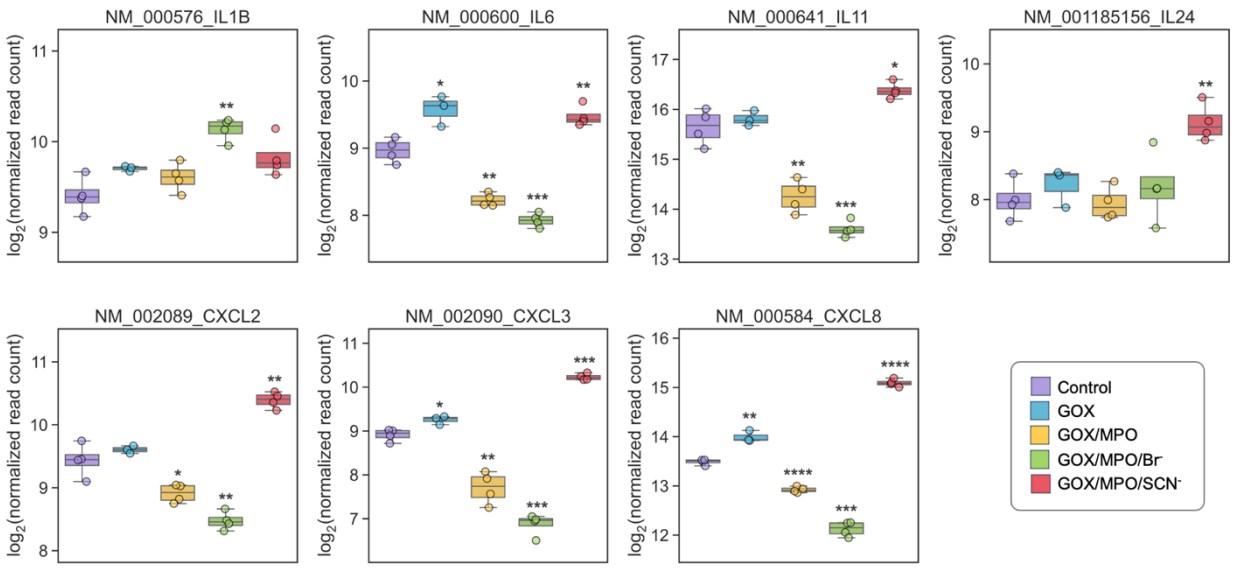

Figure 3.14 HOX significantly influence the expression of immune response genes for cytokines and chemokines. Data are $\log_2$ normalized read counts. One-way ANOVA with Benjamini-Hochberg post hoc test; *p<0.05, **p<0.005, ***p<0.0005, ****p<0.00005 compared to control.

~2-fold increase in *IL1A* while the other two groups had more of a modest effect. GOX/MPO and GOX/MPO/Br^- both decreased the gene expression of the cytokines IL-6 and IL-11, which have been implicated as both pro- and anti-inflammatory cytokines[31,32]. The final cytokine gene we explored encodes for IL-24, which exhibits both pro- and anti-inflammatory roles[33], and was increased by GOX/MPO/SCN^- exposure.

HOX upregulate Nrf2-target genes

Previous studies have shown that dose- and time-dependent HOX exposure in cells can activate transcription factor Nrf2-target antioxidant gene expression[18,20,22,23]. GOX/MPO, GOX/MPO/Br^-, and GOX/MPO/SCN^- all increased the expression of numerous antioxidant enzymes as well as increased expression of *MAFG*, which encodes for a Nrf2 transcriptional cofactor (**Figure 3.15**). HOX-induced genes encoding protein involved in glutathione (GSH) metabolism included *GCLM* (glutamate-cysteine ligase modifier subunit), the first rate-limiting enzyme in GSH synthesis, and *SLC7A11* (solute carrier family 7 member 11) a cystine-glutamate antiporter. The HOX groups also increased expression of *TXNRD1* (thioredoxin reductase 1), *NQO1* (NAD(P)H quinone dehydrogenase 1), and *HMOX1* (heme oxygenase 1), which all protect the cell from oxidative stress. GOX/MPO/SCN^- had the largest impact on the expression of these genes while GOX/MPO and GOX/MPO/Br^- similarly influenced *SLC7A11*, *NQO1*, and *HMOX1* and GOX/MPO/Br^- caused a greater increase in expression of *GCLM*, *TXNRD1* and *MAGF* compared to GOX/MPO, but not GOX/MPO/SCN^-.

HOSCN significantly upregulates a diverse set of potential cytoprotective genes

We have previously shown in our HOX exposure model that 24 hours of exposure to GOX/MPO/SCN^- was not cytotoxic to AECs, however, 24 hours of exposure to GOX/MPO and GOX/MPO/Br- caused cell death[11]. GOX/MPO/SCN^- increased a suite of genes involved in

pathways such as MAPK and EGFR/FGFR signaling that contribute to cell homeostasis, growth, and survival that could convey cytoprotective effects to AECs (**Table 3.1**).

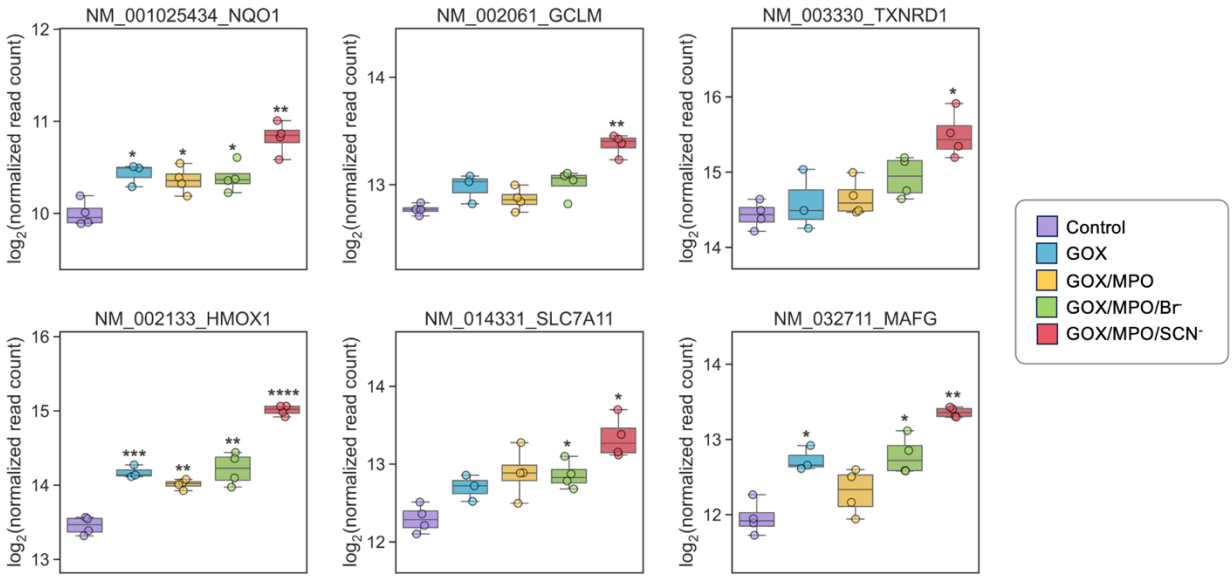

Figure 3.15 HOX significantly induced Nrf2-target antioxidant response element genes.

Data are $\log_2$ normalized read counts. One-way ANOVA with Benjamini-Hochberg post hoc test; *p<0.05, **p<0.005, ***p<0.0005, ****p<0.00005 compared to control.

REFSEQ	SYMBOL	GENE NAME	log2FC	p-value	q-value
NM_003840	TNFRSF10D	TNF receptor superfamily member 10d	1.29	6.62E-245	1.61E-240
NM_004089	TSC22D3	TSC22 domain family member 3	1.87	1.56E-218	1.90E-214
NM_016270	KLF2	Kruppel like factor 2	2.71	4.72E-150	3.82E-146
NM_000584	CXCL8	C-X-C motif chemokine ligand 8	1.60	2.17E-121	1.32E-117
NM_001945	HBEGF	heparin binding EGF like growth factor	1.13	5.32E-96	2.58E-92
NM_018948	ERRFI1	ERBB receptor feedback inhibitor 1	1.52	7.24E-95	2.51E-91
NM_003407	ZFP36	ZFP36 ring finger protein	1.28	6.48E-95	2.51E-91
NM_002228	JUN	Jun proto-oncogene, AP-1 transcription factor subunit	1.47	6.25E-85	1.69E-81
NM_003897	IER3	immediate early response 3	1.09	8.46E-84	2.05E-80
NR_024430	MIR100HG	mir-100-let-7a-2-mir-125b-1 cluster host gene	1.42	1.29E-71	2.08E-68
NM_004040	RHOB	ras homolog family member B	2.05	1.02E-66	1.24E-63
NM_002133	HMOX1	heme oxygenase 1	1.55	4.67E-66	5.15E-63
NM_001008394	EID3	EP300 interacting inhibitor of differentiation 3	1.96	6.09E-53	5.10E-50
NM_203344	SERTAD3	SERTA domain containing 3	1.16	1.00E-45	7.16E-43
NM_014143	CD274	CD274 molecule	1.30	8.43E-31	2.66E-28
NR_028502	MIR22HG	MIR22 host gene	1.28	3.49E-25	7.84E-23
NM_002090	CXCL3	C-X-C motif chemokine ligand 3	1.32	9.09E-21	1.37E-18
NM_014330	PPP1R15A	protein phosphatase 1 regulatory subunit 15A	1.10	1.91E-19	2.49E-17
NM_032711	MAFG	MAF bZIP transcription factor G	1.39	4.37E-19	5.41E-17
NM_002575	SERPINB2	serpin family B member 2	1.39	4.27E-16	3.93E-14
NR_073048	DEDD2	death effector domain containing 2	1.38	1.90E-15	1.62E-13
NR_036515	MIR23AHG	miR-23a/27a/24-2 cluster host gene	1.00	2.33E-15	1.95E-13
NM_004464	FGF5	fibroblast growth factor 5	1.17	8.13E-15	6.32E-13
NR_002440	SNORD16	small nucleolar RNA, C/D box 16	1.60	7.19E-14	4.98E-12
NR_028504	MIR22HG	MIR22 host gene	1.53	7.35E-14	5.05E-12
NM_182981	OSGIN1	oxidative stress induced growth inhibitor 1	1.21	4.51E-13	2.87E-11
NM_001206540	CAPZB	capping actin protein of muscle Z-line subunit beta	2.42	5.18E-13	3.25E-11
NM_001011515	PDLIM5	PDZ and LIM domain 5	1.06	1.12E-12	6.76E-11
NR_133913	LINC01629	long intergenic non-protein coding RNA 1629	1.31	3.42E-12	1.93E-10
NR_036682	BCL7B	BAF chromatin remodeling complex subunit BCL7B	1.03	1.29E-11	6.68E-10
NM_033143	FGF5	fibroblast growth factor 5	1.26	2.08E-11	1.03E-09
NR_029635	MIR221	microRNA 221	1.44	5.43E-11	2.54E-09
NM_182763	MCL1	MCL1 apoptosis regulator, BCL2 family member	1.14	8.74E-11	3.93E-09
NM_014331	SLC7A11	solute carrier family 7 member 11	1.05	1.31E-10	5.74E-09
NM_001281742	UBE2C	ubiquitin conjugating enzyme E2 C	1.63	1.46E-10	6.36E-09

Table 3.1 Potential cytoprotective genes significantly induced by GOX/MPO/SCN^-.

Displayed are the top 35 most statistically significant DEGs from AECs treated with GOX/MPO/SCN^- compared to untreated control AECs.

3.5 Discussion

We previously demonstrated substrate-dependent effects of HOX on cytotoxicity in AECs by 24 h of exposure, as well as a divergence of metabolomic responses as early as 2 h of exposure[11]. Therefore, we hypothesized that the metabolomic differences we observed would be reflected early in the transcriptome of HOX-exposed AECs. To test this hypothesis, we profiled the transcriptome of AECs (BEAS-2B cells) treated with experimental conditions that favored the formation of HOCl (GOX/MPO), HOBr (GOX/MPO/Br^-), or HOSCN (GOX/ MPO/SCN^-). We observed a diversity of transcriptional changes that were unique to each oxidant group, which could be expected given the previously observed differences in reactivity and specificity of HOCl, HOBr, and HOSCN in modifying biomolecules and eliciting diverse cellular responses.

While most of this discussion will focus on the unique AEC transcriptome alterations by HOX, there are a few noteworthy similarities in gene expression changes and implications in biological pathways between HOX oxidant groups. GOX/MPO, GOX/MPO/Br^-, and GOX/MPO/SCN^- all increased the expression of Nrf2-target genes, albeit at varying levels, which suggests they can all induce antioxidant signaling pathways in AECs. HOCl and HOSCN can induce the expression for Nrf2-target genes in various cell-types, which is in concordance with our results[18,22,23]. A prior study has shown that HOCl strongly induces the expression of the Nrf2 transcriptional cofactors MAFF and MAFG and the expression of phase II detoxification enzymes *TXNRD1*, *ALDH1A3*, *HMOX1*, *NQO1*, *GCLM* in primary and cell line AECs[23].GOX/MPO in our study only slightly elevates the expression of *MAGF*, *TXNRD1*, *HMOX1*, *NQO1*, and *GCLM* compared to untreated control. A plausible explanation for the discrepancy in results could be due to differences in experimental conditions – we performed the exposures in nutrient-rich media where it is expected that components in the media will likely

interact with HOCl and form secondary products, thus buffering AECs from direct HOCl exposure and preventing a stronger induction of Nrf2 genes. Therefore, we cannot conclude whether the transcriptional changes we observed are due to direct or indirect HOX exposure. We also observed that all HOX groups increased the expression of the pro-inflammatory cytokines IL-1α and IL-1β, implying that they may all have the ability to induce inflammasome signaling. This may occur as a downstream effect of NF- κB signaling pathway activation in AECs, similar to prior data in macrophages exposed to HOCl and HOSCN[19,20]. Lastly, the GO analysis revealed that all the HOX groups significantly impacted biological pathways involved in apoptosis, response to growth factors, and regulation of cellular response to stress, among others. However, the transcriptional program for each of these pathways diverged significantly between the HOX groups.

Overall, our analyses showed that HOX exposure causes significant global changes in the transcriptome of AECs by 2 hours and that the acquired transcriptional profile is highly dependent on the MPO substrates Cl^-, Br^-, and SCN^- that influence which HOX is formed. GOX/MPO induced the smallest transcriptional changes (tens of genes), while GOX/MPO/Br^- and GOX/MPO/SCN^- impacted hundreds of genes compared to untreated control. HOCl cannot be produced by any other mammalian peroxidase than MPO, which confines its role to neutrophil host defense. This contrasts with HOBr which can also be produced by peroxidasin in the extracellular matrix, an essential step in forming sulfilimine crosslinks in collagen IV within the basement membrane[34]. The smaller transcriptional effects seen with HOCl compared to HOSCN or HOBr suggest a lesser role for the former in AEC adaptation during inflammation. Notably, GOX/MPO/Br^- had the greatest decrease in gene expression for many of the pro-inflammatory genes compared to untreated control. This could potentially serve to protect AECs

from an exacerbated immune response if HOBr interacts with them on the basolateral side (interface with the ECM).

In congruence with our prior study, others have observed that HOSCN is less cytotoxic than HOCl, and that SCN^- supplementation protects cells from HOCl-induced cell death[20,35–37]. HOSCN promotes a cytoprotective response in AECs and greater adaptability to oxidative stress compared to the other oxidants. The significant transcriptional changes that occur due to GOX/MPO/SCN^- exposure was anticipated given the specificity and selectivity of HOSCN for thiols and selenols. It has become increasingly apparent that HOSCN acts as a finely tuned signaling molecule for redox and cellular signaling pathways that influence cell fate and inflammation. In our study, GOX/MPO/SCN^- significantly upregulated a number of signal transduction pathways including MAPK signaling, which has been observed in prior studies[17,23]. GOX/MPO/SCN^- also significantly induced the expression of genes involved in cellular adaptation, survival, and growth including *TNFRSF10D* (TNF receptor superfamily member 10d), which encodes for a tumor necrosis factor-related apoptosis-inducing ligand (TRAIL) receptor called TRAIL-R4 (DcR-2/TRUNDD). TRAIL-R4, unlike other TRAIL receptors, has a truncated death domain that renders it nonfunctional and can inhibit TRAIL-induced apoptosis, as well as activate signaling pathways that confer cell survival and growth[38,39]. GOX/MPO/SCN^- also significantly increased TSC22D3 (TSC22 domain family member 3), which encodes for the protein GILZ that has demonstrated anti-inflammatory activity[40,41]. Additionally, GOX/MPO/SCN^- enhanced the expression of KLF2 (KLF transcription factor 2), a gene that encodes for a transcription factor that can promote survival and proliferation[42,43].

The upregulation of pro-inflammatory genes, including genes that can induce chemotaxis in neutrophils (i.e. *CXCL8*), by GOX/MPO/SCN^- seems paradoxical given that thiocyanate is

associated with increased lung function in humans and resolution of inflammation in animal models[35,36]. The increased mRNA expression of *CXCL8* (IL-8) by HOSCN has also been observed, but an *in vivo* study demonstrated a decrease in expression of the mouse analog to IL-8 chemokine when nebulized with SCN^-[19,35,44]. It is unclear if the upregulated expression of *CXCL8* in our study corresponds to an increase in the IL-8 chemokine protein followed by secretion into the extracellular environment where neutrophil recruitment is plausible. One consistent observation has been the increase of *IL1B* and IL-1β by HOSCN, although IL-1β expression has shown to be reduced in mice infected with bacteria and treated with SCN^-[19,35]. This suggests SCN^- inhibits cytokines during bacterial clearance, but induction of IL-1β by SCN^- outside of an infection context lacks clarity. Excess IL-1β has been implicated as part of the pathophysiological changes that occur in various diseases[45], but it could potentially have a homeostatic role in AECs during HOSCN exposure since IL-1β is regarded as being pleiotropic[46]. A plausible explanation for the increase of pro-inflammatory genes by HOSCN and conditions favoring HOSCN in AECs could perhaps be owed to a well calibrated and efficacious immune response in the local microenvironment that is accompanied by the upregulation of cytoprotective genes to circumvent stress.

An inherent limitation to our study is the inability to decipher whether the alterations to genes in AECs are directly or indirectly due to HOX or its oxidative byproducts, which are likely to occur given the exposure media, Medium-199, contains many viable HOX targets, particularly for HOCl and HOBr (e.g., ~100μM Met)[47]. However, our model aims to recapitulate the extracellular microenvironment of AECs where a diversity of biomolecules is present in homeostatic conditions and elevated in pathophysiological conditions, as observed in chronic airway diseases[48–50]. While HOX generation is a routine part of the innate immune system to

ward off invading pathogens, it can become problematic in chronic airway diseases where excess HOCl is produced without adequate levels of antioxidants present. Therefore, SCN^- therapy is a promising potential treatment option for chronic lung diseases that feature chronic neutrophilic inflammation due to its antioxidant properties. As we have observed *in vitro* in our HOX exposure model, SCN^- supplementation induces pathways that could aid host cells to adapt to the recurring oxidative stress and damage. Future studies will be necessary to confirm the gene targets identified here and their involvement in adaptive signaling pathways within HOX-exposed cells.

3.6 References

1. Nauseef, W. M. How human neutrophils kill and degrade microbes: an integrated view. Immunological Reviews 219, 88–102 (2007).
2. Schultz, J. & Kaminker, K. Myeloperoxidase of the leucocyte of normal human blood. I. Content and localization. Archives of Biochemistry and Biophysics 96, 465–467 (1962).
3. Furtmüller, P. G., Burner, U., Jantschko, W., Regelsberger, G. & Obinger, C. The reactivity of myeloperoxidase compound I formed with hypochlorous acid. Redox Report 5, 173–178 (2000).
4. Chapman, A. L. P., Skaff, O., Senthilmohan, R., Kettle, A. J. & Davies, M. J. Hypobromous acid and bromamine production by neutrophils and modulation by superoxide. Biochem J 417, 773–781 (2009).
5. van Dalen, C. J., Whitehouse, M. W., Winterbourn, C. C. & Kettle, A. J. Thiocyanate and chloride as competing substrates for myeloperoxidase. Biochem J 327, 487–492 (1997).
6. Thomas, E. L. Myeloperoxidase-Hydrogen Peroxide-Chloride Antimicrobial System: Effect of Exogenous Amines on Antibacterial Action Against Escherichia coli. Infect Immun 25, 110–116 (1979).
7. Klebanoff, S. J. & Hamon, C. B. Role of myeloperoxidase-mediated antimicrobial systems in intact leukocytes. J Reticuloendothel Soc 12, 170–196 (1972).
8. Klebanoff, S. J. Myeloperoxidase-Halide-Hydrogen Peroxide Antibacterial System. J Bacteriol 95, 2131–2138 (1968).
9. Chandler, J. D. Global Profiling of Cell Responses to (Pseudo)Hypohalous Acids. in Mammalian Heme Peroxidases (CRC Press, 2021).

10. Chandler, J. D. et al. Myeloperoxidase oxidation of methionine associates with early cystic fibrosis lung disease. Eur Respir J 52, 1801118 (2018).
11. Kim, S. O. et al. Substrate-dependent metabolomic signatures of myeloperoxidase activity in airway epithelial cells: Implications for early cystic fibrosis lung disease. Free Radical Biology and Medicine (2023) doi:10.1016/j.freeradbiomed.2023.06.021.
12. Dickerhof, N. et al. Oxidized glutathione and uric acid as biomarkers of early cystic fibrosis lung disease. Journal of Cystic Fibrosis 16, 214–221 (2017).
13. Davies, M. J. & Hawkins, C. L. The Role of Myeloperoxidase in Biomolecule Modification, Chronic Inflammation, and Disease. Antioxid Redox Signal 32, 957–981 (2020).
14. Kettle, A. J. et al. Oxidation contributes to low glutathione in the airways of children with cystic fibrosis. European Respiratory Journal 44, 122–129 (2014).
15. Skaff, O., Pattison, D. I. & Davies, M. J. Hypothiocyanous acid reactivity with low-molecular-mass and protein thiols: absolute rate constants and assessment of biological relevance. Biochem J 422, 111–117 (2009).
16. Skaff, O. et al. Selenium-containing amino acids are targets for myeloperoxidase-derived hypothiocyanous acid: determination of absolute rate constants and implications for biological damage. Biochem J 441, 305–316 (2012).
17. Lane, A. E., Tan, J. T. M., Hawkins, C. L., Heather, A. K. & Davies, M. J. The myeloperoxidase-derived oxidant HOSCN inhibits protein tyrosine phosphatases and modulates cell signalling via the mitogen-activated protein kinase (MAPK) pathway in macrophages. Biochem J 430, 161–169 (2010).

18. Woods, C. G. et al. Dose-dependent transitions in Nrf2-mediated adaptive response and related stress responses to hypochlorous acid in mouse macrophages. Toxicology and Applied Pharmacology 238, 27–36 (2009).
19. Pan, G. J., Rayner, B. S., Zhang, Y., van Reyk, D. M. & Hawkins, C. L. A pivotal role for NF-κB in the macrophage inflammatory response to the myeloperoxidase oxidant hypothiocyanous acid. Arch Biochem Biophys 642, 23–30 (2018).
20. Guo, C., Davies, M. J. & Hawkins, C. L. Role of thiocyanate in the modulation of myeloperoxidase-derived oxidant induced damage to macrophages. Redox Biology 36, 101666 (2020).
21. Liu, T., Zhang, L., Joo, D. & Sun, S.-C. NF-κB signaling in inflammation. Sig Transduct Target Ther 2, 1–9 (2017).
22. Pi, J. et al. Activation of Nrf2-mediated oxidative stress response in macrophages by hypochlorous acid. Toxicology and Applied Pharmacology 226, 236–243 (2008).
23. Zhu, L. et al. Identification of Nrf2-dependent airway epithelial adaptive response to proinflammatory oxidant-hypochlorous acid challenge by transcription profiling. Am J Physiol Lung Cell Mol Physiol 294, L469-477 (2008).
24. Tonelli, C., Chio, I. I. C. & Tuveson, D. A. Transcriptional Regulation by Nrf2. Antioxidants & Redox Signaling 29, 1727–1745 (2018).
25. Zhou, Y. et al. Metascape provides a biologist-oriented resource for the analysis of systems-level datasets. Nat Commun 10, 1523 (2019).
26. Pattison, D. I., Davies, M. J. & Hawkins, C. L. Reactions and reactivity of myeloperoxidase-derived oxidants: differential biological effects of hypochlorous and hypothiocyanous acids. Free Radic Res 46, 975–995 (2012).

27. Furtmüller, P. G., Burner, U. & Obinger, C. Reaction of Myeloperoxidase Compound I with Chloride, Bromide, Iodide, and Thiocyanate. Biochemistry 37, 17923–17930 (1998).
28. Sokol, C. L. & Luster, A. D. The Chemokine System in Innate Immunity. Cold Spring Harb Perspect Biol 7, a016303 (2015).
29. Matsushima, K., Yang, D. & Oppenheim, J. J. Interleukin-8: An evolving chemokine. Cytokine 153, 155828 (2022).
30. Baggiolini, M., Walz, A. & Kunkel, S. L. Neutrophil-activating peptide-1/interleukin 8, a novel cytokine that activates neutrophils. J Clin Invest 84, 1045–1049 (1989).
31. Fung, K. Y. et al. Emerging roles for IL-11 in inflammatory diseases. Cytokine 149, 155750 (2022).
32. Luo, Y. & Zheng, S. G. Hall of Fame among Pro-inflammatory Cytokines: Interleukin-6 Gene and Its Transcriptional Regulation Mechanisms. Frontiers in Immunology 7, (2016).
33. Zhong, Y., Zhang, X. & Chong, W. Interleukin-24 Immunobiology and Its Roles in Inflammatory Diseases. Int J Mol Sci 23, 627 (2022).
34. Colon, S., Page-McCaw, P. & Bhave, G. Role of Hypohalous Acids in Basement Membrane Homeostasis. Antioxid Redox Signal 27, 839–854 (2017).
35. Chandler, J. D. et al. Antiinflammatory and Antimicrobial Effects of Thiocyanate in a Cystic Fibrosis Mouse Model. Am J Respir Cell Mol Biol 53, 193–205 (2015).
36. Xu, Y., Szép, S. & Lu, Z. The antioxidant role of thiocyanate in the pathogenesis of cystic fibrosis and other inflammation-related diseases. Proc Natl Acad Sci U S A 106, 20515–20519 (2009).
37. Wagner, B. A. et al. Role of thiocyanate, bromide and hypobromous acid in hydrogen peroxide-induced apoptosis. Free Radic Res 38, 167–175 (2004).

38. LeBlanc, H. N. & Ashkenazi, A. Apo2L/TRAIL and its death and decoy receptors. Cell Death Differ 10, 66–75 (2003).

39. Lalaoui, N. et al. TRAIL-R4 promotes tumor growth and resistance to apoptosis in cervical carcinoma HeLa cells through AKT. PLoS One 6, e19679 (2011).

40. Ronchetti, S., Migliorati, G. & Riccardi, C. GILZ as a Mediator of the Anti-Inflammatory Effects of Glucocorticoids. Front Endocrinol (Lausanne) 6, 170 (2015).

41. Bereshchenko, O., Migliorati, G., Bruscoli, S. & Riccardi, C. Glucocorticoid-Induced Leucine Zipper: A Novel Anti-inflammatory Molecule. Front Pharmacol 10, 308 (2019).

42. Ohguchi, H. et al. The KDM3A–KLF2–IRF4 axis maintains myeloma cell survival. Nat Commun 7, 10258 (2016).

43. Rabacal, W. et al. Transcription factor KLF2 regulates homeostatic NK cell proliferation and survival. Proc Natl Acad Sci U S A 113, 5370–5375 (2016).

44. Wang, J.-G. et al. The principal eosinophil peroxidase product, HOSCN, is a uniquely potent phagocyte oxidant inducer of endothelial cell tissue factor activity: a potential mechanism for thrombosis in eosinophilic inflammatory states. Blood 107, 558–565 (2006).

45. Ren, K. & Torres, R. Role of interleukin-1β during pain and inflammation. Brain Res Rev 60, 57–64 (2009).

46. Bent, R., Moll, L., Grabbe, S. & Bros, M. Interleukin-1 Beta—A Friend or Foe in Malignancies? International Journal of Molecular Sciences 19, 2155 (2018).

47. 11150 - Medium 199 - US. https://www.thermofisher.com/us/en/home/technical-resources/media-formulation.86.html.

48. Walmsley, S. et al. A prototypic small molecule database for bronchoalveolar lavage-based metabolomics. Sci Data 5, 180060 (2018).

49. Halper-Stromberg, E. et al. Bronchoalveolar Lavage Fluid from COPD Patients Reveals More Compounds Associated with Disease than Matched Plasma. Metabolites 9, 157 (2019).
50. Wolak, J. E., Esther, C. R. & O'Connell, T. M. Metabolomic analysis of bronchoalveolar lavage fluid from cystic fibrosis patients. Biomarkers 14, 10.1080/13547500802688194 (2009).

Chapter 4

General discussion

4.1 Summary of findings

4.2 Implications & future directions

4.3 Conclusions

4.4 References

4.1 Summary of findings

Sustained neutrophilic inflammation is central to the pathogenesis of chronic inflammatory lung diseases (e.g., chronic obstructive pulmonary disease, COPD; cystic fibrosis, CF; neutrophilic asthma) and contributes to deterioration of lung function over time[1–4]. As an integral part of innate immunity, neutrophils generate hypohalous acids (HOX) through myeloperoxidase (MPO) to destroy pathogens[5,6], but excessive HOX production coupled to inadequate neutralization can result in oxidative damage to the airway epithelium. HOX (i.e., HOCl, HOBr, HOSCN) have specific reactivity profiles for biomolecules that warrant studying their individual impact on AECs. Understanding the complex role of HOX in airway epithelial cells (AECs) could help inform therapeutic interventions targeting neutrophilic inflammation in chronic airway disease (e.g., COPD, CF, and neutrophilic asthma) to ultimately mitigate disease progression.

The research presented in this dissertation provides novel insight to the holistic (patho)physiological changes in human AECs during HOX exposure. We found that cells exposed to conditions favoring HOSCN formation (GOX/MPO/SCN^-) for up to 24 h, our longest time point, had virtually no impact on cell viability in AECs unlike the exposures that favored H_2O_2 (GOX), HOCl (GOX/MPO), and HOBr (GOX/MPO/Br^-) formation, which all had profound cytotoxic effects in AECs by 24 h (**Chapter 2**). While this seems contradictory considering HOSCN is an oxidant, it is the mildest and most selective oxidant out of the HOX (based on reduction potential and pK_a) and prior evidence has suggested a cytoprotective role for HOSCN in AECs[7,8]. GOX/MPO/SCN^- altered primary metabolic pathways that could be indicative of AECs adaptation to cellular oxidative stress during HOSCN exposure through broad metabolic reprogramming. For example, GOX/MPO/SCN^- caused a significant alteration to the

pentose phosphate pathway (PPP), potentially through rerouting of glycolytic flux to PPP, which would supply the cell with the reducing power of NADPH to combat oxidative stress under chronic exposures. This could consequently lead to a diminished pyruvate supply for the ATP-generating tricarboxylic acid (TCA) cycle. However, GOX/MPO/SCN^- also impacted pathways that could be contributing to the increase of TCA cycle intermediates malate and fumarate at 6 h such as Gln/Glu metabolism, which provide a source for TCA intermediate α-ketoglutarate (α-KG), and/or the Leu/Ile degradation pathway, which can feed into the TCA cycle via succinyl CoA and acetyl CoA, to prevent loss of energy homeostasis.

Additionally, AECs exposed to GOX/MPO and GOX/MPO/Br^- had the most similarities in cytotoxicity, metabolite profile, and effects on metabolic pathways, which is not surprising given their similar reactivities. Both increasingly impacted Cys/Met metabolism in AECs the highest, oxidizing thus depleting Met and producing methionine sulfoxide (MetO) and dehydromethionine (dhMet). Initially, we were unaware of the identity of dhMet due to the lack of commercial availability of a dhMet standard and lack of annotation or presence from public MS/MS structural databases, but it was significant in our statistical analyses and similarily to MetO, was increased uniquely by GOX/MPO and GOX/MPO/Br^-. Upon further investigation, we validated the compound as dhMet, a secondary Met oxidation product that significantly correlated to lung damage (i.e., bronchiectasis) in BAL of children with CF, as did MetO.

We observed profoundly distinct gene expression profiles of AECs exposed to each of the exposure groups for 2 h, which reflects an early inflammatory event (**Chapter 3**). The most notable convergence we observed in the HOX was the upregulation of Nrf2-target genes (i.e., *GCLM*, *SLC7A11*, *TXMRD1*, *NQO1*, *HMOX1*) with GOX/MPO and GOX/MPO/Br^- causing a modest increase, and GOX/MPO/SCN^- causing a significantly greater increase in these genes.

The transcription factor Nrf2 is a master regulator of antioxidant and metabolic genes that compensate for oxidative stress and toxicity and promotes the expression of enzymes involved in redox homeostasis and detoxification[9–11]. Our data supports the role of HOX in early cellular signaling and adaptation to oxidative stress in AECs. Additionally, we present evidence for HOX role in inflammasome signaling, potentially through NF-κB signaling pathway as most of the immune response genes HOX impact are targets of the transcription factor NF-κB. All HOX exposure groups increased the cytokine genes encoding for IL-1α and IL-1β with GOX/MPO/SCN^- increasing IL-1α the greatest and GOX/MPO/Br^- increasing IL-1β the most. Interestingly, GOX/MPO/SCN^- increased cytokine genes (i.e., *IL6*, *IL24*) and chemokine genes (i.e., *CXCL8*, *CXCL3*, *CXCL2*), while GOX/MPO and GOX/MPO/Br^- decreased the expression of these genes except for *IL24*, in which they had no effect. Lastly, we provide evidence of GOX/MPO/SCN^- in the involvement of MAPK signaling in AECs through the upregulated expression of genes (e.g., *MAPK1*, *JUN*, *DUSP1*) involved in MAPK signaling, which regulates a repertoire of cellular responses and fates. The vastly distinct transcriptional profiles exemplify the various roles HOX plays in inflammation.

4.2 Implications & future directions

In CF, neutrophilic inflammation manifests as early as infancy and contributes to the progression of structural lung disease (i.e., bronchiectasis), significantly impacting longevity and quality of life[12–20]. Identifying early biomarkers of lung disease derived from neutrophilic processes could refine disease monitoring, therapy, and prevention of lung disease progression in CF. A number of neutrophil components have been identified as biomarkers of CF lung damage in BAL (e.g., MPO[15,21], MetO[15], azurocidin[21], neutrophil CD63 for NE exocytosis[22], NE

activity[13]), sputum (e.g., NE activity[23]), and urine (e.g., GSA[17]). Our *in vitro* model of AECs exposed to enzymatically generated HOX elucidated GOX/MPO and GOX/MPO/Br^- specific methionine oxidation products MetO and dhMet. The metabolite MetO had previously been linked to bronchiectasis in BAL from children with CF[15], and thus our work provides mechanistic insight to MetO as a biomarker of structural lung damage derived from HOCl, or possibly HOBr, exposure. In a prior study, dhMet was implicated as a modification on the protein calprotectin in CF BAL, which was associated with bacterial burden[24]. Our work demonstrates for the first time that dhMet, as a free metabolite, correlates to bronchiectasis score in children with CF and had a stronger association to lung damage than NE, which is regarded as the most sensitive sputum biomarker for lung function[25]. This analysis contributes new data to the CF community with implications for potential biomarkers of early lung disease progression. Further validation of MetO and dhMet as biomarkers of CF lung disease is warranted in prospective clinical studies with a larger cohort.

Furthermore, this work has implications for SCN^- as a therapeutic intervention for neutrophilic inflammation. SCN^- is the preferred substrate for many peroxidases, including MPO, and has demonstrated antimicrobial and antioxidant properties against HOCl[8,26–29]. SCN^- and HOSCN have a protective role in the airway and our data shows that AECs are robust to GOX/MPO/SCN^- exposure. AECs appear to employ cytoprotective mechanisms via metabolic and transcriptional reprogramming, which will need to be further validated for direct mechanism of action and biological targets in subsequent studies. SCN^- therapy could be beneficial not only for chronic inflammatory diseases, but also for a conglomeration of respiratory pathologies that are exacerbated by neutrophilia. That includes lung cancer, acute respiratory distress syndrome, idiopathic pulmonary fibrosis, primary ciliary dyskinesia, and pneumonia[3,31–34]. In addition,

SCN^- therapy has plausible value as an antidote to chlorine gas exposure, which currently has no known antidote[35].

4.3 Conclusion

To conclude, this dissertation has built upon the idea that specific HOX elicit distinct cytotoxic, metabolomic, and transcriptomic effects that determine the (mal)adaptation of AECs during HOX-induced oxidative insult (**Figure 4.1**). We comprehensively identified primary metabolic pathways altered and transcriptomic responses induced by HOX in AECs using sensitive multi-omic methodology. Our *in vitro* findings allowed us to discover potential *in vivo* targets of HOX – we identified free metabolite dhMet, as well as validate the significance of MetO[15], as candidate biomarkers of early lung disease in clinical BAL samples of children with CF. The need for therapeutic intervention, such as SCN^- therapy, for recurring neutrophilia remains as CF and other chronic inflammatory respiratory diseases continue to present significant health challenges[2,36,37] The findings from this body of work will support continued efforts in understanding the role of HOX in the airway epithelium, within the context of physiological exposures and pathological contributions to chronic inflammatory lung diseases.

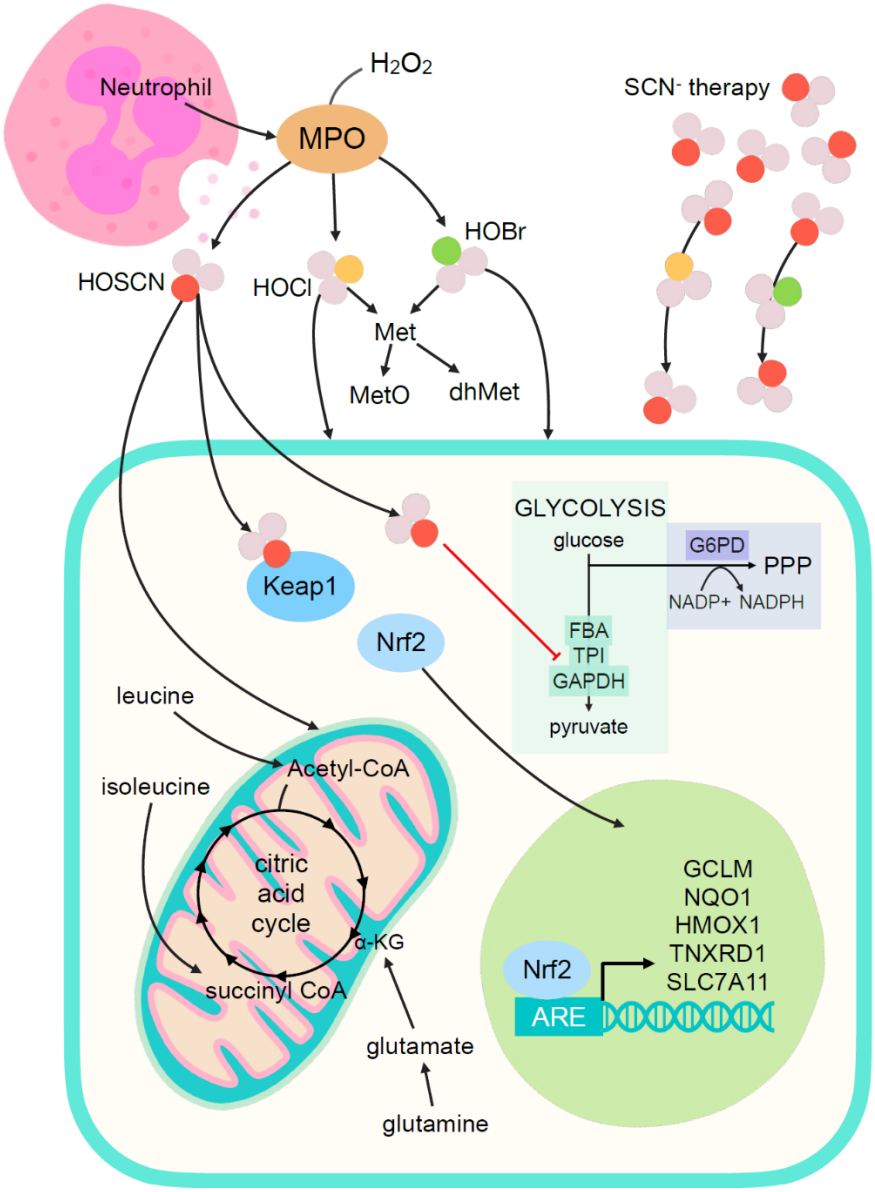

Figure 4.1 Potential mechanisms of adaptation in AECs exposed to HOSCN. Based on our observations, AECs may adapt to HOSCN exposure by 1) activating the Nrf2 pathway to upregulate antioxidant response element (ARE) genes, 2) inhibiting glycolysis so that glucose flux reroutes to the pentose phosphate pathway (PPP) to increase NADPH, and 3) altering the citric acid cycle through Leu/Ile degradation pathway and/or Gln/Glu metabolism. Also illustrated here is the impact of HOCl and HOBr on Met and the utility of SCN^- therapy on HOCl and HOBr exposure.

4.4 References

1. Wang, G. & Nauseef, W. M. Neutrophil dysfunction in the pathogenesis of cystic fibrosis. Blood 139, 2622–2631 (2022).
2. Yamasaki, A., Okazaki, R. & Harada, T. Neutrophils and Asthma. Diagnostics (Basel) 12, 1175 (2022).
3. Jasper, A. E., McIver, W. J., Sapey, E. & Walton, G. M. Understanding the role of neutrophils in chronic inflammatory airway disease. F1000Res 8, F1000 Faculty Rev-557 (2019).
4. Butler, A., Walton, G. M. & Sapey, E. Neutrophilic Inflammation in the Pathogenesis of Chronic Obstructive Pulmonary Disease. COPD: Journal of Chronic Obstructive Pulmonary Disease 15, 392–404 (2018).
5. Davies, M. J. & Hawkins, C. L. The Role of Myeloperoxidase in Biomolecule Modification, Chronic Inflammation, and Disease. Antioxid Redox Signal 32, 957–981 (2020).
6. Davies, M. J. Myeloperoxidase-derived oxidation: mechanisms of biological damage and its prevention. J Clin Biochem Nutr 48, 8–19 (2011).
7. Zhu, L. et al. Identification of Nrf2-dependent airway epithelial adaptive response to proinflammatory oxidant-hypochlorous acid challenge by transcription profiling. Am J Physiol Lung Cell Mol Physiol 294, L469-477 (2008).
8. Chandler, J. D., Nichols, D. P., Nick, J. A., Hondal, R. J. & Day, B. J. Selective Metabolism of Hypothiocyanous Acid by Mammalian Thioredoxin Reductase Promotes Lung Innate Immunity and Antioxidant Defense. Journal of Biological Chemistry 288, 18421–18428 (2013).

9. He, F., Ru, X. & Wen, T. NRF2, a Transcription Factor for Stress Response and Beyond. Int J Mol Sci 21, 4777 (2020).
10. Ma, Q. Role of Nrf2 in Oxidative Stress and Toxicity. Annu Rev Pharmacol Toxicol 53, 401–426 (2013).
11. Tonelli, C., Chio, I. I. C. & Tuveson, D. A. Transcriptional Regulation by Nrf2. Antioxidants & Redox Signaling 29, 1727–1745 (2018).
12. Gangell, C. et al. Inflammatory responses to individual microorganisms in the lungs of children with cystic fibrosis. Clin Infect Dis 53, 425–432 (2011).
13. Sly, P. D. et al. Risk Factors for Bronchiectasis in Children with Cystic Fibrosis. N Engl J Med 368, 1963–1970 (2013).
14. Esther, C. R. et al. Metabolomic biomarkers predictive of early structural lung disease in cystic fibrosis. Eur Respir J 48, 1612–1621 (2016).
15. Chandler, J. D. et al. Myeloperoxidase oxidation of methionine associates with early cystic fibrosis lung disease. Eur Respir J 52, 1801118 (2018).
16. Dickerhof, N. et al. Oxidative stress in early cystic fibrosis lung disease is exacerbated by airway glutathione deficiency. Free Radic Biol Med 113, 236–243 (2017).
17. Dickerhof, N. et al. Oxidized glutathione and uric acid as biomarkers of early cystic fibrosis lung disease. Journal of Cystic Fibrosis 16, 214–221 (2017).
18. Ali, H. A., Fouda, E. M., Salem, M. A., Abdelwahad, M. A. & Radwan, H. H. Sputum neutrophil elastase and its relation to pediatric bronchiectasis severity: A cross-sectional study. Health Science Reports 5, e581 (2022).
19. Brusselle, G. G. & Van Braeckel, E. Sputum Neutrophil Elastase as a Biomarker for Disease Activity in Bronchiectasis. Am J Respir Crit Care Med 195, 1289–1291 (2017).

20. Ls, M. et al. Progression of early structural lung disease in young children with cystic fibrosis assessed using CT. Thorax 67, 509–516 (2011).
21. Renwick, J. et al. Early Interleukin-22 and Neutrophil Proteins Are Correlated to Future Lung Damage in Children With Cystic Fibrosis. Front. Pediatr. 9, 640184 (2021).
22. Margaroli, C. et al. Elastase Exocytosis by Airway Neutrophils Is Associated with Early Lung Damage in Children with Cystic Fibrosis. Am J Respir Crit Care Med 199, 873–881 (2019).
23. Fouda, E. M., Ali, H. A., Salem, M. A. A. & Radwan, H. H. Sputum Neutrophil Elastase in pediatric cystic fibrosis and non-cystic fibrosis bronchiectasis. QJM: An International Journal of Medicine 114, hcab113.027 (2021).
24. Magon, N. J. et al. Oxidation of calprotectin by hypochlorous acid prevents chelation of essential metal ions and allows bacterial growth: Relevance to infections in cystic fibrosis. Free Radical Biology and Medicine 86, 133–144 (2015).
25. Bene, Z. et al. Laboratory biomarkers for lung disease severity and progression in cystic fibrosis. Clinica Chimica Acta 508, 277–286 (2020).
26. Chandler, J. D. & Day, B. J. Biochemical mechanisms and therapeutic potential of pseudohalide thiocyanate in human health. Free Radic Res 49, 695–710 (2015).
27. Chandler, J. D., Min, E., Huang, J., Nichols, D. P. & Day, B. J. Nebulized thiocyanate improves lung infection outcomes in mice: Thiocyanate improves lung infection outcomes. Br J Pharmacol 169, 1166–1177 (2013).
28. Ashby, M. T., Carlson, A. C. & Scott, M. J. Redox Buffering of Hypochlorous Acid by Thiocyanate in Physiologic Fluids. J. Am. Chem. Soc. 126, 15976–15977 (2004).

29. Xu, Y., Szép, S. & Lu, Z. The antioxidant role of thiocyanate in the pathogenesis of cystic fibrosis and other inflammation-related diseases. Proc Natl Acad Sci U S A 106, 20515–20519 (2009).
30. Barrett, T. J. & Hawkins, C. L. Hypothiocyanous Acid: Benign or Deadly? Chem. Res. Toxicol. 25, 263–273 (2012).
31. Hunninghake, G. W., Gadek, J. E., Lawley, T. J. & Crystal, R. G. Mechanisms of neutrophil accumulation in the lungs of patients with idiopathic pulmonary fibrosis. J Clin Invest 68, 259–269 (1981).
32. Yang, S.-C., Tsai, Y.-F., Pan, Y.-L. & Hwang, T.-L. Understanding the role of neutrophils in acute respiratory distress syndrome. Biomed J 44, 439–446 (2021).
33. Blanter, M. et al. Sputum from patients with primary ciliary dyskinesia contains high numbers of dysfunctional neutrophils and inhibits efferocytosis. Respiratory Research 23, 359 (2022).
34. Grudzinska, F. S. et al. Neutrophils in community-acquired pneumonia: parallels in dysfunction at the extremes of age. Thorax 75, 164–171 (2020).
35. Chlorine: Exposure, Decontamination, Treatment | Chemical Emergencies | CDC. https://www.cdc.gov/chemicalemergencies/factsheets/chlorine.html (2023).
36. Adeloye, D. et al. Global, regional, and national prevalence of, and risk factors for, chronic obstructive pulmonary disease (COPD) in 2019: a systematic review and modelling analysis. The Lancet Respiratory Medicine 10, 447–458 (2022).
37. Turcios, N. L. Cystic Fibrosis Lung Disease: An Overview. Respiratory Care 65, 233–251 (2020).